HOST SPECIFICITY, NEGATIVE FEEDBACKS, AND PATHOGEN DEFENSE IN THE PLANT PHYLLOSPHERE MICROBIOME

Briana Kathleen Whitaker

Submitted to the faculty of the University Graduate School
in partial fulfillment of the requirements
for the degree
Doctor of Philosophy
in the Department of Biology,
Indiana University
July 2018

Accepted by the Graduate Faculty, Indiana University, in partial fulfillment of the requirements for the degree of Doctor of Philosophy.

Doctoral Committee

_____
Keith Clay, PhD

_____
Jay Lennon, PhD

_____
Curt Lively, PhD

_____
Heather Reynolds, PhD

June 22, 2018

Acknowledgements

During the course of my dissertation research, I was funded as a National Science Foundation Graduate Research Fellows, as well as by the National Institutes of Health Genetics, Cellular & Molecular Sciences Training Grant and the Department of Biology at Indiana University (IU). Funding support for the described research was provided by IU's McCormick Science Grant, the Provost's Travel Award for Women in Science at IU, the IU Research and Teaching Preserve (RTP), the Indiana Academy of Science, the Prairie Biotic Research Inc. Small Grant Award, the G.W. Brackenridge Fellowship, the Fred Seward Award, and the Indiana Daffodil Society Scholarship, as well as in part by a grant to Dr. J. Bever by NSF DEB#1556664. A portion of this research was conducted through research agreements with the U.S. DOE Fermilab National Environmental Research Park, the Fermi Research Alliance (FRA), the USDA Forest Service, and Shawnee National Forest System, orchestrated by scientists and staff on site: Dr. R. Walton, Mr. R. Campbell, and Mr. R. McClanahan. I was also assisted by research scientists and staff at Argonne National Laboratories and the IU Center for Genomics and Bioinformatics to perform the molecular and bioinformatic techniques used in this research. The IU Greenhouse and RTP Staff helped establish and maintain the Bayles Road field site and greenhouse experiments on the IU campus. I would like to personally thank the Clay and Bever labs for innumerable support over the past five years, in particular: Dr. J. Bever, Dr. N. Christian, Z. Shearin, Q. Chai, Dr. J. Bauer, M. Zaret, K. Hoban, I. Carrico, and M. Iang. Additionally, Dr. E. Knox, Dr. M. Vaughan, J. Brown, L. Cole, Q. Zhu, Dr. T. Cheeke, J. Teresi, J. Bender, and Dr. M. Busman provided expertise and assistance for the described research. I am very thankful to Dr. M. Bakker for hosting me as a graduate research intern student through the NSF-Graduate Research Internship Program, sponsored by the U.S. Department of Agriculture – Agricultural Research Service in

Peoria, IL. Lastly, I would like to thank the members of my committee, Drs. J. Lennon, C. Lively, and H. Reynolds, as well as my major advisor Dr. K. Clay, for the support, direction, advice, and constructive criticism they have provided me with over the past five years.

Briana Kathleen Whitaker

HOST SPECIFICITY, NEGATIVE FEEDBACKS, AND PATHOGEN DEFENSE IN THE PLANT PHYLLOSPHERE MICROBIOME

My dissertation research spans several topics in plant microbial ecology. In two research projects, I have explored whether host specificity influences fungal endophyte community structure in plant leaves across several ecotypes of switchgrass (*Panicum virgatum*) and across 19 plant species within the Asteraceae family. In these works, I found contrasting results for the importance of host specificity, where fungal endophytes did not preferentially colonize specific host ecotypes within a single species, but did preferentially colonize specific host species within a single family. Additionally, I also found that more phylogenetically related host species within the Asteraceae family shared more similar fungal endophyte communities than more phylogenetically distant hosts. In another portion of my research, I applied a novel extension of the plant-soil feedback framework to microbiota associated with aboveground tissues, termed "plant-phyllosphere feedback". In this work, I found that all four species tested experienced strong negative plant-phyllosphere feedback suggesting that phyllosphere, like rhizosphere (belowground), microbiota can potentially mediate plant species coexistence via negative feedbacks. In a final work, I tested whether traits displayed by bacterial endophytes *in vitro* can be used to reliably predict disease reduction outcomes *in planta* across variable climatic conditions using wheat plants and the fungal pathogen *Fusarium graminearum*. I did not ultimately find that *in vitro* trait assessments were good predictors of disease reduction outcomes *in planta*. However, my analyses did reveal differences among bacterial endophytes in their resilience to variable climatic conditions and degree of pathogen antagonism, emphasizing the

importance of considering the abiotic environment for studies of putatively beneficial plant microbiota. Through my dissertation research, I have provided evidence for the extent and limitations of host specificity in the aboveground plant microbiome, the potential role of aboveground plant microbes in mediating species coexistence, and their role in reducing pathogenic outcomes in an agriculturally relevant host.

_____
Keith Clay, PhD

_____
Jay Lennon, PhD

_____
Curt Lively, PhD

_____
Heather Reynolds, PhD

Table of Contents

Introduction

A major goal of community ecology is to connect interactions between species within communities across spatial and temporal scales (Ricklefs 2004, Vellend 2010). For example, within the macro-organismal world, this can mean studying the physiology and behavior of predator-prey interactions locally and then scaling upwards to understand the effects of these behavior dynamics on a surrounding system of interconnected habitat patches. Or similarly, determining nutrient use efficiencies of individual plant species, and using that information to understand nutrient cycling across an entire forest. However, for the micro-organismal world it can be difficult to determine what spatial scale is the most relevant one for study (Mihaljevic 2012), due to the inherently microscopic nature of microbial interactions combined with their potentially macroscopic effects on host immunity and fitness or on ecosystem processes such as nutrient cycling. For example, some estimates suggest that a single handful of soil can contain tens to hundreds of millions of microorganisms belonging to over 5,000 species (Ramirez et al. 2015). For microbial colonizers of macroscopic hosts, community ecologists could choose to study microbial community composition and function within a single host tissue or organ (e.g., the gut or a leaf), at the level of a single host, across a population of hosts or a mixed community of potential hosts, or regionally across landscapes. My body of dissertation research is focused on the cross-section of several spatial scales in plant-microbial ecology.

Using a combination of traditional, culture-based and next-generation sequencing approaches, I tested the competing mechanisms of host specificity and local environment in driving plant microbiome community assembly. Secondly, I tested how microbial inoculum sources in the aboveground plant microbiome (i.e., the phyllosphere) alters plant fitness and whether plant fitness consequences are conditional on the identity of phyllosphere inoculum

from con- versus heterospecific hosts. These results were then placed in a plant-plant interaction framework to test whether phyllosphere microbial communities are a potential mechanism for the stabilization of plant-species interactions through negative feedbacks. Lastly, at the level of a single plant organ, I tested whether the interactions between potentially plant-growth promoting bacterial species and a fungal pathogen of wheat inflorescences are altered by the abiotic environment and whether *in planta* outcomes can be predicted by *in vitro* interaction traits. These research questions are summarized into the following four chapter titles.

Chapter 1 – Foliar fungal endophyte communities are structured by environment but not host ecotype in *Panicum virgatum* (switchgrass) – in revision at *Ecology*

Chapter 2 – Phylogenetic relatedness of Asteraceae hosts predicts foliar microbiome community structure in a common garden environment – in revision at *Molecular Ecology*

Chapter 3 – Negative plant-phyllosphere feedbacks in native Asteraceae hosts – a novel extension of the plant-soil feedback framework – published in *Ecology Letters* (2017)

Chapter 4 – Bacterial endophyte antagonism against a fungal pathogen *in vitro* does not predict efficacy *in planta* – in preparation

In the following section, I introduce the primary study system used in this research: the plant phyllosphere microbiome.

Study System – Phyllosphere Microbiome

The phyllosphere microbiome, defined as the microbial colonizers of aerial plant tissues and organs, has received significantly less attention than the rhizosphere microbiome (Peñuelas

and Terradas 2014). However, we know that phyllosphere, like rhizosphere, microbiota can also form diverse and complex communities spanning the bacterial, archaeal, and eukaryotic kingdoms, with a variety of functional and trophic roles (Porras-Alfaro and Bayman 2011). Previously, researchers were only able to use culture-dependent techniques to characterize these communities; relying on the culturability of microbial taxa alone to understand their ecology within hosts. With the advent of Next Generation Sequencing and the discovery of previously un-characterized microbiota, our knowledge of the diversity of these systems has rapidly advanced. However, culture-dependent approaches remain an important tool in a microbial ecologist's toolkit due to the ability to directly measure traits on microbial symbionts in culture, study entire genomes in search of functional genes, or inoculate microbial species back onto asymptomatic or gnotobiotic hosts (Busby et al. 2017).

Many different techniques have been used over the past few decades to identify mechanisms of community assembly for phyllosphere microbiota. These techniques have tended to divide the phyllosphere into two compartments, "endo-" and "epi-" spheres, which refer to the internal or external residence of symbionts on plant tissues, respectively. Leaf exclosure experiments (i.e., "bagging"; (Kaneko and Kaneko 2004), along with rainwater collection in forest understories (Wilson 1996), and exposure of developing seedlings to conspecific leaf litter (Christian et al. 2017) indicate that these communities primarily arise via three core 'seed banks': air, rain, and leaf litter (Christian et al. 2015). Yet few studies to date have directly manipulated these inocula sources, in conjunction with manipulating recipient host genetic identity to determine the relative influence on microbial community assembly.

My research exploring the identity of the specific microbial taxa inhabiting aboveground plant tissues has focused on the endosphere. Fungal and bacterial endophytes are thought to

colonize aboveground plant tissues via stomata (Huang et al. 2018), wounds, or other natural openings in plant tissues (e.g., anther/stigma extrusion at flowering;Graham and Browne 2009). Upon colonization, fungal endophytes in particular are known for their impacts on plant tissue chemistry via the production of secondary metabolites (Strobel and Daisy 2003). These metabolites are thought to be involved in plant defense via the creation of a spatially-heterogeneous chemical landscape that renders the host tissue unpalatable for insect herbivores or unfavorable for colonization by pathogenic microbes (Herre et al. 2007). However, both fungal and bacterial endophytes are thought to act as part of the plant immune system via direct competition with pathogenic microbiota, or indirectly via immune system priming (Porras-Alfaro and Bayman 2011).

Unfortunately, the precise molecular interactions used by plants for the recruitment and maintenance of most types of phyllosphere microbiota remains unknown. Despite these uncertainties, many questions regarding the ecology and natural history of these microbiomes are ripe for study through the use of manipulatory experiments and inoculation studies. Through my dissertation research I hope to provide insights into multiple scales of the plant phyllosphere microbiome. Specifically, testing how microbial species interact within single plant organs, how the environment and host genetic filtering structure phyllosphere microbial communities, and whether phyllosphere microbiota can influence plant-plant interactions.

Literature Cited

Busby, P. E., C. Soman, M. R. Wagner, M. L. Friesen, J. Kremer, A. Bennett, M. Morsy, J. A. Eisen, J. E. Leach, and J. L. Dangl. 2017. Research priorities for harnessing plant microbiomes in sustainable agriculture. PLoS Biology 15:e2001793.

Christian, N., E. A. Herre, L. C. Mejia, and K. Clay. 2017. Exposure to the leaf litter microbiome of healthy adults protects seedlings from pathogen damage. Proceedings of the Royal Society: Biological Sciences 284:1–8.

Christian, N., B. K. Whitaker, and K. Clay. 2015. Microbiomes: unifying animal and plant systems through the lens of community ecology theory. Frontiers in Microbiology 6:1–15.

Graham, S., and R. A. Browne. 2009. Anther extrusion and fusarium head blight resistance in European wheat. Journal of Phytopathology 157:580–582.

Herre, E. A., L. C. Mejía, D. A. Kyllo, E. Rojas, Z. Maynard, A. Butler, and S. A. Van Bael. 2007. Ecological implications of anti-pathogen effects of tropical fungal endophytes and mycorrhizae. Ecology 88:550–558.

Huang, Y.-L., N. Zimmerman, and A. E. Arnold. 2018. Observations on the early establishment of foliar endophytic fungi in leaf discs and living leaves of a model woody angiosperm, *Populus trichocarpa* (Salicaceae). Journal of Fungi 4:1–15.

Kaneko, R., and S. Kaneko. 2004. The effect of bagging branches on levels of endophytic fungal infection in Japanese beech leaves. Forest Pathology 34:65–78.

Mihaljevic, J. R. 2012. Linking metacommunity theory and symbiont evolutionary ecology. Trends in Ecology and Evolution 27:323–329.

Peñuelas, J., and J. Terradas. 2014. The foliar microbiome. Trends in Plant Science 19:278–280.

Porras-Alfaro, A., and P. Bayman. 2011. Hidden fungi, emergent properties: endophytes and

microbiomes. Annual Review of Phytopathology 49:291–315.

Ramirez, K. S., M. Döring, N. Eisenhauer, C. Gardi, J. Ladau, J. W. Leff, G. Lentendu, Z. Lindo, M. C. Rillig, D. Russell, S. Scheu, M. G. St. John, F. T. De Vries, T. Wubet, W. H. van der Putten, and D. H. Wall. 2015. Toward a global platform for linking soil biodiversity data. Frontiers in Ecology and Evolution 3:1–7.

Ricklefs, R. E. 2004. A comprehensive framework for global patterns in biodiversity. Ecology Letters 7:1–15.

Strobel, G., and B. Daisy. 2003. Bioprospecting for microbial endophytes and their natural products. Microbiology and Molecular Biology Reviews 67:491–502.

Vellend, M. 2010. Conceptual synthesis in community ecology. The Quarterly Review of Biology 85:183–206.

Wilson, D. 1996. Manipulation of infection levels of horizontally transmitted fungal endophytes in the field. Mycological Research 100:827–830.

Title: Foliar fungal endophyte communities are structured by environment but not host ecotype in *Panicum virgatum* (switchgrass)

Authors: Briana K. Whitaker (BKW)[1*], Heather L. Reynolds (HLR)[1], Keith Clay (KC)[1]

[1] Department of Biology, Indiana University, Bloomington, IN

Emails: brkawhit@indiana.edu; hlreynol@indiana.edu; clay@indiana.edu

Author for correspondence: Briana K. Whitaker

Address: Department of Biology, Jordan Hall, 1001 E. 3rd St, Indiana University, Bloomington, IN, 47405-3700; Tel: (+1) 8128551674; Fax: (+1) 8128556705; Email: brkawhit@indiana.edu

Article Type: Article; **Word Count:** Abstract (307), Total (4208), Introduction (992), Materials and Methods (1575), Results (595), Discussion (1046);References (61), Figures (5), Color Figures (5), Tables (1), Text Boxes (0)

Keywords switchgrass, ecotype, community assembly, host specificity, biotic adaption, fungal endophyte, GxE

Abstract

Experimental tests of community assembly mechanisms for host-associated microbiomes in nature are lacking. Asymptomatic foliar fungal endophytes are a major component of the plant microbiome and are increasingly recognized for their impacts on plant performance, including pathogen defense, hormonal manipulation, and drought tolerance. However, it remains unclear whether fungal endophyte colonization is simply a function of spore type and abundance within the local environment, or whether certain host ecotypes or genotypes are preferentially colonized, reflecting some degree of biotic adaptation in the symbioses. Whether local environment, host ecotype, or some combination of both controls the pattern of microbiome formation across hosts represents a new dimension to the age-old debate of nature versus nurture. Here we used a reciprocal transplant design to explore the extent of host specificity and biotic adaptation in the plant microbiome, as evidenced by differential colonization of host genetic types by endophytes. Specifically, replicate plants from three locally-adapted ecotypes of the native grass *Panicum virgatum* (switchgrass) were transplanted at three geographically distinct field sites (one home and two away) in the Midwestern US. At the end of the growing season, plant leaves were harvested and the fungal microbiome characterized using culture-dependent sequencing techniques. Our results demonstrated that fungal endophyte community structure was determined by local environment (i.e., site), but not by host ecotype. Fungal richness and diversity also strongly differed by site, with lower fungal diversity at a riparian field site, whereas host ecotype had no effect. By contrast, there were significant differences in plant phenotypes across all ecotypes and sites, indicating ecotypic differentiation of host phenotype. Our results indicate that community structure in the switchgrass fungal microbiome is driven primarily by environmental factors. From an applied perspective, this suggests that applications

of putative plant-growth promoting foliar fungi to hosts for improved yields may not be effective if local environmental inocula displace inoculated fungi.

Introduction

Host-associated microbial communities are increasingly well-characterized throughout the tree of life (Christian et al. 2015), yet an understanding of the factors controlling their ecological assembly under field conditions is still lacking (Peay 2014). In particular, it is unclear to what extent environmentally-transmitted microbiomes are structured by host factors such as host age (Hawlena et al. 2013) and host resistance (Hale et al. 2014), versus environmental factors such as local climate (Bálint et al. 2015), soil conditions (Bakker et al. 2014), and the surrounding community of alternate host species (Bakker et al. 2014, Laforest-Lapointe et al. 2017). Furthermore, host and environmental factors can be non-independent; local environment can shape host phenotype (Johnson and Agrawal 2005), which can then feed back to shape microbiome community assembly (Gehring et al. 2014). While local adaption to abiotic conditions is a well-studied mechanism driving genetic diversity within heterogeneous environments (Howe et al. 2003), population divergence (Agren and Schemske 2012), and patterns of population distributions across space and time (Hereford 2009). These patterns can also be driven by local adaptation to biotic conditions, such as the presence of mutualists (Warren II and Bradford 2014), antagonists (Nosil 2004) or preferred hosts for colonization (Laine et al. 2014).

For example, local adaptation of rust pathogens to ecotypes of wild flax has been demonstrated where 'avirulence' loci in the pathogen were strongly differentiated by host ecotype but not by distance (Laine et al. 2014). Similarly, greater virulence has been

demonstrated for sympatric wheat cultivar-pathogen combinations relative to allopatric combinations (Ahmed et al. 1995). Local adaptation to host species has also been documented for vertically-transmitted symbionts, including fungal endophytes of grasses (Afkhami et al. 2014) and bacterial symbionts of parasitic nematodes (Chapuis et al. 2009). In these instances, at least one member of the partnership has restricted gene flow due to their reliance on vertical transmission during host reproduction.

However, whether local adaptation to biotic conditions is possible for asymptomatic, horizontally-transmitted microbes is less certain (Greischar and Koskella 2007). Long-distance dispersal events and horizontal gene transfer can homogenize genetic variation in microbial taxa (Hanson et al. 2012) and reduce biotic adaptation to host types (Papke and Ward 2004), or increase the likelihood of maladaptation (Sullivan and Faeth 2004). Conversely, the rapid evolution of microbial taxa, relative to their hosts, could increase genetic variation within microbial populations and strengthen biotic adaptation to local host ecotypes (Hanson et al. 2012). Biotic adaptation within host-symbiont interactions is directly analogous to the concept of host specificity, where biotic adaptation is defined as local adaptation that alters species interactions (Urban 2011) and host specificity is defined as preferential colonization of specific host genetic types (Barrett and Heil 2012). Both concepts depend on the relative migration rates and dispersal asymmetries between the symbiont and its host across both partners' geographic ranges (Gandon et al. 1996, Nuismer et al. 1999). The strongest test for biotic adaptation, and host specificity, is reciprocal inoculation or exposure to local sources of inocula (Kawecki and Ebert 2004).

In plants, foliar fungal endophytes (FFE) comprise a major component of the phyllosphere (i.e., aboveground) microbiome, and increasingly are the subject of much empirical

and theoretical research (Christian et al. 2015). FFE are defined by their asymptomatic infection of plant tissues during at least a portion of their life cycle, and have been isolated from every plant species studied to date (Rodriguez et al. 2009). These symbionts span diverse functional and trophic roles, such as mutualists, pathogens, and latent saprotrophs (Porras-Alfaro and Bayman 2011). Among FFE, colonization of new hosts is predominately horizontal through air-, rain-, and litter- borne spores (reviewed in Christian *et al.* 2015), along with occasional re-colonization of new tissues from the previous season's buds and petioles (Kaneko and Kaneko 2004) or colonization of seeds via spores dispersed with pollen grains (Hodgson et al. 2014).

Correlational studies support local environment as an important force structuring FFE communities (Christian et al. 2016, Giauque and Hawkes 2016). Environment-specific differences in FFE community structure can arise through dispersal limitation, but few studies have explicitly examined the dispersal limits of individual FFE species. Some FFE species (or species complexes) have ranges spanning hundreds to thousands of kilometers (e.g., *Lophodermium australe*, Oono *et al.* 2014; *Colletotrichum gloesporieodes*, Rojas *et al.* 2015), while other FFE communities appear to have a more limited geographic distribution (U'Ren et al. 2012). Results from studies testing the role of host specificity as a driver of FFE community structure have also been mixed. For example, researchers have shown strong variation in FFE composition across co-occurring fern species (Del Olmo-Ruiz and Arnold 2014), tree species (Vincent et al. 2016), and among tree genotypes (Ahlholm et al. 2002). By contrast, a study on understory tropical grasses found that FFE composition was independent of host species identity (Higgins et al. 2014).

To quantify the effect of host specificity and biotic adaptation, as measured by differential colonization of hosts, relative to the effect of local environment in structuring FFE

communities, requires using host populations in both their home and away ranges. Reciprocal transplant studies can distinguish among competing mechanisms for microbial community assembly across geographically and phenotypically-defined host ecotypes. We used a reciprocal transplant study to assess whether FFE differentially colonize *Panicum virgatum L.* (switchgrass) ecotypes, defined here as a locally-adapted, genetically-based phenotype, or whether FFE community structure is determined primarily by the local environment and inocula sources, or whether both processes act simultaneously to structure FFE communities. We predicted that both host ecotype and the local environment would interactively affect FFE community structure, whereby certain FFE species would preferentially colonize certain host types (Bálint et al. 2015), but that local inocula sources of FFE from the surrounding environment would strongly influence FFE community structure across sites (Giauque and Hawkes 2016). However, our results support a dominant role for local environment in structuring FFE communities and more generally provide insights into the factors affecting switchgrass microbiomes that may be applicable to a wider range of plant systems.

Materials and Methods

Description of Host Study System and Sites

Switchgrass is a perennial C4 grass native to tallgrass prairies, riparian zones, and many other habitats of North America (Casler et al. 2011). Its geographic distribution extends from Mexico to Canada (Casler et al. 2011). Periodic glaciation, causing alternatively high gene flow and high population isolation, has led to the large phenotypic variation observed across the plant's range, with many described ecotypes (e.g., 'Alamo', 'Kanlow', 'Blackwell', 'Pathfinder', etc.; Casler et al. 2011, Lowry et al. 2014). This high degree of natural phenotypic variation in the grass makes it an ideal model system for the study of FFE community structure. Switchgrass

is also of great interest as an alternative biofuel source and is used widely for horticultural practices in the United States (Casler et al. 2011, Lowry et al. 2014).

Three sites were used in this study: a remnant riparian zone, a restored mesic prairie, and an old successional field (Supporting Information SI Fig. S1). Each site (i.e., "Madison", "Fermi", and "Shawnee") was chosen to represent a historic home for a given switchgrass ecotype (i.e., "Madison", "Fermi", and "Cave-in-Rock", respectively). The sites were separated by at least 350 km, suggesting high genetic divergence amongst the switchgrass ecotypes. Across sites, total rainfall during the course of the experiment (i.e., 10 weeks) ranged from 11.9cm at the old successional field to 23.3cm at the restored mesic prairie (Midwestern Regional Climate Center cli-MATE program). A description of all three experimental sites and associated seed collection efforts is presented in the SI Methods, as well as a table of site-level climate details (SI Table S1).

Germination & Field Transplantation

Seeds from all three ecotypes were surface-sterilized in a 0.5% bleach solution for 5min and then rinsed in distilled water. Seed coats were removed using sterile sand paper and incubated on moist filter paper in sterile 6cm petri dishes for a period of 2-5 weeks during April and May 2014. Upon germination, seedlings were transplanted into 164mL conetainers (Stuewe and Sons, Yellow, SC10) with a 1:1 mix of pasteurized compost soil and sand. Plants were grown in the greenhouses at Indiana University for 6-10 weeks and watered as needed. Two weeks before transplantation in the field, each plant was planted into a dual-pot. To create the dual-pot, the bottom of one 3.8L plastic pot was removed using an electric saw, then nested inside a second intact pot and filled with pasteurized compost soil. A single switchgrass plant was then transplanted into each pot and fertilized with 4.9mL of 13-13-13 Osmocote fertilizer,

after which the plants received no additional fertilizer during the course of the experiment. After moving plants to the field sites, the outer, intact pot was removed and the inner, bottomless pot sunk into the ground, flush with the soil surface. This ensured natural root growth at the field sites, while inhibiting rhizomatous spread into the surrounding plant communities. Transplantation occurred between July 9th and 12th, 2014 across the three sites.

Eight plants per ecotype-site combination were used as treatment replication (*8 host plants x 3 sites x 3 ecotypes*). Due to low seed germination, only n=7 CIR were planted at the Fermi and Madison sites (*N=70*). Exposure to environmental sources of FFE inocula began upon transplantation at the field sites. Plant height and tiller number were recorded for all plants prior to field transplantation and microbial exposure (Fig. 1). Both pre-planting height ($F_{2,57} = 7.95$, $p = 0.0009$; Fig. 1A) and tiller count (Poisson model for count data; $\chi^2_{2,61} = 13.79$, $p = 0.0010$; Fig. 1B*)* differed significantly among ecotypes, confirming genetic variation among ecotypes when grown in a common greenhouse environment. CIR ecotype plants were taller, while Madison ecotype plants produced more tillers.

Each plant was trimmed at the time of transplantation to a height of approximately 15cm to reduce transplant shock. Before planting, each field plot was cleared of existing vegetation to a height of approximately 15cm height and the resulting litter removed. Plots were either 2.7m x 7.3m or 3.7m x 5.5m depending on the space available at each site. Spacing between plants was 0.91m and planting order was randomized across individuals at each field site. Local soil was used to lightly cover the base of experimental plants and pots (approx. 2cm). Following planting, each plant was watered with 5.7L of water after which no additional water was applied.

Sampling Method & Molecular Procedures

After 10 weeks of growth, three leaves were sampled from each plant at mid-tiller (i.e., mid-canopy) height in September 2014 for FFE community characterization. Two Fermi ecotype plants died at the Madison site before leaves could be collected, leaving N=68 host plants. To characterize FFE communities, leaf tissues were sub-sampled. Leaves were first cut into 4-8cm segments, which were then cut into ½-cm squares using grid paper. From these, six leaf squares were haphazardly selected and quartered into 2.5mm square fragments, yielding 24 small leaf fragments per plant which were surface sterilized. This leaf size has been shown to be ideal for reducing fungal isolation to a single FFE per square yet also capturing the greatest overall community diversity (Gamboa et al. 2002). Leaf fragments were submerged sequentially in 70% ethanol (3min), a 0.5% bleach solution (2min), and sterile water (1min) using a metal tea strainer (Mejia et al. 2008). The strainer and leaf fragments were dried on a sterile Kimwipe (1min) after which 16 leaf fragments per individual plant were haphazardly selected and plated individually on 750uL of corn meal agar (CMA) in a sterile 2 mL microcentrifuge tube (U'Ren et al. 2009). Tetracycline was added to the CMA to prevent bacterial growth.

Tubes were then sealed with parafilm and incubated at 23°C on a 12-hr light cycle for 6 weeks. All leaf fragments which yielded fungal growth were sub-cultured onto 6cm CMA plates to produce pure cultures. CMA plates were sealed with parafilm and fungal cultures incubated for an additional 4 weeks, after which individual fungal colonies were grouped on the basis of colony morphology, color, and growth rate (Lacap et al. 2003), resulting in 44 putative morphotypes. For each defined morphotype at least one, but typically two or more isolates were subjected to DNA extraction and sequencing (Shipunov et al. 2008). In addition, all cultures that had ambiguous morphological characteristics, or that appeared to be morphologically unique (i.e., singletons) were sequenced. In total, DNA was extracted, amplified, and sequenced for 381

FFE cultures. Vouchers of living mycelia were suspended in sterile water and stored at room temperature at Indiana University. Detailed molecular procedures for fungal DNA extraction and amplification are presented in the SI Methods

Consensus sequences for each sequenced FFE isolate were manually inspected, assembled, and edited using CodonCode (v.7.1.2, CodonCode Corporation, Centerville, MA) and grouped at the 95% sequence similarity level with a minimum of 40% overlap. Putative names were assigned to each operational taxonomic unit (OTU) using the RDP naïve Bayesian classifier (v.2.12) and the Warcup fungal ITS database (Deshpande et al. 2015). Results and confidence thresholds from this classification are presented in Table S2. Representative sequences from each OTU were submitted to GenBank under accession numbers MH178669-MH178739.

Statistical Analyses

All statistical analyses were conducted in R (v3.4.2). Species accumulation curves and estimates of total richness were inferred for fungal OTUs using the 'specaccum' function in the 'vegan' package (Oksanen et al. 2017). Linear models were constructed to test whether the FFE species richness and diversity (Shannon index) per host differed across ecotype and site treatment groups. Tukey's post-hoc test was used to test significance of pairwise comparison between groups within treatments for continuous, non-integral response variables. Plant height and tiller number at the time of leaf sampling, as well as relative growth rate based on changes in plant size from transplantation to sampling, were tested as covariates in the models of FFE richness and diversity, but all were insignificant and thus are not presented. We used the Bray-Curtis dissimilarity index to test for differences in FFE community structure using a permutational multivariate analysis of variance (PERMANOVA; 'adonis' function, 'vegan'

package, 1000 permutations; Oksanen et al. 2017). A Hellinger transformation was applied to the FFE community matrix to limit the influence of abundant OTUs (Legendre and Gallagher 2001). All putative singletons were excluded from community structure analysis (Higgins et al. 2014). Differences in FFE community structure were visualized using non-metric multidimensional scaling (NMDS). To determine how much variance was explained by host ecotype and planting site (Legendre and Gallagher 2001), we performed a variance partitioning analysis (RDA; 'varpart' function, 'vegan' package; Oksanen et al. 2017) with the transformed FFE community matrix as the response variable. Constrained RDA followed by a pseudo-F test was used to assess significance. To determine which FFE OTUs best characterized the microbial communities as a function of switchgrass ecotype and planting site, we performed Dufrêne and Legendre's indicator species analysis (1997) using the 'labdsv' package (10,000 randomizations; Roberts 2016). Indicator OTUs are identified by their relative fidelity to a specific group (i.e., ecotypes or sites) and weighted by their relative abundance across all groups. Linear models were also constructed to test whether plant height and tiller count at leaf sampling differed across ecotype and site treatment groups. For the tiller counts, a negative binomial model was used due to overdispersion in the data. For the post-treatment size analyses, two Madison-ecotype plants grown at the Fermi site were not included due to mislabeling at harvest (leaving N=66 plants for the post-treatment size analyses).

Results

From 68 plants spanning three geographic sites and three switchgrass ecotypes, we cultured 813 isolates from 1088 leaf fragments. Of the leaf fragments plated, 74.7% yielded fungal growth. From 768 isolates, we identified 71 fungal OTUs based on sequencing data. The other 45 isolates either failed to yield high quality sequence data or were difficult to regrow from

vouchers. These isolates (1 morphotype and 43 putative singletons) constituted 5.5% of the dataset and were excluded from further analyses. Of the 71 fungal OTUs identified, 38 OTUs were isolated more than once and 33 OTUs were isolated only once (i.e., singletons). Across sites, 37 OTUs were identified from plants grown at the Fermi site, 15 OTUs from the Madison site, and 47 OTUs from the Shawnee site. Similarly, for the Fermi, Madison, and CIR ecotypes, 43, 42, and 39 fungal OTUs were identified, respectively. The most abundant OTU represented 28.7% of individual isolates and the top ten most abundant OTUs accounted for 71.2% of all isolates (Fig. 2A; Table S2). Species accumulation curves, depicting the number of accumulated taxa per plant host, remained non-asymptomatic, but the estimated richness fell within the 95% confidence interval for the total experiment (Fig 2B) and showed similar rates of accumulation across sites (Fig. 2C). Thus, the dataset was considered sufficient for the community analyses described below (Del Olmo-Ruiz and Arnold 2014).

FFE OTU richness per-plant ranged from 1 to 10. Average per-plant FFE richness varied across sites (Fig. 3B, $\chi^2_{2,59} = 13.6, p = 0.0011$), but not by ecotype (Fig. 3A, $p = 0.9823$). In particular, average per-plant FFE richness was significantly lower at the Madison site relative to the other two sites (Fig. 3B). Average per-plant FFE diversity also varied significantly across sites (Fig. 3D, $F_{2,59} = 18.7, p < 0.0001$), but not among ecotypes (Fig. 3C, $p = 0.8988$), such that average per-plant FFE diversity was also lower at the Madison site relative to the Fermi and Shawnee sites (Fig. 3D). Overall, FFE diversity per-plant ranged from 0, for one plant where all isolates were identical, up to 2.30. There was no significant interaction between host ecotype and site for either FFE richness or diversity.

FFE community structure differed significantly by site (*pseudo*-$F_{2,59} = 31.6, p = 0.0010$; Fig. 4B), but not by host ecotype ($p = 0.5465$; Fig. 4A). There was no interaction between site

and host ecotype in driving FFE community structure ($p = 0.7103$). Variance partitioning analysis showed that site explained 42.53% of the variation in FFE community structure (*pseudo-*$F_{2,63} = 24.5$, $p = 0.001$). Host ecotype did not explain any variation in FFE community structure ($p = 0.540$) and there was a large amount of unexplained variation (58.85%). Indicator species analysis identified two fungal OTUs that had high specificity and relative abundance to specific switchgrass ecotypes at a threshold $\alpha < 0.10$ (Table 1). By contrast, 22 fungal OTUs were indicative of specific sites ($\alpha < 0.10$; Table 1).

Plant height at time of FFE sampling differed among ecotypes ($F_{2,57} = 8.67$, $p = 0.0005$), where the Fermi ecotype was significantly taller than both the Madison and CIR ecotypes, which did not differ from each other (Fig. 5A). Plant height also varied by site ($F_{2,57} = 76.8$, $p < 0.0001$), such that all two-way comparisons between sites were significant ($p < 0.0001$ *for all*; Fig. 5B), but there was no interaction between ecotype and site on plant height ($p = 0.6658$). Plant tiller count at time of harvest varied by ecotype ($\chi^2_{2,57} = 8.10$, $p = 0.0174$; Fig. 5C), but not by site ($p = 0.3208$).

Discussion

Our results demonstrate that site, encompassing local environmental conditions and local sources of microbial inoculum, is the primary force structuring switchgrass FFE communities. Site was a significant predictor of FFE species richness, diversity, and community structure, and explained the majority of the variation in community structure across hosts. Contrary to our original prediction, switchgrass host ecotype had no direct effect, and did not interact with local site, in driving FFE richness, diversity, or structure. Our reciprocal transplant design provided a strong test for the role of biotic adaptation in FFE communities, but in this study we did not detect differential colonization of host ecotypes even within a single site. On the other hand, both

site and ecotype had significant effects on plant phenotype after 10 weeks of growth under field conditions, indicating genetic differences among switchgrass ecotypes for phenotype but not for the assembly of FFE communities.

There are several potential explanations for the strong effects of site, versus host ecotype, as the primary driver of FFE community structure in switchgrass. It is possible that the three ecotypes used in this study were too genetically similar. However, genetic differences in plant phenotype were detected when grown in a common greenhouse environment (Fig. 1) and at the three field sites (Fig. 5), but those phenotypic differences did not correspond to differences in FFE communities (Fig. 4). Previous research has demonstrated host-genotype specific differences in FFE community structure for balsam poplar (Bálint et al. 2015) and birch trees (Ahlholm et al. 2002). Differences were also found among several cereal species and cultivars across two sites in the structure of their epiphytic and endophytic fungal colonizers (Sapkota et al. 2015). Here, the geographic distance among sites (≥350km) and the attendant environmental and biological variation may have overwhelmed differences in FFE communities due to genetic differences among ecotypes. The three sites differed in local climate, surrounding vegetation, and soil type and texture, which can have important influences on microbial community structure (Bakker et al. 2014, Giauque and Hawkes 2016). Additionally, while spore dispersal across large distances may be possible, the effective dispersal of most fungi, and other microbial groups, is unknown (Hanson et al. 2012) and may have been limited among the three sites. Lastly, while rapid temporal turnover in FFE communities is well documented (e.g., "seasonality", Jumpponen and Jones 2010), it may be that the 10-week period of host exposure favored local environmental effects at the expense of host-specific effects, which may require more time to become evident.

Deciphering the importance of specific mechanisms driving FFE community structure at the local site level is complex. Previous research has shown that local plant community diversity can drive differences in soil microbial communities (Bakker et al. 2014) and leaf bacterial communities (Laforest-Lapointe et al. 2017), and disturbance regimes can impact FFE community assembly (Kandalepas et al. 2015). The low FFE diversity at the Madison site might therefore be related to the site's relatively low plant community diversity (personal observation) and high level of disturbance due to water-level fluctuations along the Ohio River where native switchgrass and the Madison transplant site occurred. Future research should test whether FFE communities are determined in part by local plant community diversity and how differential disturbance regimes affect FFE communities.

Increasing attention is being paid to the microbial associations of switchgrass due to its biofuel and forage crop potential (Casler et al. 2011). Previous research on plant-growth promoting microbiota in switchgrass has focused on ectomycorrhizal (i.e., *Serbacina vermifera*; (Ghimire and Craven 2011) and leaf-colonizing bacteria symbioses (i.e., *Burkholderia phytofirmans* strain *PsJN*; (Lowman et al. 2016, Wang et al. 2016). Fewer studies have examined FFE community differences in switchgrass (but see (Ghimire et al. 2011, Giauque and Hawkes 2013). One study that examined the plant-growth promoting effects of FFE on developing switchgrass seedlings found a large range in effects of individual FFE from beneficial to antagonistic (Kleczewski et al. 2012). In our study, little evidence was found for host-specific colonization by FFE taxa or host-specific fitness effects. However, a large number of previously unidentified FFE species were found at all three sites. Specifically, of the 71 OTUs isolated, only 34 could be identified to the species level with confidence, indicating that the phyllosphere microflora of prairies, old fields, and riparian areas remains largely uncharacterized.

Given the potential importance of the switchgrass microbiome for agriculture, we conducted a comparative analysis of the fungal genera identified here with the results of Ghimire *et al.* (2011), Giauque & Hawkes (2013), and Kleczewski *et al.* (2012) (Table S3). Five genera were common to switchgrass across all four studies (e.g., *Alternaria*, *Davidiella*, *Gibberella*, *Khuskia*, and *Phoma*) and an additional five genera were identified in three of the four studies (e.g., *Cochliobolus*, *Epicoccum*, [*Eu-*]*Penicillium*, *Glomerella*, *Phaeosphaeria*). Of these fungal genera, three were among the top ten most frequently isolated in our study (e.g., *Alternaria*, *Khuskia*, and *Phaeosphaeria*). This comparison among studies indicates that, despite the broad geographic range of these studies, differences in sampling methods, and use of sequence databases for fungal classification, there are many fungal genera that may be widespread colonizers of switchgrass aboveground tissues.

While the interaction between genetics and environment is recognized as an important determinant of host fitness (Hereford 2009) and species interactions (Johnson and Agrawal 2005), our results strongly support local environment as the primary determinant of FFE community structure in switchgrass. FFE communities did not exhibit ecotype specificity either within sites or across sites. It remains an open question whether these results would hold for other plant groups (e.g., trees, forbs, or other grasses) or across sites that are less geographically disparate or ecologically divergent. Our results also suggest that researchers should test whether pre-inoculation with plant-growth promoting FFE in switchgrass is effective, or if putative host varieties are rapidly colonized by local environmental inocula that then outcompete the inoculated FFE. Controlled tests using transplants across either spatial or abiotic gradients (e.g., precipitation patterns, prevailing wind direction, soil pH, slope, etc.) represent the next steps to determine how FFE communities are structured and how FFE communities impact plant

function. Overall, our results enhance our understanding of the dominant drivers of microbiome structure in an ecologically and economically-important grass species that furthermore may be applied to a wider range of host varieties and plant study systems.

Acknowledgements

The authors would like to thank Dr. R. Walton, Mr. R. Campbell, and Mr. R. McClanahan for their assistance at Fermilab and Shawnee National Forest. This work was conducted through research agreements with the U.S. DOE Fermilab National Environmental Research Park, the Fermi Research Alliance (FRA), the USDA Forest Service, and Shawnee National Forest System. We thank Z. Shearin, Q. Chai, N. Christian, K. Hoban, and M. Zaret for assistance with the project. B.K.W. was supported by the NIH Genetics, Cellular & Molecular Sciences Training Grant and as an NSF Graduate Research Fellow during the course of the experiment and through writing of the manuscript. Travel funding to field sites was provided by the Provost's Travel Award for Women in Science at IU. The research was funded by IU's McCormick Science Grant, as well as the G.W. Brackenridge Fellowship, Fred Seward Award, Indiana Daffodil Society Scholarship, and the Prairie Biotic Research Inc. Small Grant Award.

Literature Cited

Afkhami, M. E., P. J. Mcintyre, and S. Y. Strauss. 2014. Mutualist-mediated effects on species' range limits across large geographic scales. Ecology Letters 17:1265–1273.

Agren, J., and D. W. Schemske. 2012. Reciprocal transplants demonstrate strong adaptive differentiation of the model organism *Arabidopsis thaliana* in its native range. New Phytologist 194:1112–1122.

Ahlholm, J. U., M. Helander, J. Henriksson, M. Metzler, and K. Saikkonen. 2002. Environmental conditions and host genotype direct genetic diversity of *Venturia ditricha*, a fungal endophyte of birch trees. Evolution 56:1566–1573.

Ahmed, H. U., C. C. Mundt, and S. M. Coakley. 1995. Host-pathogen relationship of geographically diverse iolates of *Septoria tritici* and wheat cultivars. Plant Pathology 44:838–847.

Bakker, M. G., D. C. Schlatter, L. Otto-Hanson, and L. L. Kinkel. 2014. Diffuse symbioses: roles of plant-plant, plant-microbe and microbe-microbe interactions in structuring the soil microbiome. Molecular Ecology 23:1571–1583.

Bálint, M., L. Bartha, R. B. O'Hara, M. S. Olson, J. Otte, M. Pfenninger, A. L. Robertson, P. Tiffin, and I. Schmitt. 2015. Relocation, high-latitude warming and host genetic identity shape the foliar fungal microbiome of poplars. Molecular Ecology 24:235–248.

Barrett, L. G., and M. Heil. 2012. Unifying concepts and mechanisms in the specificity of plant-enemy interactions. Trends in Plant Science 17:282–292.

Casler, M. D., C. M. Tobias, S. M. Kaeppler, C. R. Buell, Z.-Y. Wang, P. Cao, J. Schmutz, and P. Ronald. 2011. The Switchgrass genome: tools and strategies. The Plant Genome 4:273–282.

Chapuis, É., V. Emelianoff, V. Paulmier, N. Le Brun, S. Pagès, M. Sicard, and J. B. Ferdy. 2009. Manifold aspects of specificity in a nematode-bacterium mutualism. Journal of Evolutionary Biology 22:2104–2117.

Christian, N., C. Sullivan, N. D. Visser, and K. Clay. 2016. Plant host and geographic location drive endophyte community composition in the face of perturbation. Microbial Ecology 72:621–632.

Christian, N., B. K. Whitaker, and K. Clay. 2015. Microbiomes: unifying animal and plant systems through the lens of community ecology theory. Frontiers in Microbiology 6:1–15.

Deshpande, V., Q. Wang, P. Greenfield, M. Charleston, A. Porras-Alfaro, C. R. Kuske, J. R. Cole, D. J. Midgley, and N. Tran-Dinh. 2015. Fungal identification using a Bayesian classifier and the Warcup training set of internal transcribed spacer sequences. Mycologia 108:1–5.

Dufrene, M., and P. Legendre. 1997. Species assemblages and indicator species: the need for a flexible asymmetrical approach. Ecological Monographs 67:345–366.

Gamboa, M. A., S. Laureano, and P. Bayman. 2002. Measuring diversity of endophytic fungi in leaf fragments: does size matter? Mycopathologia 156:41–45.

Gandon, S., Y. Capowiez, Y. Dubois, Y. Michalakis, and I. Olivieri. 1996. Local adaptation and gene-for-gene coevolution in a metapopulation model. Proceedings of the Royal Society B: Biological Sciences 263:1003–1009.

Gehring, C., D. Flores-Rentería, C. M. Sthultz, T. M. Leonard, L. Flores-Rentería, A. V Whipple, and T. G. Whitham. 2014. Plant genetics and interspecific competitive interactions determine ectomycorrhizal fungal community responses to climate change. Molecular Ecology 23:1379–1391.

Ghimire, S. R., N. D. Charlton, J. D. Bell, Y. L. Krishnamurthy, and K. D. Craven. 2011. Biodiversity of fungal endophyte communities inhabiting switchgrass (*Panicum virgatum* L.) growing in the native tallgrass prairie of northern Oklahoma. Fungal Diversity 47:19–27.

Ghimire, S. R., and K. D. Craven. 2011. Enhancement of switchgrass (*Panicum virgatum* L.) biomass production under drought conditions by the ectomycorrhizal fungus *Sebacina vermifera*. Applied and Environmental Microbiology 77:7063–7067.

Giauque, H., and C. V Hawkes. 2013. Climate affects symbiotic fungal endophyte diversity and performance. American Journal of Botany 100:1435–1444.

Giauque, H., and C. V. Hawkes. 2016. Historical and current climate drive spatial and temporal patterns in fungal endophyte diversity. Fungal Ecology 20:108–114.

Greischar, M. A., and B. Koskella. 2007. A synthesis of experimental work on parasite local adaptation. Ecology Letters 10:418–434.

Hale, I. L., K. Broders, and G. Iriarte. 2014. A Vavilovian approach to discovering crop-associated microbes with potential to enhance plant immunity. Frontiers in Plant Science 5:492.

Hanson, C. A., J. A. Fuhrman, M. C. Horner-Devine, and J. B. H. Martiny. 2012. Beyond biogeographic patterns: processes shaping the microbial landscape. Nature Reviews Microbiology 10:497–506.

Hawlena, H., E. Rynkiewicz, E. Toh, A. Alfred, L. A. Durden, M. W. Hastriter, D. E. Nelson, R. Rong, D. Munro, Q. Dong, C. Fuqua, and K. Clay. 2013. The arthropod, but not the vertebrate host or its environment, dictates bacterial community composition of fleas and ticks. The ISME Journal 7:221–223.

Hereford, J. 2009. A quantitative survey of local adaptation and fitness trade-offs. American Naturalist 173:579–588.

Higgins, K. L., A. E. Arnold, P. D. Coley, and T. A. Kursar. 2014. Communities of fungal endophytes in tropical forest grasses: highly diverse host- and habitat generalists characterized by strong spatial structure. Fungal Ecology 8:1–11.

Hodgson, S., C. de Cates, J. Hodgson, N. J. Morley, B. C. Sutton, and A. C. Gange. 2014. Vertical transmission of fungal endophytes is widespread in forbs. Ecology and Evolution 4:1199–1208.

Howe, G. T., S. N. Aitken, D. B. Neale, K. D. Jermstad, N. C. Wheeler, and T. H. Chen. 2003. From genotype to phenotype: unraveling the complexities of cold adaptation in forest trees. Canadian Journal of Botany 81:1247–1266.

Johnson, M. T., and A. A. Agrawal. 2005. Plant genotype and environment interact to shape a diverse arthropod community on evening primrose (*Oenothera biennis*). Ecology 86:874–885.

Jumpponen, A., and K. L. Jones. 2010. Seasonally dynamic fungal communities in the *Quercus macrocarpa* phyllosphere differ between urban and nonurban environments. New Phytologist 186:496–513.

Kandalepas, D., M. J. Blum, and S. A. Van Bael. 2015. Shifts in symbiotic endophyte communities of a foundational salt marsh grass following oil exposure from the Deepwater Horizon oil spill. Plos One 10:e0122378.

Kaneko, R., and S. Kaneko. 2004. The effect of bagging branches on levels of endophytic fungal infection in Japanese beech leaves. Forest Pathology 34:65–78.

Kawecki, T. J., and D. Ebert. 2004. Conceptual issues in local adaptation. Ecology Letters

7:1225–1241.

Kleczewski, N. M., J. T. Bauer, J. D. Bever, K. Clay, and H. L. Reynolds. 2012. A survey of endophytic fungi of switchgrass (*Panicum virgatum*) in the Midwest, and their putative roles in plant growth. Fungal Ecology 5:521–529.

Lacap, D., K. Hyde, and E. Liew. 2003. An evaluation of the fungal "morphotype" concept based on ribosomal DNA sequences. Fungal Diversity 12:53–66.

Laforest-Lapointe, I., A. Paquette, C. Messier, and S. W. Kembel. 2017. Leaf bacterial diversity mediates plant diversity and ecosystem function relationships. Nature 546:145–147.

Laine, A.-L., J. J. Burdon, A. Nemri, and P. H. Thrall. 2014. Host ecotype generates evolutionary and epidemiological divergence across a pathogen metapopulation. Proceedings of the Royal Society B: Biological Sciences 281:20140522.

Legendre, P., and E. D. Gallagher. 2001. Ecologically meaningful transformations for ordination of species data. Oecologia 129:271–280.

Lowman, S., S. Kim-Dura, C. Mei, and J. Nowak. 2016. Strategies for enhancement of switchgrass (*Panicum virgatum* L .) performance under limited nitrogen supply based on utilization of N-fixing bacterial endophytes. Plant Soil 405:47–63.

Lowry, D. B., K. D. Behrman, P. Grabowski, G. P. Morris, J. R. Kiniry, and T. E. Juenger. 2014. Adaptations between ecotypes and along environmental gradients in *Panicum virgatum*. The American Naturalist 183:1–11.

Mejia, L. C., E. I. Rojas, Z. Maynard, S. Van Bael, A. E. Arnold, P. Hebbar, G. J. Samuels, N. Robbins, and E. A. Herre. 2008. Endophytic fungi as biocontrol agents of *Theombroma cacao* pathogens. Biological Control 46:4–14.

Nosil, P. 2004. Reproductive isolation caused by visual predation on migrants between divergent

environments. Proceedings of the Royal Society B: Biological Sciences 271:1521–1528.

Nuismer, S. L., J. N. Thompson, and R. Gomulkiewicz. 1999. Gene flow and geographically structured coevolution. Proceedings of the Royal Society B: Biological Sciences 266:605–609.

Oksanen, J., F. G. Blanchet, M. Friendly, R. Kindt, P. Legendre, D. McGlinn, P. R. Minchin, R. B. O'Hara, G. L. Simpson, P. Solymos, M. H. H. Stevens, E. Szoecs, and H. Wagner. 2017. "vegan" Community Ecology Package.

Del Olmo-Ruiz, M., and A. E. Arnold. 2014. Interannual variation and host affiliations of endophytic fungi associated with ferns at La Selva, Costa Rica. Mycologia 106:8–21.

Oono, R., F. Lutzoni, A. E. Arnold, L. Kaye, J. M. U'Ren, G. May, and I. Carbone. 2014. Genetic variation in horizontally transmitted fungal endophytes of pine needles reveals population structure in cryptic species. American Journal of Botany 101:1362–1374.

Papke, R. T., and D. M. Ward. 2004. The importance of physical isolation to microbial diversification. FEMS Microbiology Ecology 48:293–303.

Peay, K. G. 2014. Back to the future: natural history and the way forward in modern fungal ecology. Fungal Ecology 12:4–9.

Porras-Alfaro, A., and P. Bayman. 2011. Hidden fungi, emergent properties: endophytes and microbiomes. Annual Review of Phytopathology 49:291–315.

Roberts, D. W. 2016. "labdsv" Package: Ordination and Multivariate Analysis for Ecology.

Rodriguez, R. J., J. F. White Jr., A. E. Arnold, and R. S. Redman. 2009. Fungal endophytes: diversity and functional roles. The New Phytologist 182:314–330.

Rojas, E. I., S. A. Rehner, G. J. Samuels, S. A. Van Bael, E. A. Herre, P. Cannon, R. Chen, J. Pang, R. Wang, Y. Zhang, Y.-Q. Peng, and T. Sha. 2015. *Colletotrichum gloeosporioides*

s.l. associated with *Theobroma cacao* and other plants in Panama: multilocus phylogenies distinguish host-associated pathogens from asymptomatic endophytes. Mycologia 102:1318–1338.

Sapkota, R., K. Knorr, L. N. Jørgensen, K. A. O'Hanlon, and M. Nicolaisen. 2015. Host genotype is an important determinant of the cereal phyllosphere mycobiome. New Phytologist 207:1134–1144.

Shipunov, A., G. Newcombe, A. K. H. Raghavendra, and C. L. Anderson. 2008. Hidden diversity of endophytic fungi in an invasive plant. American Journal of Botany 95:1096–108.

Sullivan, T. J., and S. H. Faeth. 2004. Gene flow in the endophyte Neotyphodium and implications for coevolution with *Festuca arizonica*. Molecular Ecology 13:649–656.

U'Ren, J. M., J. W. Dalling, R. E. Gallery, D. R. Maddison, E. C. Davis, C. M. Gibson, and A. E. Arnold. 2009. Diversity and evolutionary origins of fungi associated with seeds of a neotropical pioneer tree: a case study for analysing fungal environmental samples. Mycological Research 113:432–449.

U'Ren, J. M., F. Lutzoni, J. Miadlikowska, A. D. Laetsch, and A. E. Arnold. 2012. Host and geographic structure of endophytic and endolichenic fungi at a continental scale. American Journal of Botany 99:898–914.

Urban, M. C. 2011. The evolution of species interactions across natural landscapes. Ecology Letters 14:723–732.

Vincent, J. B., G. D. Weiblen, and G. May. 2016. Host associations and beta diversity of fungal endophyte communities in New Guinea rainforest trees. Molecular Ecology 25:825–841.

Wang, B., J. R. Seiler, and C. Mei. 2016. A microbial endophyte enhanced growth of switchgrass

under two drought cycles improving leaf level physiology and leaf development. Environmental and Experimental Botany 122:100–108.

Warren II, R. J., and M. A. Bradford. 2014. Mutualism fails when climate response differs between interacting species. Global Change Biology 20:466–474.

Figures and Tables

Table 1 – Dufrene Legendre Indicator species associated with each host species.

	OTU	Putative Fungal Name	Indicator Group	Indicator Value	Significance
By Ecotype	20	*Hypoxylon spp.*	Madison	0.1368	*0.0935*
	21	*Unk. Ascomycota*	Fermi	0.1515	*0.0645*
By Site	1	*Glomerella spp.*	Madison	0.9502	*0.0001*
	2	*Alternaria spp.*	Fermi	0.8017	*0.0001*
	3	*Phaeosphaeria spp.*	Fermi	0.7999	*0.0001*
	4	*Cercospora apii*	Shawnee	0.4852	*0.0002*
	5	*Arthrinium phaeospermum*	Madison	0.7748	*0.0001*
	6	*Creosphaeria sassafras*	Shawnee	0.7083	*0.0001*
	7	*Hypoxylon perforatum*	Shawnee	0.4715	*0.0001*
	8	*Glomerella spp.*	Madison	0.4540	*0.0001*
	9	*Glomerella spp.*	Fermi	0.3913	*0.0001*
	10	*Khuskia spp.*	Fermi, Shawnee	0.2091, 0.1329	*0.0866*
	11	*Unk. Xylariaceae*	Shawnee	0.3273	*0.0044*
	12	*Lecythophora fasciculata*	Madison	0.2212	*0.0074*
	13	*Phoma spp.*	Fermi	0.3913	*0.0001*
	15	*Hypoxylon perforatum*	Shawnee	0.1983	*0.0236*
	16	*Hypoxylon investiens*	Madison	0.2078	*0.0164*
	17	*Whalleya microplaca*	Shawnee	0.2917	*0.0014*
	18	*Unk. Xylariaceae*	Shawnee	0.2917	*0.0006*
	21	*Unk. Ascomycota*	Fermi	0.2174	*0.0049*
	22	*Diaporthe spp.*	Shawnee	0.1667	*0.0300*
	23	*Annulohypoxylon truncatum*	Shawnee	0.2083	*0.0098*
	24	*Leptosphaerulina chartarum*	Fermi	0.1304	*0.0666*
	28	*Eupenicillium spp.*	Fermi	0.1304	*0.0572*

Operational taxonomic units (OTUs) with significant indicator values ($p < 0.10$) are listed in order of frequency of isolation (i.e., from common to rare). For 'unknown' taxonomic levels, the abbreviation '*Unk.*' is used.

Fig. 1. Average plant height (a) and tiller number (b) differed between ecotypes when grown in a common greenhouse environment prior to field transplantation. Each point represents an individual plant. Vertical lines depict the data range out to 1.5 times the interquartile range. Letters depict significant pairwise differences among groups in concordance with post-hoc analyses.

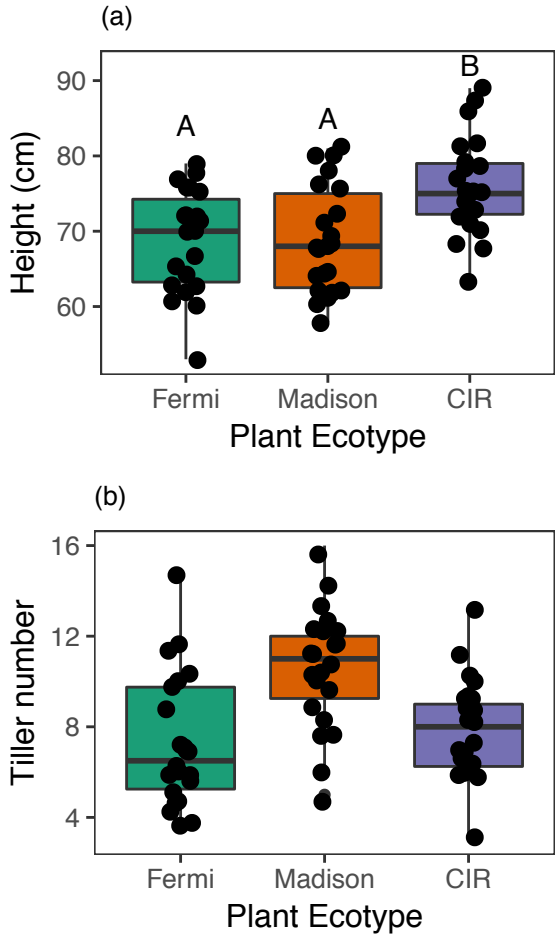

Fig. 2 – Relative abundance distribution for top ten most frequently isolated foliar fungal endophytes and species accumulation curves. In (a), the colored bars indicate the relative colonization per OTU across the three switchgrass ecotypes. In (b), the number of observed OTUs, the bootstrap estimate of total species richness (S), and the 95 % confidence interval (CI) around the estimated richness is shown for the overall experiment. In (c), the bootstrap estimate of species richness is shown for each site.

(*see next page*)

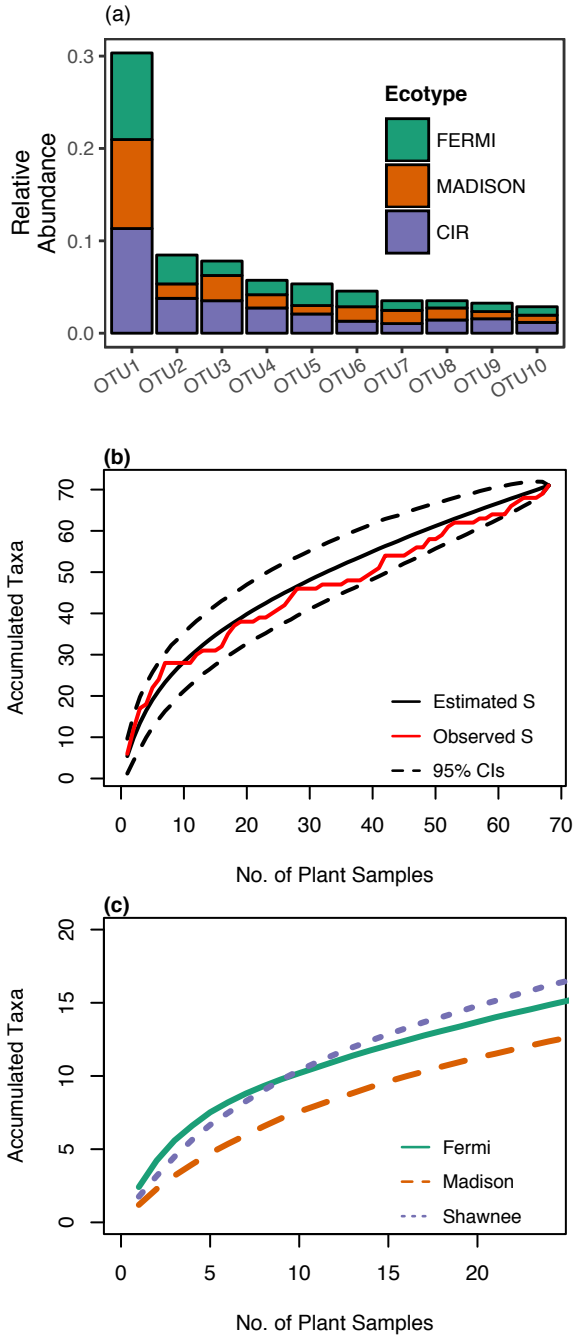
(a)
Relative Abundance
0.0
0.1
0.2
0.3
Ecotype
FERMI
MADISON
CIR
OTU1
OTU2
OTU3
OTU4
OTU5
OTU6
OTU7
OTU8
OTU9
OTU10
(b)
Accumulated Taxa
0
10
20
30
40
50
60
70
Estimated S
Observed S
95% CIs
No. of Plant Samples
(c)
Accumulated Taxa
0
5
10
15
20
Fermi
Madison
Shawnee
No. of Plant Samples

Fig. 3. FFE community richness (a,b) and Shannon diversity (c,d) varied by site, but not by ecotype. Each point represents an individual plant. Vertical lines depict the data range out to 1.5 times the interquartile range. Letters depict significant pairwise differences among groups in concordance with post-hoc analyses.

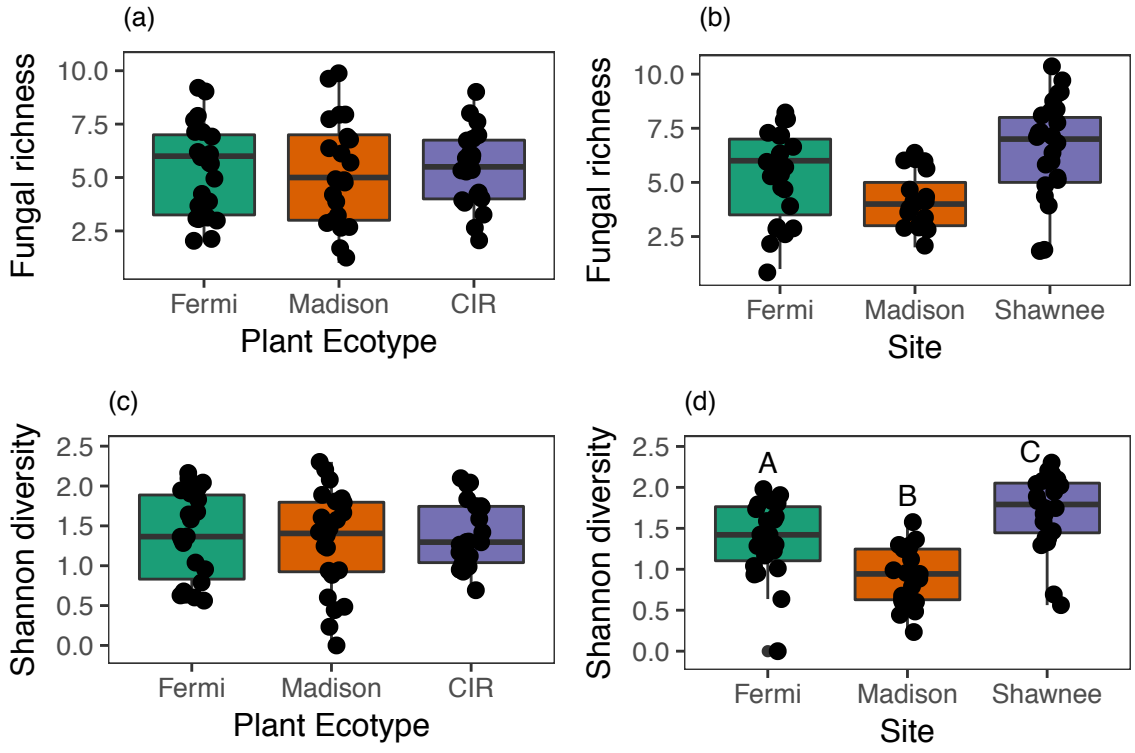

Fig. 4. FFE community structure did not vary by ecotype (a), but did vary by site (b). The location of each host individual in ordination space is denoted by a hatched circle. The ellipses represent the centroid and standard deviation for each treatment group (*green = Fermi, orange = Madison, purple = Shawnee/Cave-in-Rock for site [a] and ecotype [b]*).

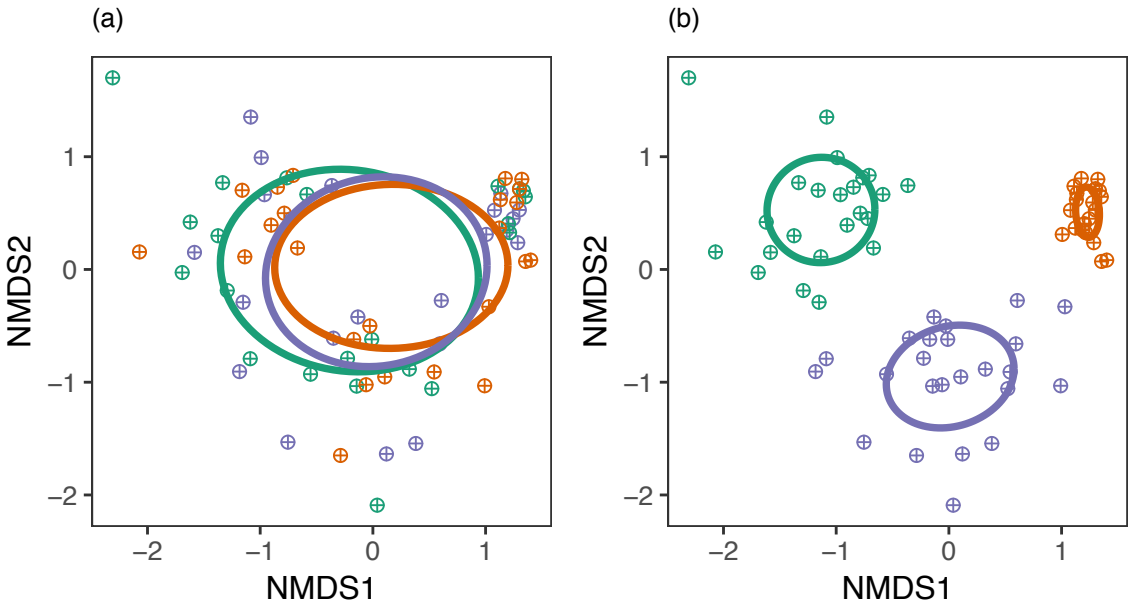

Fig. 5. Average plant height differed between ecotypes (A) and field site (B), and tiller number differs between ecotypes (C) at time of leaf collection. Each point represents an individual plant. Vertical lines depict the data range out to 1.5 times the interquartile range. Letters depict significant pairwise differences among groups in concordance with post-hoc analyses.

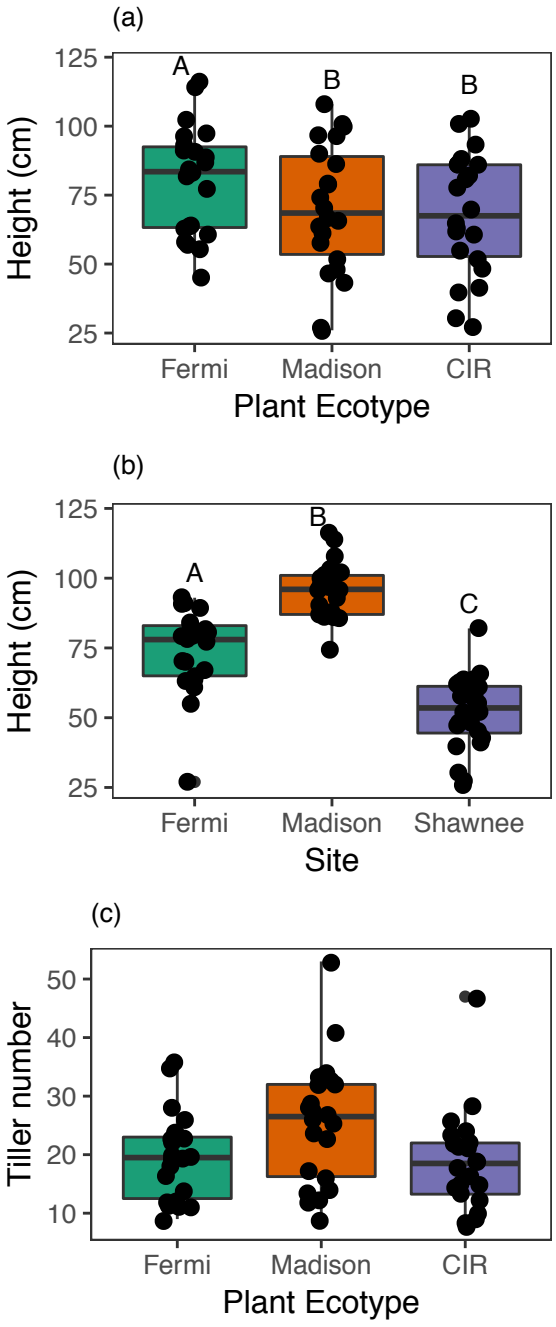

Supporting Information

Fig. S1. Map of field site physical locations. Labels indicate "M" for Madison IN, "F" for Fermi IL, and "S" for Shawnee

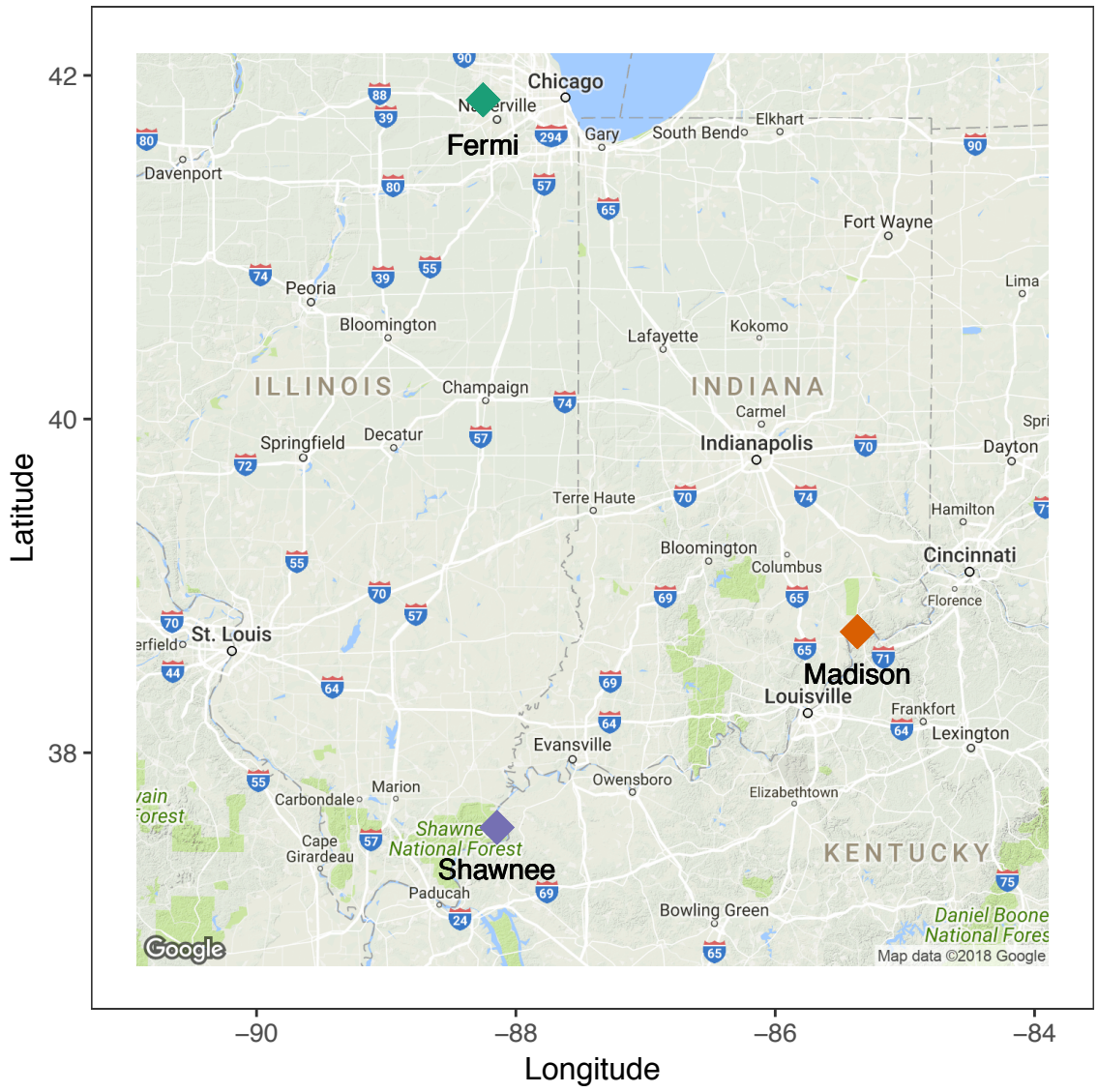

SI Methods

Description of Sites

Madison: Seed for the Madison ecotype was collected in 2008 by H. Reynolds from a riparian zone along the Ohio River in Madison, IN. The transplant plot used in this experiment was located within the Madison City Campgrounds on a 30-degree slope and 8m above the river waterline at the time of planting (38°43'54.2"N, 85°21'58.7"W). The soil type is a mixture of silt and gravel over the rocky shoreline and the resident plant community included *Sorghum halepense* (Johnson grass), *Cyperus esculentus* (Yellow Nutsedge), and *Ipomoea spp.* (Morning Glory), as well as switchgrass.

Fermi: The Fermi ecotype seed was also collected in 2008 by H. Reynolds from a restored tallgrass prairie in Batavia, IL. The prairie is managed by the Fermilab National Accelerator Laboratory (Fermilab). Land managers restored Fermilab Prairie Tract 23, the site used in this experiment (41°51'35.2"N, 88°15'10.9"W), in 2000 using locally-sourced seed from nearby natural areas – for example, from the Gensburg-Markham remnant prairies 106 kilometers away (Betz et al. 1996). The site is burned, as needed, on a seasonal basis. The resident plant community includes many prairie natives, such as switchgrass, *Helianthus grosseserratus* (Sawtooth Sunflower), *Monarda fistulosa* (Wild Bergamot), and *Andropogon gerardii* (Big Bluestem grass). The soil type is a silty clay loam.

Cave-In-Rock (CIR): Seed from the agricultural cultivar Cave-In-Rock (CIR) was also used in this experiment. CIR is an upland octoploid accession (Zalapa et al. 2011), released for use by the U.S. Department of Agriculture in 1973 with no history of breeding or selection (Casler et al. 2011). The accession was derived from a natural population of switchgrass from southern Illinois, although the precise location was not recorded, and is named for the nearby

town of Cave-In-Rock, IL surrounded by the Shawnee National Forest and Cave-In-Rock State Forest. We chose an old successional field located in Shawnee National Forest), located 11km from Cave-in-Rock, IL, as a surrogate historic home site for this ecotype (37°32'39.7"N, 088°08'43.3"W. The site has similar climatic (e.g., dry-episodic rain) and soil (e.g., clay-enriched subsoil) conditions to those identified by the USDA for the original CIR accession. The resident plant community surrounding the field plot used at Shawnee includes *Solidago spp.* (Goldenrod), *Daucus carota* (Queen Anne's Lace), and several other genera of grasses, and is also periodically burned.

Molecular Methods

Total genomic DNA was extracted from fresh mycelium using the PowerPlant® Pro DNA Isolation Kit (MO BIO Laboratories, Carlsbad, CA, USA) following the manufacturer's instructions, save for changes to the tissue homogenization step (MP Biomedicals FastPrep®-24 Tissue Homogenizer, Solon, OH; once at 4m/s for 60sec). The fungal Internal Transcribed Spacer (ITS) region (ITS1, 5.8S rRNA subunit, and ITS2) was amplified via PCR using the fungal-specific primers ITS5 and ITS4 (White et al. 1990). PCR was performed using GoTaq® DNA Polymerase (Promega Corporation, Madison, WI, USA) as per manufacturer's recommendations, in a 25 µL reaction with 1 µL of sample template. A Tetrad PTC-225 Peltier Thermal Cycler (MJ Research, MA, USA) was used for PCR reactions, with the thermal cycler program recommended by Promega: 2.5 min at 95°C, followed by 25 cycles (30 s at 95°C, 30 s at 60.2°C, 45 s at 72°C), then 5 min at 72°C. Gel electrophoresis with Sybr® Safe (Invitrogen, Eugene, OR, USA) stain was used to check for contamination and visualize successful amplification. Amplicons were then purified using the MicroElute® Cycle-Pure Kit (Omega

Bio-Tek, Inc., GA, USA) following manufacturer's instructions. Forward (ITS5) and reverse (ITS4) sequencing was performed on the purified DNA product using BigDye Terminator v3.1 with the Applied Biosystems 3730 Genetics Analyzer at the Indiana Molecular Biology Institute at Indiana University.

References for SI Methods

Betz, R. F., R. J. Lootens, and M. K. Becker. 1996. Two decades of prairie restoration at Fermilab Batavia, Illinois. Page No. FERMILAB-CONF-96-440.

Casler, M. D., C. M. Tobias, S. M. Kaeppler, C. R. Buell, Z.-Y. Wang, P. Cao, J. Schmutz, and P. Ronald. 2011. The Switchgrass genome: tools and strategies. The Plant Genome 4:273–282.

White, T. J., T. Bruns, S. Lee, and J. Taylor. 1990. Amplification and direct sequencing of fungal ribosomal RNA genes for phylogenetics. Pages 315–322*in* M. Innis, D. Gelfland, J. Sninsky, and T. White, editors.PCR protocols: A guide to methods and applications. Academic Press, San Diego.

Zalapa, J. E., D. L. Price, S. M. Kaeppler, C. M. Tobias, M. Okada, and M. D. Casler. 2011. Hierarchical classification of switchgrass genotypes using SSR and chloroplast sequences: ecotypes, ploidies, gene pools, and cultivars. Theoretical and Applied Genetics 122:805–817.

Table S1. Site-level climate details. Site-level precipitation (prcp.) in inches, maximum daily temperature (T_{max}) in Fahrenheit and minimum daily temperature (T_{min}) in Fahrenheit. Sums and averages of precipitation and temperature, respectively, begin from the day of planting at each site, which is shown by etched shading of table cells.

Midwestern Regional Climate Center - cli-MATE: MRCC Application Tools Environment									
Station Name	**WEST CHICAGO DUPAGE AP (IL)**			**ROSICLARE 5 NW (IL)**			**CLIFTY CREEK (IN)**		
Station ID	**USW00094892**			**USC00117487**			**USC00121615**		
Ecotype/ Site	**Fermi**			**Shawnee/CIR**			**Madison**		
Date	**Prcp. (in)**	**T_{max} (F)**	**T_{min} (F)**	**Prcp. (in)**	**T_{max} (F)**	**T_{min} (F)**	**Prcp. (in)**	**T_{max} (F)**	**T_{min} (F)**
6/28/14	0.01	87	71	0.06	82	68	0.62	M	M
6/29/14	0.28	86	69	T	84	68	0.03	M	M
6/30/14	1.83	87	67	T	77	69	0.12	M	M
7/1/14	T	80	66	0	88	73	0.00	M	M
7/2/14	0.22	69	57	0.91	87	67	0.45	M	M
7/3/14	0.06	77	53	0	80	57	0.06	M	M
7/4/14	0	82	56	0	71	54	0.00	M	M
7/5/14	0.03	77	58	0	79	51	0.00	M	M
7/6/14	0	87	62	0	81	54	0.00	M	M
7/7/14	0.27	86	70	0	83	60	0.00	M	M
7/8/14	0.1	82	65	0.06	88	68	0.06	M	M
7/9/14	0	80	59	0	83	62	0.00	M	M
7/10/14	0	82	55	0	85	63	0.00	M	M
7/11/14	0	81	57	0	83	59	0.00	M	M
7/12/14	1.1	80	69	0	87	61	0.00	M	M
7/13/14	0	85	67	0	87	67	0.00	M	M
7/14/14	0.23	79	57	0.38	91	69	1.21	M	M
7/15/14	T	69	53	0	84	60	0.34	M	M
7/16/14	0	74	51	0	75	51	0.00	M	M
7/17/14	0	79	52	0	76	52	0.00	M	M
7/18/14	0	81	56	0	78	53	0.00	M	M
7/19/14	0	83	54	0	79	57	0.00	M	M
7/20/14	0	81	58	0	78	55	0.00	M	M
7/21/14	0	85	60	0	81	56	0.00	M	M

7/22/14	0.16	91	67	0	87	57	0.00	M	M
7/23/14	0	77	53	0	91	63	0.00	M	M
7/24/14	0	77	52	0.49	76	54	0.04	M	M
7/25/14	T	74	53	0	79	53	0.00	M	M
7/26/14	T	83	66	0	78	56	0.12	M	M
7/27/14	0.01	86	64	0	90	60	0.03	M	M
7/28/14	0	73	57	0	91	61	2.38	M	M
7/29/14	T	81	55	0	79	50	0.00	M	M
7/30/14	0	80	58	0	79	51	0.00	M	M
7/31/14	0	83	57	0	80	55	0.00	M	M
8/1/14	T	85	57	0	83	56	0.00	M	M
8/2/14	0	86	56	0	84	62	0.00	M	M
8/3/14	0	87	62	0	85	60	0.00	M	M
8/4/14	0.66	87	63	0	86	59	0.00	M	M
8/5/14	0	83	63	0	88	59	0.00	M	M
8/6/14	0	82	59	0	88	60	0	M	M
8/7/14	0	82	58	0	89	65	0	M	M
8/8/14	0	83	62	0.75	83	68	0	M	M
8/9/14	0	81	62	0.02	79	68	0.2	M	M
8/10/14	T	85	64	0	86	69	0	M	M
8/11/14	1.41	84	66	0.25	86	69	0	M	M
8/12/14	0.25	72	59	0	83	65	0.1	M	M
8/13/14	0	82	53	0	80	53	0	M	M
8/14/14	M	76	53	0	81	53	0	M	M
8/15/14	0	79	50	0	84	53	0.1	M	M
8/16/14	0	81	58	0	85	57	0	M	M
8/17/14	0	77	61	1.23	M	M	0	M	M
8/18/14	0	83	64	M	M	M	0.1	M	M
8/19/14	T	86	67	M	M	M	0	M	M
8/20/14	0.01	86	62	M	M	M	0	M	M
8/21/14	1.38	81	70	M	M	M	0.09	M	M
8/22/14	1.7	86	73	M	M	M	0.02	M	M
8/23/14	0.15	86	67	M	M	M	0	M	M
8/24/14	T	89	67	M	M	M	0.89	M	M
8/25/14	T	88	69	M	M	M	0	M	M
8/26/14	0.02	87	68	M	M	M	0	M	M
8/27/14	0	84	63	M	M	M	0	M	M
8/28/14	0.09	81	63	M	M	M	0	M	M
8/29/14	T	87	69	0.09	90	67	0	M	M

8/30/14	0.19	83	68	0	91	67	0	M	M
8/31/14	0	85	68	0.52	79	70	0.14	M	M
9/1/14	0.06	83	68	0.02	83	70	0	M	M
9/2/14	T	82	63	0	82	72	0.32	M	M
9/3/14	0	84	58	0	84	63	M	M	M
9/4/14	0.23	84	70	0	86	63	0	M	M
9/5/14	0.06	88	63	0	90	64	0	M	M
9/6/14	0	76	56	0.04	91	67	0	M	M
9/7/14	0	82	52	0	73	57	0	M	M
9/8/14	0	78	54	0	80	54	0	M	M
9/9/14	0.04	80	62	0	83	53	0	M	M
9/10/14	1.41	81	54	0	84	54	0	M	M
9/11/14	0	54	49	0.9	87	64	0.93	M	M
9/12/14	M	M	M	M	M	M	0.2	M	M
	Sum	**Avg.**	**Avg.**	**Sum**	**Avg.**	**Avg.**	**Sum**	**Avg.**	**Avg.**
	9.16	81.9	60.9	7.83	83.3	60.5	8.06	NA	NA

Table S2. Table of all FFE species, there overall isolation count, and putative taxonomic assignment based on the Warcup Fungal ITS Training Set. Taxonomic confidence is provided.

OTU	Count	Warcup Best Match	Confidence (%)
1	233	Glomerella magna	49%
2	65	Alternaria longipes	59%
3	60	Phaeosphaeria sp.	97%
4	44	Cercospora apii	100%
5	41	Arthrinium phaeospermum	100%
6	35	Creosphaeria sassafras	100%
7	27	Hypoxylon perforatum	100%
8	27	Colletotrichum clavatum	74%
9	25	Colletotrichum metake	25%
10	22	Nigrospora oryzae	92%
11	19	Hypoxylon monticulosum	80%
12	12	Lecythophora fasciculata	100%
13	11	Phoma epicoccina	70%
14	11	Glomerella cingulata	37%
15	10	Hypoxylon perforatum	100%
16	10	Hypoxylon investiens	100%
17	9	Whalleya microplaca	100%
18	7	Xylaria bambusicola	51%
19	7	Daldinia childiae	100%
20	6	Hypoxylon lenormandii	88%
21	6	Scolecobasidium terreum	48%
22	5	Diaporthe stewartii	92%
23	5	Annulohypoxylon truncatum	97%
24	4	Leptosphaerulina chartarum	100%
25	4	Daldinia loculata	29%
26	4	Cladosporium rectoides	47%
27	3	Exserohilum rostratum	100%
28	3	Penicillium commune	46%
29	2	Podospora myriaspora	89%
30	2	Kabatiella bupleuri	42%
31	2	Curvularia trifolii	100%
32	2	Mycoleptodiscus indicus	99%
33	2	Hypoxylon rubiginosum	99%
34	2	Bipolaris oryzae	85%

35	2	Pestalotiopsis yunnanensis	23%
36	2	Rosellinia corticium	100%
37	2	Phaeosphaeria oryzae	92%
38	2	Hypoxylon rubiginosum	44%
39	1	Phoma paspali	100%
40	1	Colletotrichum chlorophyti	100%
41	1	Biscogniauxia atropunctata	100%
42	1	Myrothecium prestonii	9%
43	1	Hypoxylon macrocarpum	100%
44	1	Xylaria persicaria	100%
45	1	Cercophora coprophila	14%
46	1	Sporisorium mishrae	85%
47	1	Lecythophora fasciculata	84%
48	1	Whalleya microplaca	87%
49	1	Xylaria hypoxylon	52%
50	1	Hypoxylon howeanum	65%
51	1	Plectosphaerella cucumerina	100%
52	1	Xylaria venosula	97%
53	1	Penicillium brevicompactum	100%
54	1	Nemania sp.	100%
55	1	Hypoxylon anthochroum	50%
56	1	Nemania diffusa	100%
57	1	Arthrinium arundinis	100%
58	1	Colletotrichum sansevieriae	99%
59	1	Paraphaeosphaeria michotii	100%
60	1	Hypoxylon investiens	53%
61	1	Pseudozyma rugulosa	91%
62	1	Xylaria sp.	49%
63	1	Neosetophoma samarorum	64%
64	1	Fusarium equiseti	79%
65	1	Chaetomium globosum	50%
66	1	Lambertella advenula	30%
67	1	Xylaria venosula	100%
68	1	Annulohypoxylon truncatum	100%
69	1	Biscogniauxia mediterranea	100%
70	1	Daldinia loculata	44%
71	1	Epicoccum sorghi	100%

Table S3. Comparison of genera in common with three switchgrass fungal endophyte studies.

Fungal Genus	**Whitaker *et al.* OTU #**	**Ghimire *et al.* (2011)**	**Giauque & Hawkes (2013)**	**Kleczewski *et al.* (2012)**
Alternaria	2	Yes	Yes	Yes
Annulohypoxylon	23,68			
Arthrinium	5,57			
Biscogniauxia	41,69			
Chaetomium	65		Yes	
Cochliobolus	34	Yes (as Bipolaris)	Yes	
Creosphaeria	6			
Curvularia	31		Yes	
Daldinia	19,25			
Davidiella	26	Yes (as Cladosporium)	Yes (as Cladosporium)	Yes (as Cladosporium)
Diaporthe	22			
Epicoccum	71		Yes	Yes
Eupenicillium	28	Penicillium	Penicillium	
Gibberella	64	Yes (as Fusarium)	Yes (as Fusarium & Giberella)	Yes (as Fusarium)
Glomerella	1,8,9,14,40,58	Yes (as Colletotrichum)		Yes (as Colletotrichum
Hypoxylon	7,15,16,20,33,38,43,50,55			
Kabatiella	30			
Khuskia	10	Yes (as Nigrospora)	Yes (as Nigrospora & Khuskia)	Yes (as Nigrospora)
Lecythophora	12			
Leptosphaerulina	24		Yes	
Mycoleptodiscus	32			
Mycosphaerella	4			
Nemania	54,56			Yes
Paraphaeosphaeria	59			

Penicillium	53	Yes	Yes	
Phaeosphaeria	3	Yes		Yes
Phoma	13,39	Yes	Yes	Yes
Plectosphaerella	51			
Podospora	29		Yes	
Pseudozyma	61	Yes		
Rosellinia	36			
Setosphaeria	27	Yes (as Exserohilum)		
Sporisorium	46	Yes		
Whalleya	17			
Xylaria	44,49,52,67			Yes

This comparison was derived from Ghimire *et al.* 2011 (Fig. 1a), Giauque & Hawkes 2013 (Appendix 1), and Kleczewski *et al.* 2012 (Table 2). There were differences among these studies and our work in the fungal databases and classification software used to assign putative species names. Additionally, since initial publication there has likely been changes in the understanding of fungal systematics and the usage of anamorph and teleomorph naming systems. Therefore, for consistency, only information down to the fungal genus is presented and, where relevant, differential use of ana- and teleomorph classification is indicated.

Title: "Phylogenetic relatedness of Asteraceae hosts predicts foliar microbiome community structure in a common garden environment"

Running Title: Plant-microbiome driven by host phylogeny

Authors: Briana K. Whitaker (BKW)[1*], Natalie Christian (NC)[1], Qing Chai (QC)[12], Keith Clay (KC)[1]

[1] Department of Biology, Indiana University, Bloomington, IN

[2] School of Pastoral Agriculture Science and Technology, Lanzhou University, Lanzhou, China

Emails: brkawhit@indiana.edu; nschrist@indiana.edu; qingchai@indiana.edu; clay@indiana.edu

Author for correspondence: Briana K. Whitaker

Address: Department of Biology, Jordan Hall, 1001 E. 3rd St, Indiana University, Bloomington, IN, 47405-3700; Tel: (+1) 8128551674; Fax: (+1) 8128556705; Email: brkawhit@indiana.edu

Keywords: fungal endophytes, horizontal transmission, biodiversity, host specificity, Composites, Illumina sequencing

Article Type: Original Article; **Word Count:** Abstract (231), Main Text (5741), Introduction (956), Materials and Methods (2755), Results (708), Discussion (1322); **Number of:** References (63), Figures (6), Color Figures (4), Tables (2), Text Boxes (0)

ABSTRACT

Foliar fungal endophytes (FFE) are increasingly being used to address basic ecological and evolutionary questions about host-associated microbiomes. Phylogenetic distance among host species could represent a useful proxy for host traits that act as biotic filters to shape FFE community structure. However, teasing apart biotic from abiotic assembly mechanisms in these hyperdiverse, horizontally-transmitted microbial communities remains a challenge. In this study, we tested whether host phylogenetic relatedness among 18 native Asteraceae species and spatial distance between host individuals across replicated plots in a common garden affects FFE community structure. We found that FFE community structure varied significantly among host species and marginally among plots within the common garden, but not among individuals with differing leaf mass per area. FFE community dissimilarity between host individuals was significantly and positively correlated with the phylogenetic distance between host species, as well as with spatial distance among host individuals in the common garden. These results indicate that both more phylogenetically related hosts and more spatially proximate hosts shared more similar FFE communities, though the magnitude of the host phylogenetic effect was stronger than the spatial effect. Further, we found that FFE community diversity per unit leaf mass varied significantly among host species. These results demonstrate a significant role for host phylogenetic relatedness in shaping the plant endophyte microbiome in native Asteraceae and, more generally, have important implications for the structure and evolution of host-associated microbiomes.

INTRODUCTION

Studies on microbial communities and host-microbiome interactions have expanded dramatically over recent decades (Alivisatos et al. 2015). Research across plant and animal systems has revealed a wide range of taxonomic and functional diversity in their microbiomes (Christian et al. 2015). It is now widely recognized that microorganisms have been intimately associated with higher organisms from all ecological habitats for millennia (Krings et al. 2007, Ley et al. 2008). Despite the persistence and longevity of these symbioses over evolutionary time, the fact that most microbiota colonize hosts via horizontal transmission from the local environment raises the question of whether these interactions can be considered as co-evolved or co-adapted (Christian et al. 2017). In other words, do environmentally-acquired microbiota track the phylogenetic relatedness of their hosts when closely related species and genera co-occur?

Host-associated microbiomes are assembled and maintained via multiple mechanisms that act across a wide range of spatial and temporal scales. At the local level, bacterial and fungal symbionts may compete for common resources, or to gain entry and occupy a particular spatial niche within the host (Hooper et al. 2012). Co-occurring symbionts may also experience apparent competition via other predatory microbes within the host (Sharon et al. 2013), or from the host immune system itself (Hooper et al. 2012). Phenotypic traits, such as host size, chemistry, and morphology, can also influence microbial colonization (Laforest-Lapointe et al. 2017). Microbiota can disperse locally via propagules in the host's environment, including from other types of hosts (e.g., other plants, humans, pets, etc.; Azad *et al.* 2013; Parker *et al.* 2015), or from nearby abiotic sources (e.g., soil, water) and food (Hanson et al. 2012, Leff and Fierer 2013). Variation in disturbance or climatic conditions over time can also influence the persistence and abundance of microbial taxa in hosts after initial colonization (Shade et al. 2014). At the regional

scale, dispersal and extinction events of microbial taxa across host populations (Hanson et al. 2012) and geographic differences in environmental or climatic conditions (Giauque and Hawkes 2013) can have important consequences for microbial community composition and stability.

Because the richness, diversity, and structure of horizontally-transmitted microbial communities are shaped by mechanisms acting across such a wide range of spatial and temporal scales, it has been difficult to disentangle the role of evolutionary history in these symbioses from more contemporary ecological mechanisms (e.g., biotic interactions, dispersal limitation). Previous studies across a wide variety of plant-associated microbiomes have provided contrasting roles for host phylogenetic relatedness in structuring the host microbiome. For example, the probability of host jumping onto non-native, introduced hosts by foliar pathogens in grassland communities can be predicted by the phylogenetic relatedness and population densities of individual species within the resident, native plant community (Parker et al. 2015). On the other hand, the compatibility of viral species can be more restricted by host species identity (Seabloom et al. 2013). Among mutualistic plant-microbial associations, there is also evidence that root endophyte communities are strongly shaped by host phylogenetic relatedness, and secondarily by spatial distance between host plants in grassland communities (Wehner et al. 2014). Similarly, host species identity can drive the structure of foliar bacterial communities among forest tree species (Laforest-Lapointe et al. 2017). By contrast, another study found no evidence that host phylogenetic relatedness affected foliar fungal endophyte (FFE) community structure across a 50-ha tropical forest plot (Vincent et al. 2016).

FFE are a major component of the plant microbiome, and have recently emerged as a useful system for addressing basic evolutionary and ecological questions due to their relative tractability under laboratory conditions and ease of cultivation. FFE have existed within plant

hosts since land colonization (Krings et al. 2007), and can act as mutualists, commensalists, pathogens, or saprotrophs (Busby et al. 2016). Most FFE colonize via environmentally-transmitted propagules from wind, rain or the previous season's plant litter (reviewed in Christian *et al.* 2015). Previous research has provided evidence of FFE specificity to host genotypes in common gardens (Bálint et al. 2015) and to host species growing in mixed communities (Gange et al. 2007). By contrast, in other studies FFE community structure was more strongly driven by dispersal limitation with increasing spatial distance (Higgins et al. 2014, Eusemann et al. 2016) than by host genotype or host species identity in mixed communities. Detecting phylogenetic drivers of FFE community structure in nature may be difficult given the high spatial (David et al. 2015) and temporal turnover of microbial communities (Shade et al. 2014). Thus, experiments that use an explicit host phylogenetic approach and account for broad differences in spatial and temporal sampling would be the best test of these contrasting drivers.

Here we investigated the roles of phylogenetic relatedness and spatial distance between individual hosts on FFE community richness, diversity, and structure in a multispecies common garden. Specifically, we tested (i) whether host species specificity predicted the structure of FFE communities and (ii) whether FFE community dissimilarity correlated with phylogenetic divergence among host taxa. Additionally, we tested (iii) whether spatially proximate host plants shared more similar FFE communities and (iv) whether FFE community structure was affected by host leaf mass per unit area, after controlling for host species identity. Lastly, we also tested whether FFE community richness and diversity differed among host species and among plants in different locations in the common garden. To answer these questions, we used a common garden approach to control for confounding spatial and temporal factors, such as regional-scale changes in environmental and climatic conditions, dispersal limitation of FFE, and host developmental

age, by spatially randomizing all species or varieties under similar growth conditions (Kawecki and Ebert 2004). Furthermore, we focused on native species from within a single plant family, the Asteraceae, as a conservative test of the impact of phylogenetic relatedness on FFE communities.

MATERIALS AND METHODS

Study System

To characterize host-FFE interactions within a phylogenetic framework, we analyzed FFE communities of native perennials within the family Asteraceae. With close to 24,000 recognized species, it is the largest family of vascular plants and represents 10% of all flowering plants (Funk et al. 2009). Adaptive radiations and geographic spread out of South America has extended the natural range of the Asteraceae to every continent except Antarctica (Funk et al. 2009). Previous classifications segregated the Asteraceae into five major lineages, but recent phylogenetic analyses support twelve subfamilies, with the most basal clades being either wholly endemic, or largely constrained, to South America (Panero and Funk 2008). FFE have previously been cultured from species of Asteraceae (Christian et al. 2016) and a comparison of FFE communities between two host species from co-occurring genera of Asteraceae growing in southern England showed host-specific differences in FFE diversity and abundance for particular fungal taxa (Gange et al. 2007).

Species Selection and Plant Propagation

Replicate individuals from 28 species that spanned a wide phylogenetic range within the Asteraceae (Funk et al. 2009) were planted into replicated plots within the common garden. Two outgroup species were also chosen from the Campanulaceae, which is a sister family to the Asteraceae within the order Asterales (Table 1). Priority was given to species that: 1) had more

highly resolved taxonomic placement, 2) were perennial and native to Indiana (IN), USA, and 3) had provinciality in southern IN (which is biogeographically divergent from northern IN) or that had a contiguous distribution across the entire state of IN.

Seeds of the selected species were purchased from Prairie Moon Nursery (Winona, MN) and cold stratified as necessary according to vendor specifications using pasteurized sand and sterile water. The seeds were then germinated under common greenhouse conditions in 20.3cm x 20.3cm square flats filled with commercial potting mix (Metro-Mix 360, Sun Gro Horticulture, Agawam, MA), which was first sterilized by autoclaving for four hours. Two to three weeks after germination, seedlings were transplanted into conetainers™ (Stuewe & Sons, Yellow (U), RLC3, Tangent, OR) filled with sterilized Metro-Mix. After 5-6 weeks of growth under greenhouse conditions, plants were then transplanted into the common garden.

Common Garden

The common garden was established in April and May 2014 at the Indiana University Research and Teaching Preserve Bayles Road field site in Bloomington, IN (N 39.217, W -86.540; Supporting Information [SI] Figure S1). Bayles Road is a former agricultural field that has been used for ecological research for the last 20 years. The site has many resident Asteraceae species that could serve as potential FFE inoculum sources for experimental plants (personal observation). To reduce the growth of weeds and to facilitate seedling establishment, we employed weed reduction strategies prior to transplanting experimental plants. Specifically, all common garden plots were first mowed, sprayed twice over two days with a glyphosate-based herbicide at a 1.5% rate (Aquamaster; Monsanto Co., St. Louis, MO), and then tilled two times after plant dieback. To further minimize weed growth, black landscaping cloth (Hummert International, Earth City, MO) was spread across the tilled soil and secured using 15.2 cm metal

staples. These weed reduction strategies were applied across all plots and all experimental plants were treated identically. Six 9.1 m x 7.0 m plots were established in a paired plot design, with the three sets of paired plots located at the northern, central, or southern regions of the Bayles Road field site (SI Figure S1). Paired plots were used to provide replication for potential spatial effects, as well as to separate spatial effects from local site effects. Each plot within a pair was spaced at least 13 m apart. Planting arrangement for replicate individuals of all 30 species was randomized across plots, with three replicate individuals per species per plot in a full-factorial experimental design (i.e., Host Species x Plot; Total N=540). All plants were planted in a rectangular grid, with 0.91 m spacing lengthwise and 0.76 m spacing crosswise between plants. Immediately after transplantation, each plant received 0.5 L of liquid fertilizer ([3.91mL/L-H_2O], Jack's Classic All Purpose 20-20-20, JR Peters Inc., Allentown PA) to improve initial establishment in the field, after which no additional watering or fertilization was applied. When necessary, plots were hand-weeded and individual transplants protected from small mammal herbivory with wire mesh exclosures (a cylinder 15 cm tall, with 1 cm^2 mesh size).

Leaf Collection, Sterilization, and Sample Preparation

In September 2014, after three months of growth and exposure to natural sources of endophyte inocula, leaves were harvested for FFE sampling. We then used culture-independent Illumina sequencing to identify FFE taxa across hosts in our common garden, independent of visible symptoms of colonization. For this study, a subset of 19 species were chosen (18 Asteraceae, 1 Campanulaceae; Table 1), with one replicate individual per species per plot randomly selected (N=6 per species and N=114 total plants sampled). To minimize differences in sampling method among the 19 host species, which varied widely in height, growth architecture (i.e., rosette vs. upright), and leaf size, three leaves per plant (or leaf sub-sections from large-

leaved plant species) were carefully selected from mid-stem height. Leaf samples were then stored at 4˚C until processing, which occurred within 24hrs of collection. Two additional leaf disks (1cm diameter) were sampled from similar, proximate leaves within the same plant 3-4 weeks after collecting samples for Illumina sequencing, oven-dried at 60˚C for three days, and weighed to determine Leaf Mass per Area (LMA). Leaves for Illumina sequencing were cut into 0.5 x 0.5 cm square fragments and then nine fragments per individual plant were haphazardly selected for surface sterilization. Leaf fragments were surface sterilized for 3 min in 70% ethanol, 2 min in 0.5% sodium hypochlorite, 1 min in sterile water, and then allowed to air dry for 1 min (Mejía et al. 2008). Surface-sterilized leaf fragments were then placed in sterile 2 mL microcentrifuge tubes, flash frozen in liquid nitrogen, and stored at -80˚C.

All nine leaf fragments per individual host plant were bulked and DNA was extracted using the PowerPlant® Pro DNA Isolation Kit (MO BIO Laboratories, Carlsbad, CA, USA) following the manufacturer's instructions, save for changes to the tissue homogenization step (MP Biomedicals FastPrep®-24 Tissue Homogenizer, Solon, OH; twice at 4m/s for 60sec). Due to low quality DNA extractions for certain samples, we modified the extraction protocol following manufacturer's instructions to include 40 µL of Phenolic Separating Solution and 250 µL of solution PD3 (see Dryad repository for specific sample IDs).

Nested PCR was used to improve fungal amplicon yields based on preliminary tests in this Asteraceae host system, where a single round of PCR amplification typically failed to yield enough abundant, high quality Illumina reads. First, primers NSA3 and NLC2 (Martin and Rygiewicz 2005) were used to amplify an ~1000 bp region surrounding the internal transcribed spacer (ITS) region (SSU, ITS1, 5.8S, ITS2, and LSU) of the fungal nuclear ribosomal DNA gene via PCR using GoTaq® DNA Polymerase (Promega Corporation, Madison, WI, USA) as

per the manufacturer's recommendations in a 25 µL reaction with 1 µL of template diluted 1:10 in PCR-grade water. A Tetrad PTC-225 Peltier Thermal Cycler (MJ Research, MA, USA) was used for PCR reactions, with the thermal cycler program recommended by Promega: 2.5 min at 95°C, followed by 25 cycles (30 s at 95°C, 30 s at 60.2°C, 45 s at 72°C), then 5 min at 72°C. Amplicons were purified using the MicroElute® Cycle-Pure Kit (Omega Bio-Tek, Inc., GA, USA) and sent to the Biosciences Division (BIO) Environmental Sample Preparation and Sequencing Facility (ESPSF) at Argonne National Laboratory (ANL) for sequencing on the Illumina MiSeq platform. At ANL, products of the first PCR were amplified using a modified version of the fungal-specific ITS1F and ITS2 primer set (Smith and Peay 2014). The reverse amplification primer also contained a twelve-base barcode sequence that supports pooling of up to 2,167 different samples in each lane (Caporaso et al. 2010, 2012). Each 25 µL PCR reaction consisted of 9.5 µL of MO BIO PCR Water (Certified DNA-Free), 12.5 µL of QuantaBio AccuStart II PCR ToughMix (2x concentration, 1x final), 1 µL Golay barcode tagged Forward Primer (5 µM concentration, 200 pM final), 1 µL Reverse Primer (5 µM concentration, 200 pM final), and 1 µL of template DNA. Amplification was performed as follows: 3 min at 94°C, followed by 35 cycles (45 s at 94°C for, 60 s at 50°C, 90 s at 72 °C), 10 min at 72 °C.

Amplicon concentrations were quantified using PicoGreen (Invitrogen), pooled at equal-molar concentrations, cleaned using AMPure XP Beads (Beckman Coulter), and quantified using Qubit (Invitrogen). After quantification, the pool was first diluted to 2nM, denatured, and then diluted to 6.75pM with a 10% PhiX spike for paired 251-nuceotide read sequencing on the Illumina MiSeq platform. To exclude the PhiX control reads from downstream analysis, the first read of all read pairs was mapped against a PhiX reference using BWA (v.0.6.2-r126). All reads that successfully mapped to the PhiX reference were discarded. A custom Perl script was used to

demultiplex samples from the pooled sequence data. All resulting paired forward and reverse sequence reads were merged to create a single contig using Mothur (v.1.37.1) for workflow management. Resulting contigs with ambiguous bases, or with lengths greater than 350 bp, were removed as part of quality filtering. Chimeras were removed (UCHIME v.4.2.40) and reads were clustered (AbundantOTU+ v.0.93b) at 95% and 97% sequence similarity into Operational Taxonomic Units (OTUs). Eight samples either had poor quality DNA extractions or read counts of less than 10,000 and were thus removed prior to clustering, leaving N=106 individual hosts across 19 plant species for the community analyses.

Putative names were assigned to each OTU using the RDP naïve Bayesian classifier (v.2.12) and the Warcup fungal ITS database (Deshpande et al. 2015). Results from this classification, along with confidence thresholds for each level in the taxonomic hierarchy, are presented in SI Table S1. Statistical analyses did not differ substantially between the 95% and 97% sequence identity datasets, therefore only results for the 95% OTU threshold are presented here. Following initial assessment of the sequence data, we dropped observations from our FFE community matrix with less than five sequence reads in any given host sample to zero following Lindahl *et al.* (2013). This curation resulted in one individual plant having only one fungal OTU present; therefore, this host individual was removed from all final analyses (N=105).

Phylogenetic Inference

To generate a proxy for phylogenetic relatedness in our analysis of FFE communities, a single locus phylogeny was reconstructed for the 18 Asteraceae species and the single outgroup species (*Lobelia cardinalis*, Campanulaceae) using plant nuclear ITS sequences retrieved from GenBank (see SI Table S2 for accession numbers & species names). Species lacking available sequences in GenBank were replaced with available sequences from congeneric species (n= 3

hosts), or contribal species (n=3 hosts), based on previous phylogenetic inference in the Asteraceae (Schmidt and Schilling 2000, Urbatsch et al. 2000, Panero and Funk 2008, Fu et al. 2016). Plant sequences were aligned using Muscle version 3.8.31 (Edgar 2004), imported into R ('seqinr'; Charif *et al.* 2017), and converted to a DNA binary format ('ape'; Paradis *et al.* 2017). The 'Rphylip' package (Revell and Chamberlain 2014) was used as an R interface for the Phylip program for phylogenetic inference (v.3.695; Felsenstein 2013). Maximum likelihood inference methods were used on a rooted tree for the 19 host species, with 1000 bootstrap replications (function 'Rdnaml'; Fig. 1A, B). The final tree was used to provide a measure of phylogenetic distance between all species pairs in our data set.

Statistical Analyses

FFE Diversity Analyses – We used linear models to test how FFE OTU richness and diversity varied among individual plants. For these models, we used LMA to standardize FFE richness and diversity per unit leaf mass, because while the same area of leaf tissue was sampled for Illumina sequencing, leaf mass varied among host individuals and between species (SI Fig. S2). LMA was also used because it is significantly correlated with individual plant size (SI Fig. S3).

Linear models tested whether richness and diversity varied among the fixed effects of host species and plots in the common garden, as well as by total sequencing read count per host after quality filtering. Recent theoretical work suggests that models that incorporate total sequencing read count per host into hypothesis testing best account for the sequencing bias introduced by culture-independent approaches (McMurdie and Holmes 2014). Culture-independent approaches can introduce bias into the direct estimation of individual OTU abundances compared to other OTUs in the community, but they retain relative relationships among sampled units in distance-

based space (Eusemann et al. 2016). The interaction between host species identity and LMA was insignificant and therefore was not included in the final models of FFE richness or diversity.

FFE Community Structure Analyses – For the FFE community structure analysis, two predictor variables were tested as categorical variables (host species identity and common garden plot identity), while LMA and total sequencing read count per host were both tested as covariates and continuous variables. As an additional test for the effect of host phylogeny on FFE communities, host tribe and host sub-family were each substituted in place of the host species variable into the FFE community structure analysis. A Hellinger transformation was applied to the FFE community matrix to limit the influence of abundant OTUs (Legendre and Gallagher 2001). We used the Horn-Morisita dissimilarity index to test for differences in FFE community structure using a permutational multivariate analysis of variance (PERMANOVA), which uses a marginal sum of squares method to compute pseudo F-statistics for hypothesis testing ('adonis2' function, 'vegan' package, 3000 permutations; Oksanen *et al.* 2017). As in the FFE richness and diversity analyses, the interaction between host species identity and LMA was insignificant and thus not included in the final model.

Differences in FFE community structure were visualized using non-metric multidimensional scaling (NMDS). To visualize the role of host species identity and host phylogenetic relationships in structuring FFE communities, color was assigned to each sample point in the NMDS plots based on the phylogenetic inference (Fig. 1A, B). To simplify the presentation of host-specificity in structuring FFE communities, only the ellipses identifying the centroid and standard error of the seven Asteraceae tribes and the Campanulaceae outgroup species are presented, as opposed to ellipses for all 19 host species. To determine how much variance was explained by each of the four predictor variables separately, as well as their joint

effects (Legendre and Gallagher 2001), we performed a variance partitioning analysis (RDA; 'varpart' function, 'vegan' package; Oksanen *et al.* 2017) with the transformed FFE community matrix as the response variable. Constrained RDA followed by a pseudo-F test was used to assess significance of the predictor variables. Due to missing LMA data for nine host plants, only N=96 plants were included in the community richness, diversity, and structure analyses.

FFE Community Distance Analyses – A multivariate statistical framework was used to test the association of FFE community structure with host species phylogeny and also with plot location within the common garden (N=105 plants). Specifically, we performed Mantel tests to examine the correlation between the transformed Horn-Morisita dissimilarity matrix with pairwise host species phylogenetic distance, as well as with pairwise spatial distance among plots. A null distribution drawn from 9999 permutations of the Horn-Morisita matrix was used to test for statistical significance. Pairwise phylogenetic distance among all species pairs was estimated using the 'cophenetic' function of tree branch length in the 'picante' package in R (Kembel et al. 2016). Pairwise spatial distance between the centroid of all field plots in the common garden was calculated using Google Earth v.7.1.7.2602. The distance between plots was always significantly greater than the distance between plants within plots.

FFE Indicator Species Analysis – To determine which fungal OTUs best characterized the microbial communities as a function of host species identity, we performed Dufrene and Legendre's indicator species analysis (1997) using the 'labdsv' package in R (10,000 randomizations; Roberts 2016). Indicator OTUs are identified by their relative fidelity to a specific group (i.e., particular host species) and weighted by their relative abundance across all groups. The analysis was performed on only those fungal OTUs with >1000 reads across all hosts (i.e., "core" taxa) to limit the influence of rare taxa and improve performance of the

randomizations. Tentative ecological guild and trophic mode was assigned for all indicator species using the FUNGuild and U.S. Department of Agriculture's Fungal databases (Nguyen et al. 2016, Farr and Rossman 2017). All statistical analyses were run in R v.3.3.2.

RESULTS

Basic Sequencing Results – The quality-filtered sequence dataset, based on 105 plant samples, contained 556 fungal OTUs generated from 5,932,461 ITS1 reads. The average sequencing depth per sample was 56,500 reads and ranged from 15,488 to 88,855. Fungal OTUs represented 29 identified orders where the five most abundant orders were: Pleosporales (165 OTUs), Capnodiales (78 OTUs), Trichosphaeriales (39 OTUs), Xylariales (34 OTUs), and Tremellales (27 OTUs). 110 OTUs could not be identified to the order level. Additionally, 86.2% of identified OTUs belonged to the phylum Ascomycota, 13.6% belonged to the Basidiomycota, and 1 OTU matched to the Zygomycota (*Mortierella* spp.). The hierarchical classification of all fungal OTUs is presented in SI Table S3. The ten most common OTUs represented 57% of the total sequence reads after quality filtering and varied in relative abundance among the 19 host species (Fig. 1C).

FFE Species Richness, Diversity, and Community Structure – After three months of exposure to natural inocula sources, FFE OTU richness did not differ among host species ($p = 0.2153$; Fig. 2A) or among plots in the common garden ($p = 0.2491$; SI Fig. S4A). Furthermore, FFE OTU richness did not vary by the total number of read counts per individual host ($p = 0.7520$). By contrast, while FFE OTU diversity also did not vary among common garden plots ($p = 0.1634$; Fig. S4B) or by total number of read counts per individual host ($p = 0.4662$), FFE OTU diversity did vary significantly among host species ($F_{18,71} = 1.89$, $p = 0.0310$; Fig. 2B; whole

model Adj. $R^2 = 0.1566$). This significant difference among host species was maintained even after accounting for differences in the mass of leaf tissue sampled per plant host.

Similarly, there was a highly significant effect of host species identity on the structure of FFE communities (pseudo-$F_{18,70} = 1.39$, *p= 0.0010*; Fig. 3). There was also a significant effect of host tribe identity on the structure of FFE communities (pseudo-$F_{7,81} = 1.46$, *p= 0.0047*; Fig. 3), but there was no significant effect of host subfamily on FFE community structure (*p= 0.3626*). The sequencing read count per host also had an effect on community structure (pseudo-$F_{1,70} = 1.74$, *p= 0.0430*). In addition, FFE community structure differed marginally across host plants grown in different common garden plots (pseudo-$F_{5,70} = 1.27$, *p= 0.0810*; Fig 4), but LMA did not have a significant effect on FFE community structure (*p= 0.2076*). Results from the variance partitioning analysis showed that host species identity explained the most variation in community structure (4.74%; *p= 0.001*), followed by common garden plot identity (1.48%; p= 0.038) and sequencing bias (0.713%; *p= 0.033*). LMA did not significantly explain any variation in FFE community structure (0.024%; *p= 0.413*).

FFE Community Distance – Phylogenetic distance among hosts ranged from 0 for individuals of the same species to 0.71 branch length units for individuals of the two most divergent species (i.e., *Vernonia fasciculata* and *Cacalia plantaginea*; Fig 1B). The results of the Mantel test showed that dissimilarity of FFE communities among hosts was significantly and positively correlated with host phylogenetic distance (*p= 0.0200; r = 0.0785*; Fig. 5). Specifically, more closely related host species had more similar FFE communities than more distantly related host species. Similarly, results from an independent Mantel test showed that dissimilarity of FFE communities among hosts was positively correlated with the pairwise distance between plots within the common garden (Fig. 6). However, the spatial effect was

smaller than the phylogenetic effect on FFE community distance (*p= 0.0476; r = 0.0524*). The pairwise spatial distance between plots in the common garden ranged from 0 to 648 m.

Indicator Species Analysis – Indicator species analysis identified 24 fungal OTUs that were indicative of a particular host species at a threshold $\alpha < 0.05$ (Table 2). Several of these OTUs have previously been categorized as plant pathogens, including *Peltaster fructicola* from apple (*Malus* spp.) trees and *Mycosphaerella lateralis* from *Eucalyptus* trees. Similarly, several indicator taxa are known pathogens on a broad range of host species and families (e.g., *Myrothecium roridum, Colletotrichum destructivum, Nigrospora oryzae*). By contrast, no indicator taxa were listed as having an endophytic lifestyle in the FUNGuild database. It was not possible to assign putative function or trophic mode using the FUNGuild and USDA reference databases for ten indicator taxa due to low taxonomic resolution.

DISCUSSION

We found that host species identity was a significant driver of FFE community structure and diversity, after accounting for differences among individual plants in the mass of leaf tissue sampled. Furthermore, pairwise phylogenetic distance between host species was significantly and positively correlated with FFE community dissimilarity between individual hosts. Thus, more closely related host species had more similar FFE microbiomes while more distantly related host species had less similar FFE microbiomes and shared fewer FFE taxa in common. Our results are in agreement with previous studies demonstrating signatures of host phylogenetic relationships for foliar fungal pathogens (Gilbert and Webb 2007, Parker et al. 2015). However, to our knowledge, our study is the first to test host phylogenetic relationships for FFE microbiota using a common garden approach, where individual plants from different species were spatially

randomized in the same habitat. The common garden design allowed for natural variation in microbial colonization at the local level, but controlled for other factors affecting FFE community structure such as regional variation in environmental and climatic conditions, differences in host age at the time of sampling, and temporal turnover in FFE communities across seasons or years. The correlation between FFE community dissimilarity and distance between common garden plots was also positive, though weaker relative to pairwise host phylogenetic distance. Lastly, we found that while FFE community diversity per unit leaf mass varied significantly among host species, LMA itself was not a significant predictor of FFE community structure after controlling for host species identity.

Our results demonstrate an important role for phylogenetic relatedness in determining the structure of FFE communities, though much of the observed variation in FFE community structure remains to be explained. Host phylogenetic relatedness is a useful proxy for understanding complex ecological and evolutionary processes because it is often simpler to measure than an array of functional traits and relatively inexpensive with the increasing availability of genetic data (Cavender-Bares et al. 2009). However, the genotypic and phenotypic divergence among host species underlying phylogenetic relationships is complex and could include a wide array of traits not measured here that could more strongly influence the success of specific microbial taxa. For example, research on plant-pathogen interactions suggests that more closely related hosts share similar genetic pathways for cellular recognition of proteins and effector molecules during pathogen colonization and resistance (Barrett and Heil 2012). Similarly, previous work has shown that FFE community composition varies predictably with leaf carbon concentration (Yang et al. 2016), which is an important component of plant life-history strategy and influenced by both evolutionary processes and local climate (Elser et al.

2010). Physiological changes associated with leaf tissue senescence are also genetically controlled (Lim et al. 2007) and correspond with shifts in FFE community structure (Voříšková and Baldrian 2013).

Disentangling local, host-based processes, such as genotypic and phenotypic differences among individual hosts, from regional-scale, spatial processes remains a challenge in studies of microbiome assembly and function. Here we detected a spatial effect on FFE community structure across a distance of just 650m. Other recent work has shown that FFE community structure varied predictably along a 400-km precipitation gradient in two *Panicum* grass species (Giauque and Hawkes 2013), indicating a more regional effect of moisture availability on FFE community structure. Similarly, individual FFE populations can exhibit genetic structure (i.e., isolation by distance) over hundreds of kilometers (Oono et al. 2014), but functional consequences of FFE population genetics for hosts or other members within the FFE community remain unclear. To separate local and regional influences on FFE populations and communities from host genotypic effects, experimental plantings of species or genotypes across spatial or environmental gradients, followed by microbiome characterization, would be an informative direction for future research. For example, specific genotypes within a single host species that vary in LMA, other leaf traits, or immune responses could be transplanted across soil fertility or spatial distance gradients.

Indicator species analysis identified 24 core fungal OTUs that had high specificity and relative abundance to particular Asteraceae species, or to the outgroup species *Lobelia cardinalis* (Table 2). Several of these fungal genera have previously been reported as pathogens (Nguyen et al. 2016, Farr and Rossman 2017). However, fungal reference databases tend to be populated by research from agricultural systems and therefore can over-represent the importance of pathogens.

In general, the FFE colonizers of wild herbaceous hosts are less well characterized than those from tree or crop species (Christian et al. 2017). Moreover, our sampling regimen specifically targeted asymptomatic plant tissues versus diseased leaves. Thus, our results suggest that while some FFE OTUs may be closely related to the pathogens of agricultural grasses and trees, they may also exist as asymptomatic endophytes in alternate host species (Malcolm et al. 2013). Additionally, one member of the order Pucciniales (rusts) was an indicator species for the two *Vernonia* hosts, which agrees with our observations of rust pustule formation on the abaxial leaf surfaces of most *Vernonia* hosts in the field. Ultimately, elucidating the true functional role of these indicator species requires isolation and subsequent inoculation onto a range of host species.

Our common garden experiment was established with the explicit purpose of maximizing local stochastic effects (e.g., small-scale environmental conditions and microbial inocula sources), while minimizing regional effects on FFE community structure (e.g., broad geographic differences in surrounding vegetation, FFE dispersal, and climatic conditions). As a result, host species in the common garden shared many of the same FFE, despite exhibiting significant species-specific differences. Given the large differences in plant architecture, chemistry, and other phenotypic traits across host species, it is perhaps surprising that we did not see even more variation in FFE community structure. However, by minimizing environmental variation we revealed the significant role of phylogenetic relatedness in structuring FFE communities. Future research should examine how other environmental factors or host traits influence microbial colonizers. For example, micro-environmental differences (e.g., variable UV exposure, leaf age; Osono & Mori 2003), among leaves sampled from different plant hosts could be one source of this unexplained variation. In addition, recent evidence indicates that microbial colonization from conspecific and heterospecific neighboring plants can also affect microbial community structure

(Laforest-Lapointe et al. 2017). Thus, variation in the vegetation surrounding the common garden or in the identity of neighboring plants within the common garden itself may have influenced microbial community structure via short-distance dispersal, or via priority effects of initial colonizers onto newly emerged leaves (Adame-Álvarez et al. 2014).

In conclusion, our research demonstrates that host species identity is an important force structuring FFE communities and that these differences are due in part to host species phylogenetic relatedness. To our knowledge, our study is the first to demonstrate a phylogenetic signal for FFE communities using an experimental design that explicitly manipulated host phylogeny and species identity within a common garden framework. Most previous research on the role of host phylogenetic relatedness in structuring microbial communities has relied on field sampling of natural host populations and communities where host taxa occurred in different locations or microenvironments (Tedersoo et al. 2013, Wehner et al. 2014, Eusemann et al. 2016, Vincent et al. 2016), and thus did not control for regional and temporal drivers of microbial community assembly. It remains an open question whether a host phylogenetic signal would be detectable, or of similar magnitude, for other microbial groups within the foliar plant microbiome, such as bacterial endophytes or viruses, or for other plant families beyond the Asteraceae. While we sampled FFE irrespective of their functional consequences for the host, it has been demonstrated that pathogens show a higher degree of host specificity than mutualists in the rhizosphere (Cortois et al. 2016). Teasing apart the functional role of individual taxa in the foliar microbiome from their degree of host specificity is an important direction for future research. Overall, our results have broad implications for the organization and assembly of host-associated microbiota across divergent plant and animal host lineages (Clay and Schardl 2002, Ley et al. 2008, Russell et al. 2017).

ACKNOWLEDGEMENTS

B.K.W. and N.C were supported as National Science Foundation Graduate Research Fellows during the course of the experiment. B.K.W. was also additionally funded by the National Institutes of Health Genetics, Cellular & Molecular Sciences Training Grant. Q.C. was supported through the Changjiang Scholars Program and Innovative Research Team by the Ministry of Education of the People's Republic of China (IRT17R50), as well as through the China Scholarship Council at Indiana University (IU). Funding support for establishment of the common garden and sequencing of fungal taxa was provided by research grants to B.K.W. from the IU Research and Teaching Preserve (RTP) and the Indiana Academy of Science. We would like to thank M. Zaret, K. Hoban, L. Cole, Z. Shearin, Q. Zhu, T. Cheeke, and the IU Greenhouse and RTP Staff for assistance with the project, as well as the IU Herbarium Director Dr. E. Knox for assistance identifying native Asteraceae and the IU Center for Genomics and Bioinformatics for bioinformatics support. Finally, we would like to thank the Clay and Bever labs for feedback on the manuscript, as well as the anonymous reviewers who helped to improve the final paper.

LITERATURE CITED

Adame-Álvarez, R.-M., J. Mendiola-Soto, and M. Heil. 2014. Order of arrival shifts endophyte-pathogen interactions in bean from resistance induction to disease facilitation. FEMS Microbiology Letters 355:100–107.

Alivisatos, A. P., M. J. Blaser, E. L. Brodie, M. Chun, J. L. Dangl, T. J. Donohue, P. C. Dorrestein, J. A. Gilbert, J. L. Green, J. K. Jansson, R. Knight, M. E. Maxon, M. J. McFall-Ngai, J. F. Miller, K. S. Pollard, E. G. Ruby, S. A. Taha, and Unified Microbiome Initiative Consortium. 2015. A unified initiative to harness Earth's microbiomes. Science 350:507–508.

Azad, M. B., T. Konya, H. Maughan, D. S. Guttman, C. J. Field, M. R. Sears, A. B. Becker, J. A. Scott, A. L. Kozyrskyj, and C. S. Investigators. 2013. Infant gut microbiota and the hygiene hypothesis of allergic disease: impact of household pets and siblings on microbiota composition and diversity. Allergy, Asthma, and Clinical Immunology 9:1–9.

Bálint, M., L. Bartha, R. B. O'Hara, M. S. Olson, J. Otte, M. Pfenninger, A. L. Robertson, P. Tiffin, and I. Schmitt. 2015. Relocation, high-latitude warming and host genetic identity shape the foliar fungal microbiome of poplars. Molecular Ecology 24:235–248.

Barrett, L. G., and M. Heil. 2012. Unifying concepts and mechanisms in the specificity of plant-enemy interactions. Trends in Plant Science 17:282–292.

Busby, P. E., M. Ridout, and G. Newcombe. 2016. Fungal endophytes: modifiers of plant disease. Plant Molecular Biology 90:645–655.

Caporaso, J. G., J. Kuczynski, J. Stombaugh, K. Bittinger, F. D. Bushman, E. K. Costello, N. Fierer, A. G. Peña, J. K. Goodrich, J. I. Gordon, G. A. Huttley, S. T. Kelley, D. Knights, J. E. Koenig, R. E. Ley, C. A. Lozupone, D. McDonald, B. D. Muegge, M. Pirrung, J. Reeder,

J. R. Sevinsky, P. J. Turnbaugh, W. A. Walters, J. Widmann, T. Yatsunenko, J. Zaneveld, and R. Knight. 2010. QIIME allows analysis of high-throughput community sequencing data. Nature Methods 7:335–336.

Caporaso, J. G., C. L. Lauber, W. A. Walters, D. Berg-Lyons, J. Huntley, N. Fierer, S. M. Owens, J. Betley, L. Fraser, M. Bauer, N. Gormley, J. A. Gilbert, G. Smith, and R. Knight. 2012. Ultra-high-throughput microbial community analysis on the Illumina HiSeq and MiSeq platforms. ISME Journal 6:1621–1624.

Cavender-Bares, J., K. H. Kozak, P. V. A. Fine, and S. W. Kembel. 2009. The merging of community ecology and phylogenetic biology. Ecology Letters 12:693–715.

Charif, D., O. Clerc, C. Frank, J. R. Lobry, A. Necsulea, L. Palmeira, S. Penel, and G. Perriere. 2017. "seqinr" Package: Biological Sequences Retrieval and Analysis.

Christian, N., C. Sullivan, N. D. Visser, and K. Clay. 2016. Plant host and geographic location drive endophyte community composition in the face of perturbation. Microbial Ecology 72:621–632.

Christian, N., B. K. Whitaker, and K. Clay. 2015. Microbiomes: unifying animal and plant systems through the lens of community ecology theory. Frontiers in Microbiology 6:1–15.

Christian, N., B. K. Whitaker, and K. Clay. 2017. A novel framework for decoding fungal endophyte diversity. Pages 65–78*in* J. Dighton and J. F. White, editors.The fungal community: Its organization and role in the ecosystem. 4th edition. CRC Press, Boca Raton, FL, USA.

Clay, K., and C. Schardl. 2002. Evolutionary origins and ecological consequences of endophyte symbiosis with grasses. The American Naturalist 160:S99–S127.

Cortois, R., T. Schröder-Georgi, A. Weigelt, W. H. van der Putten, and G. B. De Deyn. 2016.

Plant-soil feedbacks: role of plant functional group and plant traits. Journal of Ecology 104:1608–1617.

David, A. S., E. W. Seabloom, and G. May. 2015. Plant host species and geographic distance affect the structure of aboveground fungal symbiont communities, and environmental filtering affects belowground communities in a coastal dune ecosystem. Microbial Ecology 71:912–926.

Deshpande, V., Q. Wang, P. Greenfield, M. Charleston, A. Porras-Alfaro, C. R. Kuske, J. R. Cole, D. J. Midgley, and N. Tran-Dinh. 2015. Fungal identification using a Bayesian classifier and the Warcup training set of internal transcribed spacer sequences. Mycologia 108:1–5.

Edgar, R. C. 2004. MUSCLE: Multiple sequence alignment with high accuracy and high throughput. Nucleic Acids Research 32:1792–1797.

Elser, J. J., W. F. Fagan, A. J. Kerkhoff, N. G. Swenson, and B. J. Enquist. 2010. Biological stoichiometry of plant production: metabolism, scaling and ecological response to global change. New Phytologist 186:593–608.

Eusemann, P., M. Schnittler, R. H. Nilsson, A. Jumpponen, M. B. Dahl, D. G. Wurth, A. Buras, M. Wilmking, and M. Unterseher. 2016. Habitat conditions and phenological tree traits overrule the influence of tree genotype in the needle mycobiome-Picea glauca system at an arctic treeline ecotone. New Phytologist 211:1221–1231.

Farr, D., and A. Rossman. 2017. Fungal Databases, U.S. National Fungus Collections, ARS, USDA. Retrieved June 25, 2017, https://nt.ars-grin.gov/fungaldatabases/.

Felsenstein, J. 2013. PHYLIP (Phylogeny Inference Package) version 3.695. Distributed by the author. Department of Genome Sciences, University of Washington, Seattle.

Fu, Z.-X., B.-H. Jiao, B. Nie, G.-J. Zhang, T.-G. Gao, and C. P. Consortium. 2016. A comprehensive generic-level phylogeny of the sunflower family: Implications for the systematics of Chinese Asteraceae. Journal of Systematics and Evolution 54:416–437.

Funk, V. A., A. Susanna, T. F. Stuessy, and R. J. Bayer. 2009. Systematics, evolution, and biogeography of Compositae. Page (V. Funk, A. Susanna, T. F. Stuessy, and R. Bayer, Eds.). International Association for Plant Taxonomy.

Gange, A. C., S. Dey, A. F. Currie, and B. C. Sutton. 2007. Site- and species-specific differences in endophyte occurrence in two herbaceous plants. Journal of Ecology 95:614–622.

Giauque, H., and C. V Hawkes. 2013. Climate affects symbiotic fungal endophyte diversity and performance. American Journal of Botany 100:1435–1444.

Gilbert, G. S., and C. O. Webb. 2007. Phylogenetic signal in plant pathogen-host range. Proceedings of the National Academy of Sciences 104:4979–4983.

Hanson, C. A., J. A. Fuhrman, M. C. Horner-Devine, and J. B. H. Martiny. 2012. Beyond biogeographic patterns: processes shaping the microbial landscape. Nature Reviews Microbiology 10:497–506.

Higgins, K. L., A. E. Arnold, P. D. Coley, and T. A. Kursar. 2014. Communities of fungal endophytes in tropical forest grasses: highly diverse host- and habitat generalists characterized by strong spatial structure. Fungal Ecology 8:1–11.

Hooper, L. V, D. R. Littman, and A. J. Macpherson. 2012. Interactions between the microbiota and the immune system. Science 336:1268–1273.

Kawecki, T. J., and D. Ebert. 2004. Conceptual issues in local adaptation. Ecology Letters 7:1225–1241.

Kembel, S. W., D. D. Ackerly, S. P. Blomberg, W. K. Cornwell, P. D. Cowan, M. R. Helmus, H.

Morlon, and C. O. Webb. 2016. “picante” Package: R tools for integrating phylogenies and ecology.

Krings, M., T. N. Taylor, H. Hass, H. Kerp, N. Dotzler, and E. J. Hermsen. 2007. Fungal endophytes in a 400-million-yr-old land plant: infection pathways, spatial distribution, and host responses. New Phytologist 174:648–657.

Laforest-Lapointe, I., A. Paquette, C. Messier, and S. W. Kembel. 2017. Leaf bacterial diversity mediates plant diversity and ecosystem function relationships. Nature 546:145–147.

Leff, J. W., and N. Fierer. 2013. Bacterial communities associated with the surfaces of fresh fruits and vegetables. PLoS One 8:e59310.

Legendre, P., and E. D. Gallagher. 2001. Ecologically meaningful transformations for ordination of species data. Oecologia 129:271–280.

Ley, R., C. Lozupone, M. Hamady, R. Knight, and J. I. Gordon. 2008. Worlds within worlds: evolution of the vertebrate gut microbiota. Nature Reviews 6:776–788.

Lim, P. O., H. J. Kim, and H. G. Nam. 2007. Leaf Senescence. Annual Review of Plant Biology 58:115–136.

Lindahl, B., R. H. Nilsson, L. Tedersoo, K. Abarenkov, T. Carlsen, R. Kjoller, U. Koljalg, T. Pennanen, S. Rosendahl, J. Stenlid, and H. Kauserud. 2013. Fungal community analysis by high-throughput sequencing of amplified markers – a user’s guide. New Phytologist 199:288–299.

Malcolm, G. M., G. A. Kuldau, B. K. Gugino, and M. del Mar Jiménez-Gasco. 2013. Hidden host plant associations of soilborne fungal pathogens: an ecological perspective. Phytopathology 103:538–544.

Martin, K. J., and P. T. Rygiewicz. 2005. Fungal-specific PCR primers developed for analysis of

the ITS region of environmental DNA extracts. BMC microbiology 5:28.

McMurdie, P. J., and S. Holmes. 2014. Waste not, want not: why rarefying microbiome data is inadmissible. PLoS Computational Biology 10:e1003531.

Mejía, L. C., E. I. Rojas, Z. Maynard, S. Van Bael, A. E. Arnold, P. Hebbar, G. J. Samuels, N. Robbins, and E. A. Herre. 2008. Endophytic fungi as biocontrol agents of Theobroma cacao pathogens. Biological Control 46:4–14.

Nguyen, N. H., Z. Song, S. T. Bates, S. Branco, L. Tedersoo, J. Menke, J. S. Schilling, and P. G. Kennedy. 2016. FUNGuild: An open annotation tool for parsing fungal community datasets by ecological guild. Fungal Ecology 20:241–248.

Oksanen, J., F. G. Blanchet, M. Friendly, R. Kindt, P. Legendre, D. McGlinn, P. R. Minchin, R. B. O'Hara, G. L. Simpson, P. Solymos, M. H. H. Stevens, E. Szoecs, and H. Wagner. 2017. "vegan" Community Ecology Package.

Oono, R., F. Lutzoni, A. E. Arnold, L. Kaye, J. M. U'Ren, G. May, and I. Carbone. 2014. Genetic variation in horizontally transmitted fungal endophytes of pine needles reveals population structure in cryptic species. American Journal of Botany 101:1362–1374.

Osono, T., and A. Mori. 2003. Colonization of Japanese beech leaves by phyllosphere fungi. Mycoscience 44:437–441.

Panero, J. L., and V. A. Funk. 2008. The value of sampling anomalous taxa in phylogenetic studies: Major clades of the Asteraceae revealed. Molecular Phylogenetics and Evolution 47:757–782.

Paradis, E., S. Blomber, B. Bolker, J. Claude, H. S. Cuong, R. Desper, G. Didier, B. Durand, J. Dutheil, R. J. Ewing, O. Gascuel, C. Heibl, A. Ives, B. Jones, D. Lawson, V. Lefort, P. Legendre, J. Lemon, R. McCloskey, J. Nylander, R. Opgen-Rhein, A. Popescu, M. Royer-

Carenzi, K. Schliep, K. Strimmer, and D. de Vienne. 2017. “ape” Package: Analyses of Phylogenetics and Evolution.

Parker, I. M., M. Saunders, M. Bontrager, A. P. Weitz, R. Hendricks, R. Magarey, K. Suiter, and G. S. Gilbert. 2015. Phylogenetic structure and host abundance drive disease pressure in communities. Nature 520:542–544.

Revell, L. J., and S. A. Chamberlain. 2014. Rphylip: an R interface for PHYLIP. Methods in Ecology and Evolution 5:976–981.

Roberts, D. W. 2016. “labdsv” Package: Ordination and Multivariate Analysis for Ecology.

Russell, J. A., J. G. Sanders, and C. S. Moreau. 2017. Hotspots for symbiosis: Function, evolution, and specificity of ant-microbe associations from trunk to tips of the ant phylogeny (Hymenoptera: Formicidae). Myrmecological News 24:43–69.

Schmidt, G. J., and E. E. Schilling. 2000. Phylogeny and biogeography of eupatorium (Asteraceae: Eupatorieae) based on nuclear ITS sequence data. American Journal of Botany 87:716–726.

Seabloom, E. W., E. T. Borer, C. Lacroix, C. E. Mitchell, and A. G. Power. 2013. Richness and composition of niche-assembled viral pathogen communities. PloS One 8:e55675.

Shade, A., S. E. Jones, J. G. Caporaso, J. Handelsman, R. Knight, N. Fierer, and J. A. Gilbert. 2014. Conditionally rare taxa disproportionately contribute to temporal changes in microbial diversity. mBio 5:e01371-14.

Sharon, I., M. J. Morowitz, B. C. Thomas, E. K. Costello, D. A. Relman, and J. F. Banfield. 2013. Time series community genomics analysis reveals rapid shifts in bacterial species, strains, and phage during infant gut colonization. Genome Research 23:111–120.

Tedersoo, L., M. Mett, T. A. Ishida, and M. Bahram. 2013. Phylogenetic relationships among

host plants explain differences in fungal species richness and community composition in ectomycorrhizal symbiosis. The New Phytologist 199:822–831.

Urbatsch, L. E., B. G. Baldwin, and M. J. Donoghue. 2000. Phylogeny of the coneflowers and relatives (Heliantheae: Asteraceae) based on nuclear rDNA internal transcribed spacer (ITS) sequences and chlorplast DNA restriction site data. Systematic Botany 25:539–565.

Vincent, J. B., G. D. Weiblen, and G. May. 2016. Host associations and beta diversity of fungal endophyte communities in New Guinea rainforest trees. Molecular Ecology 25:825–841.

Voříšková, J., and P. Baldrian. 2013. Fungal community on decomposing leaf litter undergoes rapid successional changes. The ISME Journal 7:477–486.

Wehner, J., J. R. Powell, L. A. H. Muller, T. Caruso, S. D. Veresoglou, S. Hempel, and M. C. Rillig. 2014. Determinants of root-associated fungal communities within Asteraceae in a semi-arid grassland. Journal of Ecology 102:425–436.

Yang, T., P. Weisenhorn, J. A. Gilbert, Y. Ni, R. Sun, Y. Shi, and H. Chu. 2016. Carbon constrains fungal endophyte assemblages along the timberline. Environmental Microbiology 18:2455–2469.

DATA ACCESSIBILITY

- All curated data input files (.CSV format) and associated R statistical scripts used for statistical analyses and figure creation will be published online after manuscript acceptance (Dryad).
- DNA sequences and associated metadata will be published online after manuscript acceptance (Genbank).

AUTHOR CONTRIBUTIONS

BKW, QC, and KC established the common garden; BKW and QC maintained it. BKW, NC, and QC performed the molecular protocols. BKW curated the raw data files, performed all statistical analyses, and wrote the first draft of the manuscript. All authors contributed substantially to project design and manuscript revisions.

FIGURES AND TABLES

Fig. 1 – Relative abundance of top ten most abundant OTUs differs among host species. (A) Color code corresponding to the phylogenetic tree and relative phylogenetic distances among host species – *as a reference for Figure 3*. (B) Phylogenetic tree of the 19 host species using maximum likelihood methods. (C) Relative abundance for the top ten most abundant fungal OTUs are shown as percentages, where each colored bar represents a different OTU. Best match names for each of the top ten OTUs are also shown. For 'unknown' taxonomic levels, the abbreviation '*Unk.*' is used. For simplicity, host species names are shortened to the first 3 letters of the genus, followed by the first 3-4 letters of the species name.

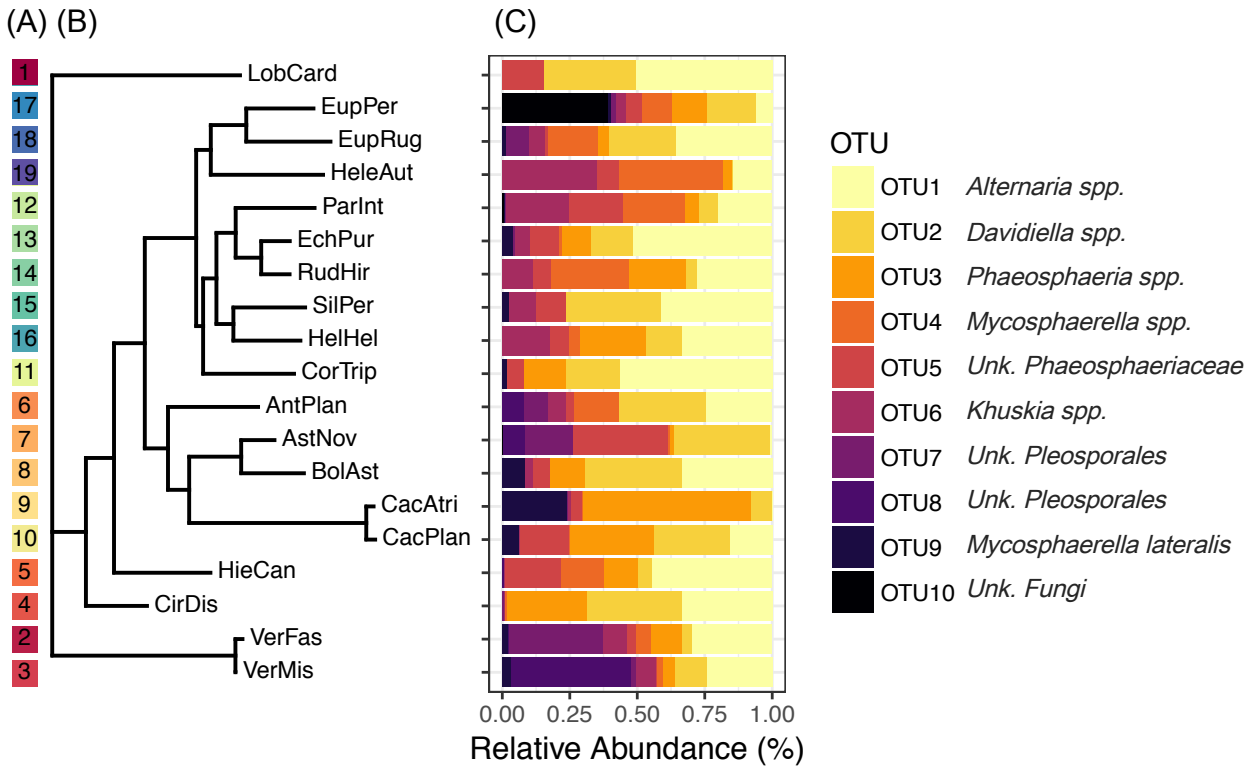

Fig. 2 – Average FFE community (A) richness and (B) diversity by host species. Boxplots are displayed for each species. For both panels, species have been sorted from least to highest FFE diversity. Richness and diversity have both been standardized by Leaf Mass per Area.

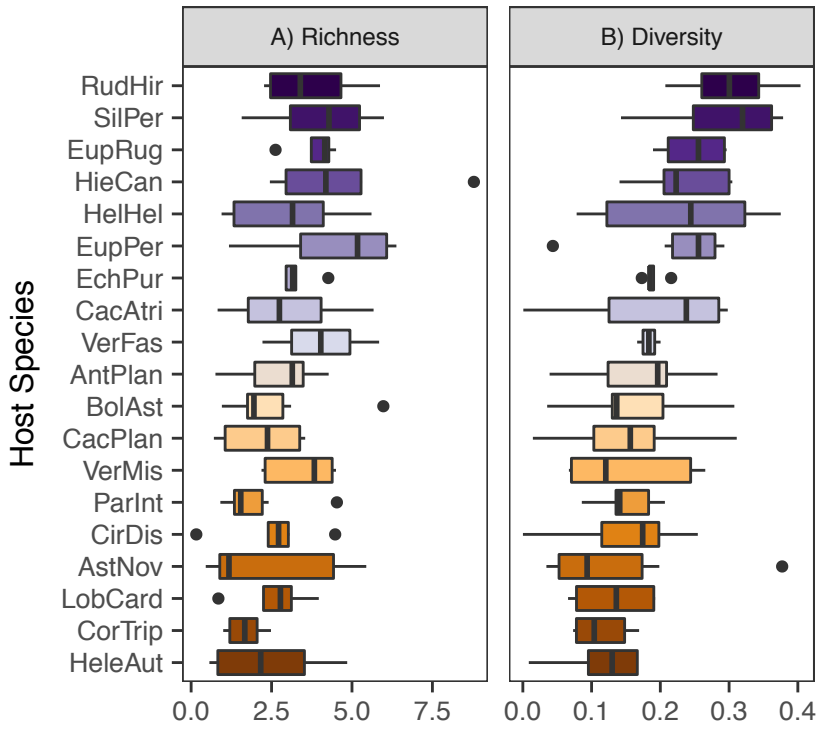

Fig. 3 – FFE community structure varied by host species. The location of each host individual in ordination space (stress = 0.249) is denoted by a filled circle, while the centroid, or average NMDS coordinates, of all 19 host species are shown as filled, numbered squares. Host species are color-coded according to their phylogenetic relationship – *as shown in Fig. 1A*. The ellipses represent the centroid and standard deviation for each of the seven host tribes and the Campanulaceae family outgroup.

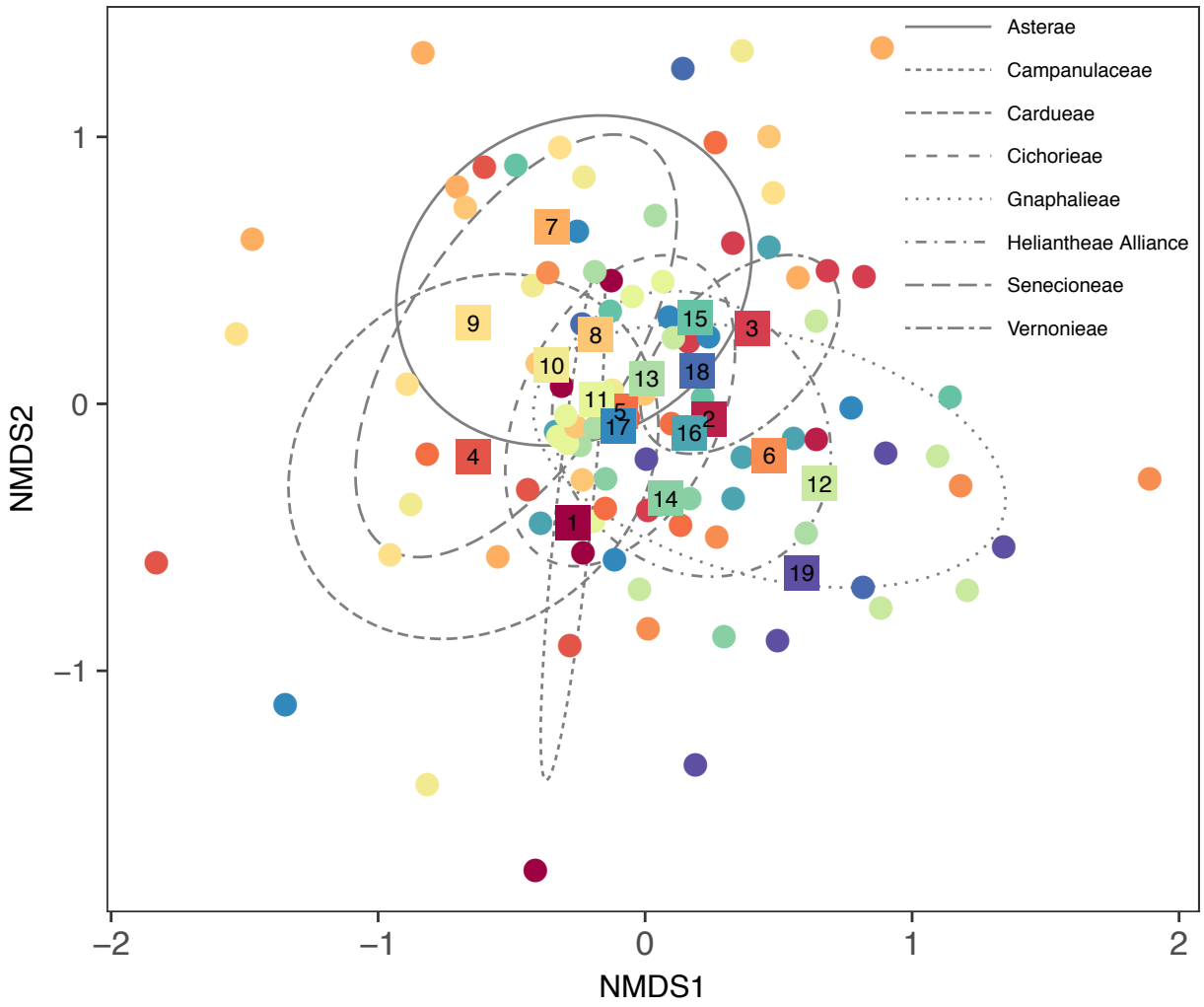

Fig. 4 – FFE community structure varied marginally among plots in the common garden. Ellipses depict the centroid and standard deviation for common garden plots. The two grey-shaded ellipses represent plots 1 & 2, the two green-shaded ellipses represent plots 3 & 4, and the two purple-shaded ellipses represent plots 5 & 6. The location of each host individual in ordination space is denoted by a filled circle and is color-coded in kind with the ellipses.

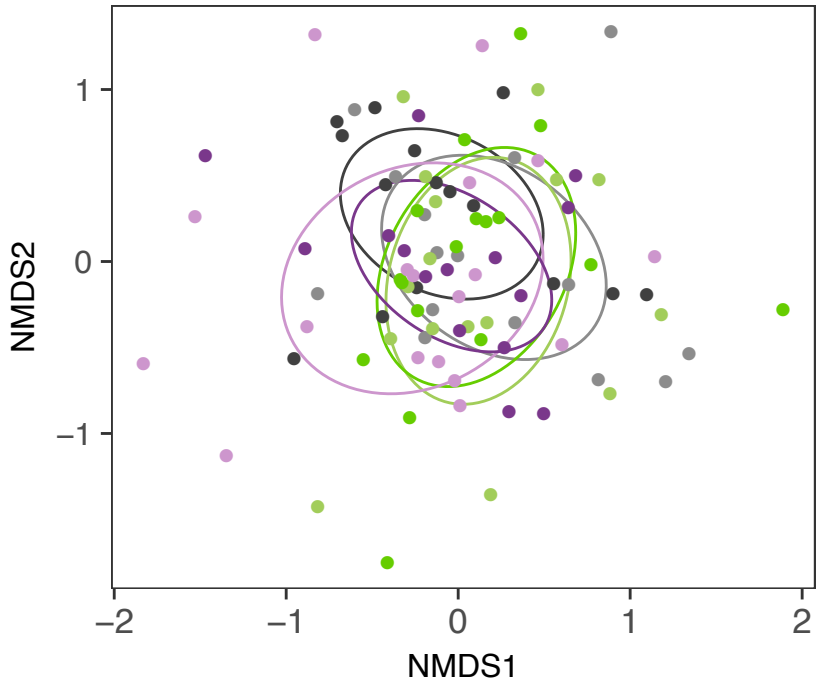

Fig. 5 – FFE community dissimilarity increased with increasing host phylogenetic distance. A regression of the pairwise dissimilarity between individual host-associated FEE communities (Horn-Morisita) plotted against the pairwise phylogenetic distance between host species is shown (blue-dashed line). Each point represents a single pairwise comparison.

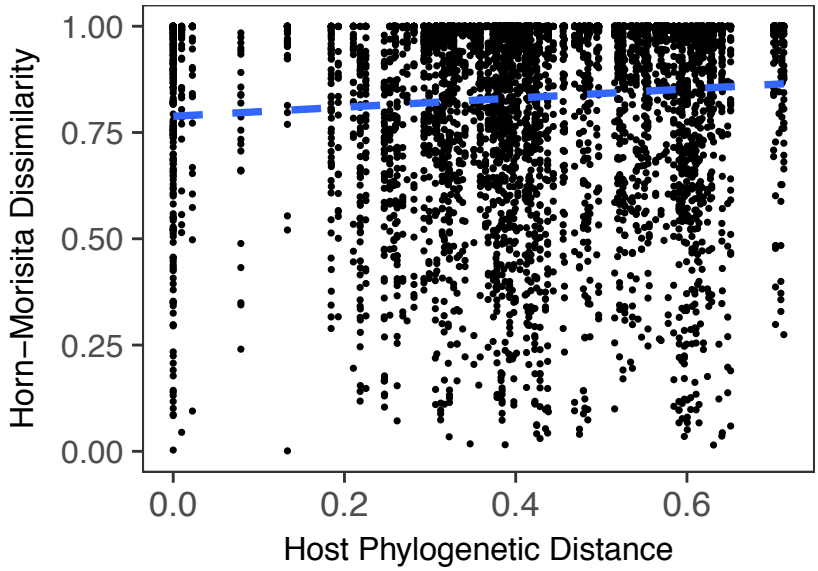

Fig. 6 – FFE community dissimilarity increased with increasing distance between common garden field plots. A regression of the pairwise dissimilarity between individual host-associated FEE communities (Horn-Morisita) plotted against the pairwise distance between plots in the common garden is shown (blue-dashed line). Each point represents a single pairwise comparison.

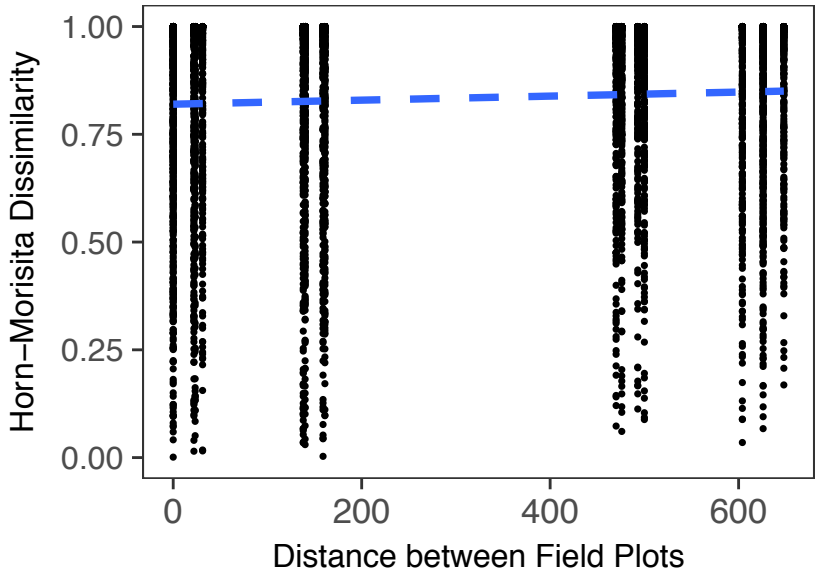

Table 1 – Common Garden plant species and taxonomic information.

Genus	Species	Abbreviation	Sub-Family	Tribe	Sub-Tribe
Plant species sampled for Illumina sequencing					
Antennaria	*plantaginifolia*	AntPlan	Asteroideae	Gnaphalieae	
Aster	*novae-angliae*	AstNov	Asteroideae	Asterae	
Boltonia	*asteroides*	BolAst	Asteroideae	Asterae	
Arnoglossum	*atriplicifolium*	CacAtri	Asteroideae	Senecioneae	
Arnoglossum	*plantagineum*	CacPlan	Asteroideae	Senecioneae	
Cirsium	*discolor*	CirDis	Carduoideae	Cardueae	Carduinae
Coreopsis	*tripteris*	CorTrip	Asteroideae	Heliantheae Alliance	Coreopsideae
Echinacea	*purpurea*	EchPur	Asteroideae	Heliantheae Alliance	Heliantheae
Eupatorium	*perfoliatum*	EupPer	Asteroideae	Heliantheae Alliance	Eupatorieae
Ageratina	*altissima*	EupRug	Asteroideae	Heliantheae Alliance	Eupatorieae
Helenium	*autumnale*	HeleAut	Asteroideae	Heliantheae Alliance	Helenieae
Heliopsis	*helianthoides*	HelHel	Asteroideae	Heliantheae Alliance	Heliantheae
Hieracium	*canadense*	HieCan	Cichorioideae	Cichorieae	Hieraciinae
Lobelia	*cardinalis*	LobCard	(*outgroup*) Campanulaceae Family		
Parthenium	*integrifolium*	ParInt	Asteroideae	Heliantheae Alliance	Heliantheae
Rudbeckia	*hirta*	RudHir	Asteroideae	Heliantheae Alliance	Heliantheae
Silphium	*perfoliatum*	SilPer	Asteroideae	Heliantheae Alliance	Heliantheae
Vernonia	*fasciculata*	VerFas	Cichorioideae	Vernonieae	Vernoniinae
Vernonia	*missurica*	VerMis	Cichorioideae	Vernonieae	Vernoniinae
Plant species not sampled for Illumina sequencing					
Eupatorium	*coelestinum*	EupCoel	Asteroideae	Heliantheae Alliance	Eupatorieae
Helianthus	*grosseserratus*	HeliGro	Asteroideae	Heliantheae Alliance	Heliantheae
Liatris	*spicata*	LiaSpic	Asteroideae	Heliantheae Alliance	Latrinae
Lobelia	*spicata*	LobSpic	(*outgroup*) Campanulaceae Family		
Prenanthes	*alba*	PreAlba	Cichorioideae	Cichorieae	Hypochaeridinae
Prenanthes	*racemosa*	PreRace	Cichorioideae	Cichorieae	Hypochaeridinae
Ratibida	*pinnata*	RatPin	Asteroideae	Heliantheae Alliance	Heliantheae
Solidago	*nemoralis*	SolNem	Asteroideae	Astereae	Solidagininae
Verbesina	*alternifolia*	ActAlt	Asteroideae	Heliantheae Alliance	Heliantheae
Verbesina	*helianthoides*	VerbHel	Asteroideae	Heliantheae Alliance	Heliantheae
Vernonia	*altissima*	VerAlt	Cichorioideae	Vernonieae	Vernoniinae

Taxonomic information is provided where applicable. For some species, plant sub-tribe is not defined.

Table 2 – Dufrene Legendre Indicator species associated with each host species.

OTU	Putative Fungal Name	Host Species	Indicator Value	Significance	FUNGuild	USDA Fungal Database
4	*Mycosphaerella spp.*	HeleAut RudHir	0.2315 0.1141	*0.0141*	*Plant Pathogen (probable)*	*Genus contains many pathogens*
8	*Unk. Order Pleosporales*	VerMis	0.4133	*0.0086*	*NA*	*NA*
9	*Mycosphaerella lateralis (#1)*	CacAtri BolAst	0.2369 0.1185	*0.0439*	*Plant Pathogen (probable)*	*Known pathogen on Eucalyptus trees*
10	*Unk. Fungi*	EupPer	0.9835	*0.0001*	*NA*	*NA*
17	*Mycosphaerella spp.*	HeleAut	0.8268	*0.0002*	*Plant Pathogen (probable)*	*Genus contains many pathogens*
20	*Unk. Order Agaricales*	SilPer	0.3471	*0.0122*	*NA*	*NA*
33	*Mycosphaerella spp.*	HeleAut	0.4988	*0.0035*	*Plant Pathogen (probable)*	*Genus contains many pathogens*
39	*Myrothecium roridum*	LobCard	0.4810	*0.0083*	*Saprotroph (probable)*	*Known pathogen – multiple hosts from multiple families*
42	*Unk. Sub-Phylum Pezizomycotina*	EchPur	0.3145	*0.0157*	*NA*	*NA*
59	*Mycosphaerella lateralis (#2)*	BolAst	0.4420	*0.0124*	*Plant Pathogen (probable)*	*Known pathogen on Eucalyptus trees*
72	*Unk. Fungi*	CorTrip	0.3017	*0.0464*	*NA*	*NA*
74	*Unk. Fungi*	VerFas	0.3333	*0.0434*	*NA*	*NA*
94	*Ramichloridium apiculatum*	AntPlan	0.3333	*0.0437*	*Plant Pathogen (probable)*	*Known pathogen, Potential saprotroph*
108	*Unk. Fungi*	EupPer	0.5000	*0.0017*	*NA*	*NA*
118	*Uwebraunia commune (#1)*	CacAtri	0.5736	*0.0009*	*Plant Pathogen (probable)*	*Known pathogen on Eucalyptus trees*
126	*Colletotrichum destructivum*	HieCan	0.5000	*0.0019*	*Plant Pathogen (probable)*	*Known pathogen – multiple hosts from multiple families*
146	*Peltaster fructicola*	VerFas	0.3333	*0.0427*	*Plant Pathogen (probable)*	*Known pathogen on apple trees*
148	*Uwebraunia commune (#2)*	CacAtri	0.5260	*0.0018*	*Plant Pathogen (probable)*	*Known pathogen on Eucalyptus trees*
171	*Unk. Family Didymellaceae*	AntPlan	0.3333	*0.0451*	*NA*	*NA*
193	*Unk. Family Trichosphaeriales inc. sed.*	ParInt	0.2789	*0.0497*	*NA*	*NA*
217	*Preussia pseudominima*	VerMis	0.3322	*0.0466*	*Saprotroph (probable)*	**No records*
218	*Unk. Order Pucciniales*	VerMis VerFas	0.5903 0.1490	*0.0002*	*NA*	*Rust Pathogen*
250	*Unk. Order Pleosporales*	EupPer	0.3295	*0.0318*	*NA*	*NA*
274	*Nigrospora oryzae*	HeleAut	0.3333	*0.0432*	*Saprotroph (probable)*	*Known pathogen, Known endophyte, Potential saprotroph*

Operational taxonomic units (OTUs) with significant indicator values ($p < 0.05$) are listed. Putative fungal names were assigned for each OTU by using the RDP naïve Bayesian classifier and Warcup and UNITE fungal databases. For simplicity, host species names are shortened to the first 3 letters of the genus, followed by the first 3-4 letters of the species name. For 'unknown' taxonomic levels, the abbreviation '*Unk.*' is used.

Supplementary Information

Figure S1. – Topographic map showing the layout of the common garden plots at Bayles Rd., Bloomington, IN. Black squares show the location of the six replicated plots.

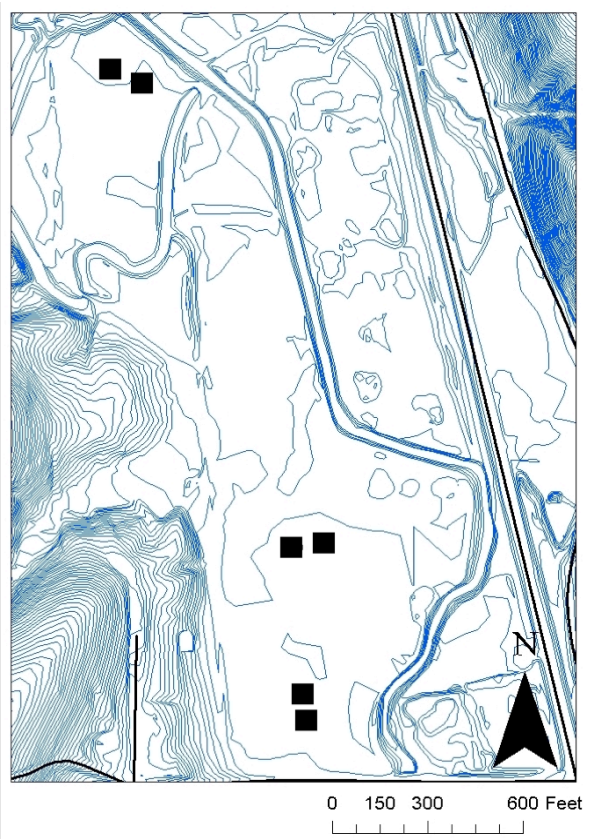

Table S1 – Putative fungal OTU taxonomic assignment (Warcup Naïve Bayesian Classifier, Fungal ITS Training Set) and confidence scores. Overall sequencing read counts provided.

OTU	Read Count	Warcup Taxonomic Assignment
1	947,714	Alternaria 1
2	575,794	Davidiella 1
3	484,732	Phaeosphaeria 0.93
4	327,148	Mycosphaerella 1

5	308,487	Phaeosphaeriaceae 0.9
6	278,743	Khuskia 0.96
7	132,997	Pleosporales 1
8	120,737	Pleosporales 0.91
9	93,856	Mycosphaerella lateralis 0.97
10	88,753	Fungi 1
11	75,944	Pezizomycotina 0.93
12	60,594	Paraphoma chrysanthemicola 0.97
13	57,103	Trichosphaeriales_Incertae sedis 0.99
14	55,476	Kabatiella 1
15	53,828	Stereum 0.98
16	51,727	Leptosphaerulina chartarum 1
17	51,685	Mycosphaerella 1
18	46,847	Lectera colletotrichoides 0.99
19	45,615	Trichosphaeriales_Incertae sedis 1
20	45,182	Agaricales 0.98
21	42,811	Paraphoma chrysanthemicola 0.95
22	42,075	Pichia jadinii 1
23	40,758	Didymellaceae 0.91
24	40,541	Hypoxylon perforatum 1
25	38,948	Mycosphaerella lateralis 0.94
26	37,345	Atheliaceae 0.94
27	36,963	Pleosporales 1
28	36,317	Fungi 1
29	35,383	Arthrinium phaeospermum 1
30	33,659	Didymella 0.9
31	33,362	Sordariomycetes 0.97
32	33,272	Pleosporales 1
33	33,032	Mycosphaerella 0.99
34	32,098	Fungi 1
35	32,041	Hypoxylon perforatum 1
36	31,956	Preussia pseudominima 0.9
37	31,832	Daldinia childiae 0.92
38	31,384	Mycosphaerella lateralis 0.97
39	25,049	Myrothecium roridum 0.94
40	24,252	Mycosphaerella lateralis 0.94
41	22,504	Peniophora 1
42	21,684	Pezizomycotina 0.92
43	21,156	Xylaria 0.93
44	20,752	Fungi 1
45	20,690	Rhodotorula mucilaginosa 0.95
46	20,646	Agaricomycotina 0.91
47	19,795	Golovinomyces 1
48	19,658	Paraconiothyrium 1
49	19,542	Fungi 1
50	19,439	Mycosphaerella 1
51	19,132	Alternaria 1
52	19,087	Khuskia 0.97
53	18,567	Fungi 1
54	18,139	Leotiomycetidae 0.92
55	18,098	Paecilomyces sinensis 1
56	16,708	Uwebraunia commune 0.96
57	16,521	Ceratobasidium sp AG_Bo 1
58	16,447	Diaporthe 1
59	15,891	Mycosphaerella lateralis 0.95
60	15,780	Exserohilum fusiforme 0.97

61	15,203	Trichosphaeriales_Incertae sedis 0.99
62	15,061	Phoma paspali 0.98
63	14,935	Agaricomycetes 1
64	14,875	Diaporthe stewartii 0.92
65	14,397	Davidiella 1
66	13,437	Pleosporales 1
67	13,431	Cryptococcus magnus 0.98
68	13,393	Eupenicillium 0.99
69	13,343	Fungi 1
70	13,127	Mycosphaerella 1
71	13,002	Cryptococcus sp AL_V 1
72	12,750	Fungi 1
73	12,471	Pleosporales 1
74	12,153	Fungi 1
75	12,010	Phaeosphaeria oryzae 0.93
76	11,835	Pleosporales 1
77	11,699	Khuskia 0.95
78	11,649	Fungi 1
79	11,223	Ceratobasidium sp AG_Fb 1
80	11,209	Abortiporus biennis 1
81	10,867	Didymellaceae 0.96
82	10,705	Pleospora 0.99
83	10,207	Phoma novae_verbascicola 0.97
84	10,153	Davidiella 1
85	9,926	Rhodotorula mucilaginosa 0.92
86	9,854	Pleosporales 1
87	9,445	Hypoxylon 0.92
88	9,384	Fungi 1
89	8,750	Didymella 0.9
90	8,612	Sordariomycetes 0.98
91	8,465	Pezizomycotina 0.9
92	8,305	Dioszegia 1
93	8,140	Pezizomycotina 0.93
94	7,987	Ramichloridium apiculatum 1
95	7,873	Dissoconium aciculare 0.99
96	7,713	Pezizomycotina 0.93
97	7,705	Candida parapsilosis 1
98	7,628	Pleosporales 1
99	7,602	Phaeosphaeria oryzae 0.96
100	7,441	Helotiales 0.96
101	7,290	Diaporthe 1
102	7,226	Trichosphaeriales_Incertae sedis 1
103	7,142	Didymella 0.9
104	6,668	Fungi 1
105	6,546	Pleosporales 1
106	6,405	Pleosporales 1
107	6,337	Mycosphaerella lateralis 0.94
108	6,316	Fungi 1
109	6,179	Khuskia 0.98
110	6,123	Mycosphaerella lateralis 0.94
111	6,106	Eurotium 1
112	5,872	Pezizomycotina 0.91
113	5,838	Davidiella 1
114	5,631	Rhodosporidium babjevae 1
115	5,436	Annulohypoxylon truncatum 0.98
116	5,121	Dokmaia monthadangii 0.99

117	5,110	Pezizomycotina 0.9
118	5,092	Uwebraunia commune 0.91
119	5,084	Daldinia 0.95
120	5,081	Sordariomycetidae 0.9
121	5,062	Didymella 0.9
122	4,983	Alternaria 1
123	4,933	Fungi 1
124	4,866	Ceriporia lacerata 0.98
125	4,703	Daldinia 1
126	4,657	Colletotrichum destructivum 0.97
127	4,626	Nectriaceae 1
128	4,459	Khuskia 0.98
129	4,447	Fungi 1
130	4,406	Khuskia 0.98
131	4,319	Dioszegia 1
132	4,195	Coprinellus velatopruinatus 1
133	4,169	Fungi 1
134	4,067	Dothideomycetes 0.98
135	4,008	Pleosporales 1
136	3,833	Mycosphaerella lateralis 0.94
137	3,798	Ascomycota 0.91
138	3,622	Xylariales 0.94
139	3,620	Mycosphaerella 0.97
140	3,585	Phoma novae_verbascicola 0.97
141	3,554	Nectriaceae 1
142	3,537	Fungi 1
143	3,513	Conocybe apala 1
144	3,487	Sordariomycetidae 0.9
145	3,372	Pleosporales 1
146	3,363	Peltaster fructicola 1
147	3,363	Uwebraunia commune 0.9
148	3,355	Uwebraunia commune 0.9
149	3,255	Fungi 1
150	3,215	Trichosphaeriales_Incertae sedis 0.99
151	3,211	Xylaria polymorpha 0.99
152	3,194	Hannaella oryzae 0.98
153	3,193	Microbotryomycetes_Incertae sedis 0.91
154	3,174	Fungi 1
155	3,094	Daldinia 0.95
156	3,074	Pleosporales 1
157	3,028	Trametes versicolor 0.97
158	2,969	Phaeosphaeria oryzae 0.92
159	2,823	Phialophora sessilis 0.96
160	2,796	Crepids mollis 0.95
161	2,796	Agaricomycetes 1
162	2,761	Sordariomycetes 0.9
163	2,616	Alternaria 1
164	2,601	Pezizomycotina 0.9
165	2,566	Phaeosphaeria oryzae 0.94
166	2,551	Glomerella 1
167	2,520	Didymella 1
168	2,506	Hypocreales_Incertae sedis 0.99
169	2,504	Whalleya microplaca 1
170	2,481	Trichosphaeriales_Incertae sedis 1
171	2,472	Didymellaceae 0.93
172	2,453	Agaricales 1

173	2,440	Xylaria longipes 1
174	2,437	Fungi 1
175	2,375	Gaeumannomyces graminis var graminis 0.95
176	2,284	Davidiella 1
177	2,267	Strelitziana 0.97
178	2,245	Pleosporales 1
179	2,224	Didymellaceae 0.91
180	2,194	Mycosphaerella 1
181	2,188	Fungi 1
182	2,174	Davidiella 1
183	2,148	Nemania sp JJP_2009a 1
184	2,120	Hypoxylon 1
185	2,119	Didymella 0.9
186	2,117	Nectriaceae 1
187	2,088	Ascomycota 0.9
188	2,058	Agaricomycotina 0.9
189	1,953	Hypoxylon 0.96
190	1,945	Didymella 0.99
191	1,917	Phoma paspali 0.98
192	1,867	Phoma paspali 0.99
193	1,861	Trichosphaeriales_Incertae sedis 0.99
194	1,835	Lectera colletotrichoides 0.99
195	1,832	Fungi 1
196	1,809	Kretzschmaria deusta 1
197	1,794	Mycosphaerella 1
198	1,793	Eutypella scoparia 0.99
199	1,781	Didymella 0.99
200	1,773	Davidiella 1
201	1,769	Fungi 1
202	1,742	Lectera colletotrichoides 0.99
203	1,740	Davidiella 1
204	1,726	Fungi 1
205	1,711	Didymella 0.9
206	1,680	Rhodotorula mucilaginosa 0.96
207	1,667	Curvularia trifolii 1
208	1,656	Daldinia 0.93
209	1,653	Hypocreales 0.97
210	1,621	Phaeosphaeria oryzae 0.94
211	1,615	Microsphaeropsis arundinis 0.92
212	1,610	Cochliobolus geniculatus 1
213	1,577	Mycosphaerella lateralis 0.94
214	1,565	Fungi 1
215	1,561	Mycosphaerella 1
216	1,544	Pleosporales 1
217	1,531	Preussia pseudominima 0.94
218	1,527	Pucciniales 1
219	1,512	Phaeosphaeria oryzae 0.93
220	1,488	Davidiella 1
221	1,480	Fungi 1
222	1,476	Fungi 1
223	1,475	Fungi 1
224	1,473	Itersonilia perplexans 1
225	1,468	Helotiales 0.98
226	1,458	Pleosporales 0.97
227	1,438	Mycosphaerella 1

228	1,428	Daldinia childiae 0.97
229	1,425	Phaeosphaeria 0.94
230	1,418	Hypocrea orientalis 1
231	1,414	Cryptococcus 0.96
232	1,402	Davidiella 1
233	1,400	Mycosphaerella 1
234	1,389	Kabatiella 1
235	1,368	Didymellaceae 0.91
236	1,364	Pleosporales 1
237	1,362	Davidiella 1
238	1,343	Agaricomycetes 0.95
239	1,325	Mrakia 1
240	1,324	Pezizomycotina 0.96
241	1,308	Magnaporthe oryzae 0.96
242	1,301	Agaricomycetidae 0.9
243	1,300	Pleosporales 1
244	1,290	Mycosphaerella lateralis 0.98
245	1,272	Didymella 0.9
246	1,253	Pleosporales 0.97
247	1,247	Pleosporales 1
248	1,245	Sordariales 0.92
249	1,240	Davidiella 1
250	1,233	Pleosporales 0.99
251	1,216	Hypoxylon macrocarpum 1
252	1,204	Hypoxylon fragiforme 0.97
253	1,186	Khuskia 0.96
254	1,182	Didymella 0.9
255	1,169	Pezizomycotina 0.9
256	1,153	Trichosphaeriales_Incertae sedis 1
257	1,152	Seimatosporium discosioides 0.96
258	1,135	Davidiella 1
259	1,123	Pleosporales 1
260	1,120	Pleosporales 1
261	1,120	Mycosphaerella 1
262	1,116	Trichosphaeriales_Incertae sedis 1
263	1,103	Fungi 1
264	1,093	Phoma 0.99
265	1,084	Fungi 1
266	1,083	Phaeosphaeria oryzae 0.98
267	1,081	Pezizomycotina 0.91
268	1,063	Uwebraunia commune 0.93
269	1,057	Uwebraunia commune 0.9
270	1,052	Agaricomycotina 0.94
271	1,051	Paraphoma chrysanthemicola 0.96
272	1,044	Davidiella 0.98
273	1,035	Hannaella oryzae 0.98
274	1,034	Nigrospora oryzae 0.91
275	1,030	Didymellaceae 1
276	1,010	Didymellaceae 1
277	1,008	Fungi 1
278	1,006	Lectera colletotrichoides 0.98
279	1,003	Fungi 1
280	1,002	Gibellulopsis 0.91
281	1,001	Sclerotiniaceae 1
282	1,001	Phoma 0.98
283	995	Coprinopsis 0.99

284	995	Alternaria 1
285	992	Didymellaceae 0.98
286	992	Phoma 0.98
287	990	Khuskia 0.98
288	975	Pleosporales 0.96
289	975	Didymella 0.98
290	966	Trichosphaeriales_Incertae sedis 1
291	960	Trichosphaeriales_Incertae sedis 0.98
292	957	Pucciniomycotina 0.97
293	941	Ascomycota 0.92
294	938	Basidiomycota 0.91
295	936	Coprinopsis strossmayeri 1
296	921	Didymella 0.98
297	915	Didymella 0.9
298	911	Rhodotorula ingeniosa 0.93
299	894	Pleosporales 1
300	889	Trichosphaeriales_Incertae sedis 0.98
301	888	Ophiognomonia 0.94
302	884	Pluteus 0.99
303	871	Xylaria oxyacanthae 1
304	871	Ascomycota 0.92
305	858	Glomerella 1
306	857	Agaricomycotina 0.95
307	845	Phoma novae_verbascicola 0.96
308	844	Phaeosphaeria oryzae 0.94
309	838	Phaeosphaeria oryzae 0.98
310	835	Paecilomyces sinensis 0.96
311	833	Daldinia 0.95
312	830	Pleosporales 1
313	828	Phoma novae_verbascicola 0.98
314	810	Trichosphaeriales_Incertae sedis 1
315	768	Sordariomycetes 0.96
316	762	Microdochium bolleyi 0.95
317	747	Khuskia 0.94
318	736	Mycosphaerella 0.99
319	733	Dothideomycetes 0.92
320	730	Paecilomyces sinensis 0.93
321	725	Eurotium 1
322	725	Mortierella 1
323	723	Uwebraunia commune 0.9
324	713	Davidiella 1
325	707	Davidiella 1
326	699	Pleosporales 1
327	697	Sordariomycetidae 0.96
328	682	Gibberella 1
329	680	Dissoconium aciculare 0.99
330	679	Agaricomycetidae 1
331	678	Tremellales_Incertae sedis 1
332	675	Trichosphaeriales_Incertae sedis 0.98
333	662	Mycosphaerella 1
334	659	Daldinia 0.9
335	658	Phoma paspali 0.99
336	656	Trichosphaeriales_Incertae sedis 0.99
337	654	Ascomycota 0.92
338	645	Plectosphaerella 0.94
339	643	Lewia 0.92

340	638	Paecilomyces 0.98
341	637	Davidiella 1
342	635	Khuskia 0.98
343	625	Phaeosphaeria oryzae 0.93
344	614	Mycosphaerella 0.91
345	603	Mycosphaerella 1
346	602	Didymella 0.99
347	598	Pichia jadinii 1
348	595	Didymella 0.92
349	592	Didymellaceae 1
350	581	Fungi 1
351	578	Ascomycota 0.91
352	562	Phaeosphaeria oryzae 0.95
353	562	Nectriaceae 1
354	561	Phaeosphaeria oryzae 0.94
355	557	Ascomycota 0.9
356	556	Pleosporales 1
357	554	Phoma 0.98
358	554	Dinemasporium strigosum 0.97
359	545	Pleosporales 1
360	537	Didymellaceae 1
361	532	Pleosporales 1
362	529	Alternaria 1
363	528	Eurotium 1
364	526	Tremellales_Incertae sedis 0.99
365	522	Cryptococcus 0.97
366	518	Phoma 0.98
367	498	Davidiella 1
368	491	Leotiomycetidae 0.9
369	481	Pestalotiopsis 1
370	477	Davidiella 1
371	475	Fungi 1
372	474	Fungi 1
373	472	Herpotrichiellaceae 0.93
374	460	Phoma paspali 0.99
375	456	Phaeosphaeria oryzae 0.92
376	456	Phaeosphaeria oryzae 0.95
377	450	Sporidiobolus 0.98
378	447	Pleosporales 1
379	441	Didymellaceae 0.91
380	440	Phaeosphaeria oryzae 0.92
381	440	Didymella 0.91
382	435	Pleosporales 1
383	434	Sphaceloma 1
384	433	Khuskia 0.98
385	425	Dokmaia monthadangii 0.99
386	422	Phaeosphaeria oryzae 0.92
387	421	Didymella 0.99
388	420	Agaricomycotina 0.96
389	418	Paraphaeosphaeria michotii 1
390	414	Uwebraunia commune 0.93
391	412	Preussia pseudominima 0.98
392	405	Mycosphaerella 1
393	401	Pleosporales 1
394	386	Eurotium 1
395	384	Didymella 0.9

396	381	Davidiella 1
397	379	Helotiales 0.97
398	374	Nectriaceae 1
399	371	Fungi 1
400	368	Khuskia 0.97
401	368	Paecilomyces sinensis 1
402	359	Pleosporales 0.96
403	352	Trichosphaeriales_Incertae sedis 1
404	350	Pezizomycotina 0.94
405	345	Didymella 0.99
406	334	Pleosporales 1
407	328	Ramichloridium apiculatum 1
408	327	Daldinia 0.94
409	326	Cryptococcus aureus 0.9
410	326	Davidiella 1
411	325	Davidiella 1
412	325	Gibellulopsis 0.95
413	319	Phoma paspali 0.99
414	318	Coprinellus disseminatus 1
415	316	Cryptococcus magnus 1
416	316	Paecilomyces sinensis 0.95
417	306	Khuskia 0.97
418	303	Pezizomycotina 0.94
419	302	Uwebraunia commune 0.9
420	302	Mycosphaerella 0.97
421	301	Glomerella 1
422	300	Didymella 0.9
423	294	Cladosporium dominicanum 1
424	288	Pleosporales 1
425	281	Khuskia 0.98
426	278	Pleosporales 1
427	272	Malassezia globosa 1
428	269	Didymella 0.99
429	266	Pleosporales 1
430	264	Eupenicillium 0.99
431	263	Didymellaceae 1
432	255	Khuskia 0.97
433	255	Plectosphaerella 0.94
434	253	Paecilomyces sinensis 0.91
435	252	Preussia pseudominima 0.97
436	248	Didymella 0.9
437	245	Cryptococcus aureus 0.95
438	239	Kabatiella 1
439	238	Cryptococcus aureus 0.95
440	231	Didymellaceae 0.99
441	230	Pleosporales 1
442	226	Kretzschmaria deusta 0.99
443	226	Auriculibuller fuscus 1
444	218	Agaricomycotina 0.91
445	218	Nectriaceae 1
446	216	Pleosporales 1
447	214	Bionectria 1
448	213	Didymellaceae 1
449	213	Davidiella 1
450	212	Didymella 0.9
451	209	Pleosporales 0.99

452	207	Fungi 1
453	206	Didymellaceae 1
454	204	Khuskia 0.96
455	200	Fungi 1
456	200	Hyphodontia flavipora 1
457	199	Trichosphaeriales_Incertae sedis 0.99
458	195	Pezizomycotina 0.96
459	194	Trichosphaeriales_Incertae sedis 0.98
460	191	Paecilomyces sinensis 0.97
461	188	Ascomycota 0.95
462	181	Mycosphaerella lateralis 0.94
463	180	Didymella 0.99
464	176	Nectriaceae 1
465	174	Phoma novae_verbascicola 0.98
466	171	Dissoconium aciculare 0.99
467	169	Dissoconium aciculare 0.99
468	165	Mycosphaerella lateralis 0.97
469	163	Diaporthe 1
470	161	Myrothecium roridum 0.97
471	160	Pezizomycotina 0.93
472	158	Daldinia 0.94
473	157	Didymella 0.99
474	155	Fungi 1
475	154	Didymellaceae 1
476	153	Didymella 0.99
477	152	Hannaella 0.92
478	151	Pezizomycotina 0.99
479	151	Didymella 0.99
480	150	Mycosphaerella lateralis 0.94
481	146	Lectera colletotrichoides 0.94
482	139	Phoma 0.98
483	134	Didymellaceae 0.96
484	134	Pezizomycotina 0.9
485	133	Fungi 1
486	131	Myrothecium 0.99
487	125	Sordariomycetes 0.94
488	125	Fungi 1
489	124	Plectosphaerella 0.94
490	124	Didymellaceae 1
491	123	Trichosphaeriales_Incertae sedis 1
492	121	Davidiella 1
493	121	Nectriaceae 1
494	117	Didymella 0.97
495	112	Davidiella 0.98
496	111	Didymellaceae 0.93
497	109	Cryptococcus aureus 0.9
498	106	Diaporthe 1
499	104	Mycosphaerella 1
500	103	Fungi 1
501	101	Fungi 1
502	99	Cryptococcus paraflavus 0.97
503	98	Davidiella 0.99
504	98	Trichosphaeriales_Incertae sedis 0.98
505	97	Phoma 0.98
506	97	Ascomycota 0.9
507	92	Phoma 0.98

508	88	Didymella 0.9
509	87	Phoma novae_verbascicola 0.97
510	86	Phoma novae_verbascicola 0.96
511	85	Mycosphaerella lateralis 0.94
512	83	Khuskia 1
513	83	Fungi 1
514	82	Phoma novae_verbascicola 0.97
515	80	Ascomycota 0.9
516	78	Ascomycota 0.9
517	77	Fungi 1
518	76	Pezizomycotina 0.97
519	69	Pezizomycotina 0.9
520	68	Khuskia 0.97
521	65	Tremellales_Incertae sedis 0.99
522	63	Pezizomycotina 0.9
523	61	Pleosporales 0.96
524	61	Phoma novae_verbascicola 0.95
525	57	Mycosphaerella lateralis 0.94
526	56	Didymella 0.99
527	52	Tremellales_Incertae sedis 1
528	51	Pleosporales 1
529	50	Cryptococcus paraflavus 0.97
530	50	Didymellaceae 1
531	49	Ascomycota 0.9
532	49	Preussia pseudominima 0.98
533	49	Alternaria 1
534	48	Pezizomycotina 0.99
535	47	Dinemasporium strigosum 0.97
536	44	Mycosphaerella lateralis 0.94
537	43	Pleosporales 1
538	41	Preussia pseudominima 0.98
539	34	Dothideomycetes 0.98
540	33	Plectosphaerella 0.94
541	33	Tremellales_Incertae sedis 0.98
542	32	Fungi 1
543	32	Xylaria 0.92
544	31	Diaporthe 0.99
545	30	Fungi 1
546	28	Cryptococcus 0.99
547	27	Pezizomycotina 0.94
548	18	Pezizomycotina 0.93
549	14	Cryptococcus 0.98
550	12	Pezizomycotina 0.96
551	11	Tremellales_Incertae sedis 1
552	11	Tremellales_Incertae sedis 1
553	9	Trichosphaeriales_Incertae sedis 1
554	8	Khuskia 0.93
555	8	Pleosporales 1
556	8	Didymellaceae 0.91
557	7	Didymella 0.98
558	7	Mycosphaerella 0.93
559	5	Hannaella oryzae 0.96

Table S2

Plant ITS GenBank accession numbers used in phylogenetic tree reconstruction. For simplicity, host species names are shortened to the first 3 letters of the genus, followed by the first 3-4 letters of the species name.

Host Spp. Code	GenBank Accession & Version No.	Sequenced Species Name
AntPlan	JX524601.1	*Antennaria plantaginifolia*
AstNov	JQ360398.1	*Symphyotrichum novae-angliae*
BolAst	AF046975.1	*Boltonia asteroides*
CacAtri	KJ418356.1	*Arnoglossum atriplicifolium*
CacPlan	KJ418354.1	*Arnoglossum plantagineum*
CirDis	KC603916.1	*Cirsium discolor*
CorTrip	KM347936.1	*Coreopsis tripteris*
EchPur	GQ864125.1	*Tithonia calva* (contribal)
EupPer	DQ415741.1	*Eupatorium perfoliatum*
EupRug	JQ737035.1	*Ageratina wrightii*
HeleAut	KF607068.1	*Helenium autumnale*
HelHel	AF374914.1	*Trichocoryne connate* (contribal)
HieCan	KT249913.1	*Hieracium umbellatum* (congeneric)
LobCard	AY350630.1	*Lobelia cardinalis*
ParInt	AY947417.1	*Parthenium hysterophorus* (congeneric)
RudHir	AF047901.1	*Helianthus niveus* (contribal)
SilPer	AY196733.1	*Silphium gracile* (congeneric)
VerFas	EF155816.1	*Vernonia fasciculata*
VerMis	KC603926.1|	*Vernonia missurica*

Table S3 – Hierarchical classification for all fungal OTUs. Putative fungal names and hierarchy were assigned for each OTU by using the RDP naïve Bayesian classifier and Warcup fungal databases. Numbers in parentheses indicate how many OTUs were identified at each level in the fungal taxonomic hierarchy.

Phylum	Class	Order	Family
Unidentified (47)			
Zygomycota (1)	Mucoromycotina Incertae sedis (1)	Mortierellales (1)	Mortierellaceae (1)
Ascomycota (439)	Unidentified (36)		
	Dothideomycetes (251)	Unidentified (3)	
		Capnodiales (78)	**Mycosphaerellaceae (78)**
		Pleosporales (165)	Unidentified (46)
			Didymellaceae (62)
			Phaeosphaeriaceae (19)
			Pleosporales Incertae sedis (14)
			Pleosporaceae (12)
			Sporormiaceae (6)
			Montagnulaceae (3)
			Leptosphaeriaceae (3)
		Dothideales (3)	Dothioraceae (3)
		Myriangiales (1)	Elsinoaceae (1)
		Dothideomycetes Incertae sedis (1)	Dothideomycetes Incertae sedis (1)
	Eurotiomycetes (17)	Chaetothyriales (3)	Herpotrichiellaceae (2)
			Chaetothyriales Incertae sedis (1)
		Eurotiales (14)	Trichocomaceae (14)
	Leotiomycetes (7)	Unidentified (2)	
		Erysiphales (1)	Erysiphaceae (1)
		Helotiales (4)	Unidentified (3)
			Sclerotiniaceae (1)
	Saccharomycetes (3)	Saccharomycetales (3)	Pichiaceae (2)
			Saccharomycetales Incertae sedis (1)
	Sordariomycetes (123)	Unidentified (8)	
		Diaporthales (7)	Diaporthaceae (6)
			Valsaceae (1)
		Hypocreales (16)	Unidentified (1)
			Nectriaceae (9)
			Hypocreales Incertae sedis (4)
			Hypocreaceae (1)
			Bionectriaceae (1)
		Sordariales (1)	Unidentified (1)

			Plectosphaerellaceae (11)
		Sordariomycetidae Incertae sedis (18)	Glomerellaceae (4)
			Magnaporthaceae (2)
			Apiosporaceae (1)
		Trichosphaeriales (39)	**Trichosphaeriales Incertae sedis (39)**
			Unidentified (1)
			Xylariaceae (27)
		Xylariales (34)	Xylariales Incertae sedis (2)
			Amphisphaeriaceae (2)
			Hyponectriaceae (1)
			Diatrypaceae (1)
	Pezizomycotina Incertae sedis (2)	Pezizomycotina Incertae sedis (2)	Pezizomycotina Incertae sedis (2)
Basidiomycota (69)	Unidentified (8)		
		Unidentified (5)	
			Unidentified (2)
			Psathyrellaceae (4)
		Agaricales (9)	Pluteaceae (1)
			Cortinariaceae (1)
			Bolbitiaceae (1)
	Agaricomycetes (23)	Atheliales (1)	Atheliaceae (1)
		Cantharellales (2)	Ceratobasidiaceae (2)
		Hymenochaetales (1)	Schizoporaceae (1)
			Polyporaceae (1)
		Polyporales (3)	Meripilaceae (1)
			Hapalopilaceae (1)
		Russulales (2)	Stereaceae (1)
			Peniophoraceae (1)
		Unidentified (1)	
	Microbotryomycetes (7)	Sporidiobolales (6)	Sporidiobolales Incertae sedis (5)
			Sporidiobolaceae (1)
	Pucciniomycetes (1)	Pucciniales (1)	Unidentified (1)
		Cystofilobasidiales (2)	Cystofilobasidiaceae (2)
	Tremellomycetes (29)	**Tremellales (27)**	Tremellales Incertae sedis (14)
			Tremellaceae (13)
	Ustilaginomycotina Incertae sedis (1)	Malasseziales (1)	Malasseziales Incertae sedis (1)

Figure S2 – Average (A) Leaf Mass per Area (LMA) and Sequencing Reads varied among host species but sequencing reads did not predict LMA (*p= 0.6661*). Boxplots are displayed for each species. Each point represents a single host individual. LMA has been square-root transformed for normality. For both panels, species are sorted alphabetically from bottom to top.

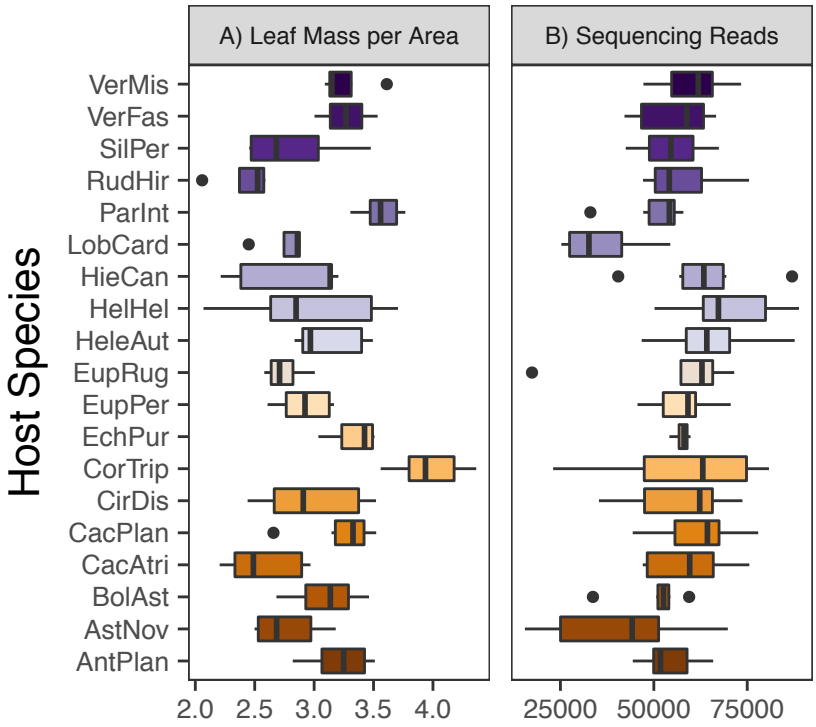

Figure S3 – Quadratic regression (blue dashed line) of Leaf-Mass Area (LMA) against individual host size. Each point represents a single host individual. Individual plant size was qualitatively assigned to one of five size classes at the time of leaf collection. (Quadratic Term *p= 0.0218*; Linear Term *p= 0.0034*).

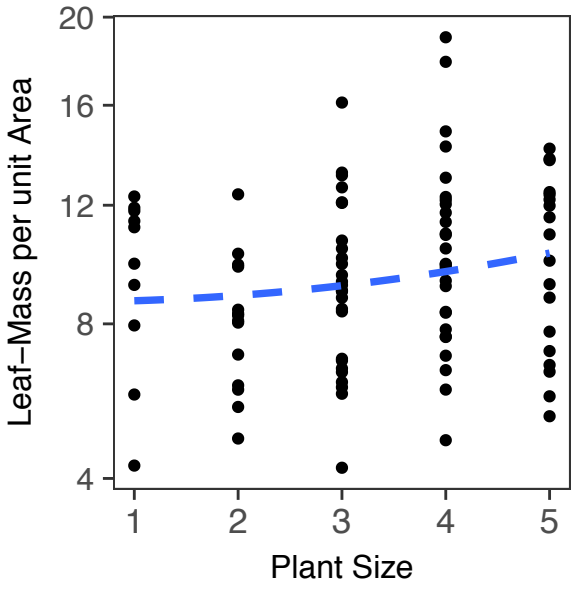

Figure S4 FFE community a) richness and b) diversity per unit leaf mass did not vary significantly among common garden plots. Boxplots are displayed for each common garden plot.

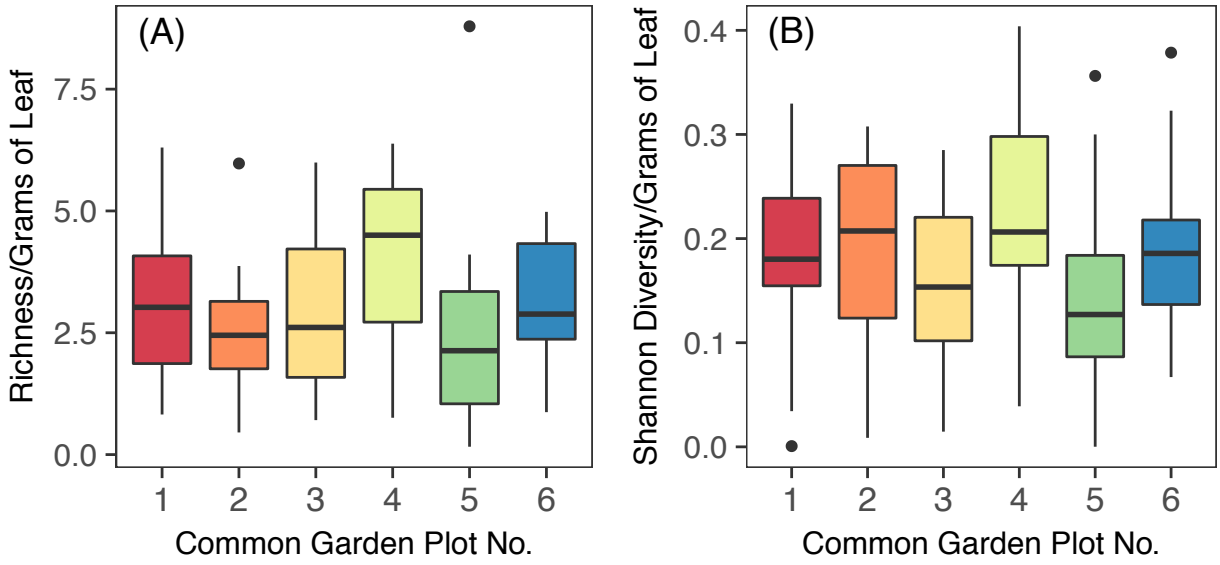

Negative plant-phyllosphere feedbacks in native Asteraceae hosts – a novel extension of the plant-soil feedback framework

Briana K. Whitaker[1], Jonathan T. Bauer[1], James D. Bever[2], Keith Clay[1]

[1] Department of Biology, Jordan Hall, 1001 E. 3rd St, Indiana University, Bloomington, IN, 47405-3700

[2] Department of Ecology and Evolutionary Biology, Higuchi Hall, 2101 Constant Ave., University of Kansas, Lawrence, KS, 66047-7503

Emails: brkawhit@indiana.edu ; jonathantbauer@gmail.com ; jbever@ku.edu ; clay@indiana.edu

Author for correspondence: Briana K. Whitaker

Address: Department of Biology, Jordan Hall, 1001 E. 3rd St, Indiana University, Bloomington, IN, 47405-3700 ; Tel: (+1) 8128551674 ; Email: brkawhit@indiana.edu

Statement of Authorship: BKW and JTB collected data. BKW curated the raw data files. BKW, JTB, and JDB performed statistical analyses. BKW wrote the first draft of the manuscript. All authors contributed substantially to project design and manuscript revisions.

Keywords: ***Negative feedback, foliar endophyte, pathogen, soil microbiota, plant population dynamics, fungi, bacteria, leaf litter, rhizosphere***

Data Accessibility Statement The raw data (.CSV format) and SAS statistical code (.SAS and .PDF formats) are available via the Dryad Digital Repository: http://dx.doi.org/10.5061/dryad.85641

Article Type: Letters ; **Word Count:** Abstract (149), Main Text (4997), Introduction (1191), Materials and Methods (1941), Results (538), Discussion (1327) ; **Number of:** References (61), Figures (5), Tables (0), Text Boxes (0)

ABSTRACT

Over the past 25 years, the plant-soil feedback framework has catalyzed our understanding of how belowground microbiota impact plant fitness and species coexistence. Here we apply a novel extension of this framework to microbiota associated with aboveground tissues, termed "plant-phyllosphere feedback". In parallel greenhouse experiments, rhizosphere and phyllosphere microbiota of con- and heterospecific hosts from four species were independently manipulated. In a third experiment, we tested the combined effects of soil and phyllosphere feedback under field conditions. We found that three of four species experienced weak negative plant-soil feedback whereas, by contrast, all four species experienced strong negative plant-phyllosphere feedback. Field-based feedback estimates were highly negative for all four species, though variable in magnitude. Our results suggest that phyllosphere microbiota, like rhizosphere microbiota, can potentially mediate plant species coexistence via negative feedbacks. Extension of the plant-soil feedback framework to the phyllosphere is needed to more fully elucidate plant-microbiota interactions.

INTRODUCTION

Theoretical and empirical advances over the past 20 years have been achieved in the study of belowground microbial dynamics by using the plant-soil feedback (PSF) framework (van der Putten et al. 1993, Bever et al. 1997, Klironomos 2002, Schnitzer et al. 2011). Advances include a greater appreciation of soil microbiota as a potential mechanism for species coexistence (Petermann et al. 2008), regulator of plant community diversity patterns and dynamics (Mangan et al. 2010), and axis of the species niche (Bauer et al. 2015). By contrast, experimental research on aboveground, phyllosphere microbiota is less common compared to research on soil microbiota (Arnold et al. 2003, Peñuelas and Terradas 2014). For example, phyllosphere research has historically focused on experimental inoculations of individual microbes or a small subset of the community onto a single host species (Meija et al. 2014), with only more recent efforts in microbiome characterization (Suryanarayanan 2013). Further, there has been less emphasis on the potential role of phyllosphere communities in regulating intra- and interspecific plant competition and population dynamics (Bever et al. 2015). Here we elucidate, for the first time, the host-specific fitness consequences of phyllosphere microbiota by extending PSF to plant-phyllosphere interactions.

The PSF Framework: The PSF framework has been used to understand the spatial distribution of plant populations (Packer and Clay 2000, Bagchi et al. 2014), plant species coexistence (Mangan et al. 2010), early-to-late successional species transitions (Kardol et al. 2006, van de Voorde et al. 2011, Bauer et al. 2015), and invasion dynamics (Mitchell and Power 2003, Callaway et al. 2004). More recently the PSF framework has been integrated with other ecological concepts, including functional trait theory (Kardol et al. 2015, Ke et al. 2015), nutrient cycling under changing climate and land use (van der Putten et al. 2016), and competition trade-

off theory (Albornoz et al. 2016). The PSF framework posits that mechanisms for plant species coexistence include not only competition (Casper and Castelli 2007), but also con- and heterospecific fitness effects mediated by belowground microbiota (Revilla et al. 2013) and soil nutrient cycling (Meisner et al. 2012). Experimental manipulation of host-specific soil inoculum independently of competitive interactions can isolate microbially-mediated PSF effects (Bever et al. 1997). Specifically, the PSF framework predicts that host fitness effects will be greatest when the soil microbiota is dominated by organisms that have high host-specificity and/or relative fitness when associated with that host (Ehrenfeld et al. 2005).

The direction of the host fitness response will depend on the degree of pathogenicity, parasitism, or mutualism displayed by the collective soil biota (van der Putten et al. 2016). If the soil biota has strong mutualistic effects on conspecific hosts, but strong antagonistic effects on co-occurring heterospecifics, positive feedback will lead to local dominance of that species receiving the greater net benefit (Bever et al. 2012). However, if the soil biota has greater antagonistic effects on conspecific hosts, relative to heterospecific hosts, negative feedback can lead to local plant species coexistence and greater system stability via greater self-limitation (Petermann et al. 2008).

Phyllosphere Microbiota: Phyllosphere microbiota form diverse and complex communities in aboveground tissues of their hosts, and include bacterial, archaeal, and eukaryotic taxa, spanning diverse functional and trophic roles (Peñuelas and Terradas 2014). Both above- and belowground tissues of all plant species are colonized by horizontally-transmitted microbiota (Rodriguez et al. 2009). By contrast, the aboveground, but not belowground, tissues of a few specialized plant lineages are infected by hereditary, seed-transmitted fungi (e.g., cool-season grasses, locoweeds, and morning glories; Rodriguez *et al.*

2009; Panaccione *et al.* 2014). More generally, host specificity of horizontally-transmitted microbiota in the phyllosphere is considered to span a spectrum from highly host specific (Laine et al. 2014) to host generalist (Suryanarayanan 2013), similarly to rhizosphere microbiota. Several approaches have been utilized to understand the assembly and diversity of these environmentally-acquired communities. Leaf exclosure experiments (Kaneko & Kaneko 2004) and rainwater collection in the understory (Wilson 1996) indicate that phyllosphere communities arise from propagules dispersed by air and rain (Christian et al. 2015). Additionally, leaf litter can be an important propagule source for phyllosphere community assembly (Herre et al. 2007, Monteil et al. 2012), particularly following seed germination and early plant development. Over longer time periods, decomposing litter can eventually contribute to rhizosphere communities (U'Ren and Arnold 2016). Several studies have measured direct, conspecific effects induced by phyllosphere microbiota using *in vivo* inoculation, or have extrapolated the functional consequences of host colonization using *in vitro* competition assays for specific taxa (Mejia et al. 2008, Li et al. 2010). Taken together, these approaches indicate that phyllosphere microbes can act as pathogens (Laine et al. 2014), mutualists (Meija et al. 2014, Busby et al. 2016), or saprotrophs (Song et al. 2016) for host plants.

While inoculation and microbiome characterization studies represent valuable first steps towards revealing the functional roles of phyllosphere microbiota, connecting phyllosphere communities to larger questions of plant population dynamics and species coexistence have rarely been addressed. For example, hosts that are colonized by phyllosphere microbiota could experience positive feedback via indirect effects, if those microbiota spill over and induce disease in less tolerant, competing hosts (Stergiopoulos & Gordon 2014; Parker *et al.* 2015). Alternatively, host species that support defensive, but costly, host-specific mutualists could

outcompete heterospecifics under conditions of high enemy pressure, also leading to positive feedback (Clay et al. 2005). Negative feedback could occur when phyllosphere communities have stronger pathogenic effects on conspecific relative to heterospecific hosts – as has been suggested by previous studies on host-specific foliar pathogens (reviewed in Mordecai 2011).

Microbiota-mediated fitness effects: Most previous plant-feedback experiments have exclusively manipulated soil inoculum to examine microbial effects or have manipulated litter inoculum to determine long-term effects due to nutrient cycling (Ehrenfeld et al. 2005, Meisner et al. 2012), without regard for the potential effects of aboveground microbiota on plant fitness and species coexistence. We therefore suggest that the PSF framework be adapted for the study of phyllosphere microbiota via experimental manipulation of phyllosphere inocula sources and host species identity. We define 'plant-phyllosphere feedbacks' (PPFs) as microbiota-mediated fitness differences between plants grown in the presence of phyllosphere communities associated with neighboring con- or heterospecific plants. This concept mirrors that of PSFs (Bever et al. 2015), and similarly focuses on measuring the net effects of phyllosphere communities on plant-plant interactions rather than characterizing microbial community makeup.

The goal of this research was to determine the fitness consequences of the phyllosphere community on hosts, and to compare these effects with those of the soil community. In particular, we predicted that 1) inoculation with conspecific phyllosphere microbiota would induce greater fitness costs relative to inoculation with heterospecific microbiota (i.e., negative feedback), in concordance with the preponderance of effects resulting from plant-soil manipulations (Kulmatiski et al. 2008). In addition, we predicted that 2) soil microbiota would also have strong negative feedback effects, due to the constant exposure of roots to soil inoculum and high degree of dispersal limitation in the soil. Lastly, we predicted that 3) the combined

effects of PSF and PPF would be magnified under field, relative to greenhouse, conditions where plants are simultaneously exposed to both soil and phyllosphere inocula, as well as a wide range of natural stressors.

MATERIALS AND METHODS

To address our predictions, we established three independent experiments to quantify rhizosphere and phyllosphere feedbacks across four plant species. Each experiment used a complete factorial (i.e., all pairwise combinations of con- and heterospecific inoculations), randomized design and was deliberately designed to mirror the other two. Two greenhouse experiments were performed to test for the presence of PSFs (Experiment 1) and PPFs (Experiment 2), respectively. We also performed a third experiment in the field (Experiment 3) to measure the simultaneous effects of both PSFs and PPFs under realistic ecological conditions (Fig. 1). Due to differences in the methodology and study conditions between experiments, as well as potential differences in microbial density between the soil and phyllosphere inoculum, direct statistical comparisons among experiments were not appropriate or performed.

The four plant species used in this experiment were: *Symphyotrichum novae-angliae* (L.) G.L. Newsom (AN; formerly *Aster novae-angliae*), *Arnoglossum atriplicifolium* (L.) H. Rob (CA; formerly *Cacalia atriplicifolia*), *Eupatorium perfoliatum* L. (EP), and *Vernonia missurica* Raf. (VM). All four species are native to the Midwestern US and are members of the family Asteraceae. Microbial inoculum sources for all three experiments and all host species were obtained from the soil and aboveground tissues of two-year old host plants (Fig. 1) growing in a common garden at the Indiana University Research and Teaching Preserve Bayles Road field site in Bloomington, IN USA (39°13'03.6"N 86°32'24.4"W). The common garden was laid out as a

six-plot, full-factorial, replicated design (Supporting Information [SI] Figure S1) and is described in the SI Methods. Control inoculum treatments differed between experiments. Control plants received sterilized, bulk field soil in experiment 1 and the absence of phyllosphere inocula in experiment 2. No sterile control treatment was possible under field conditions in experiment 3.

For each experiment, the four species were grown in the presence of both an adult conspecific's microbiota, as well as each of the three-heterospecific species' microbiota. Experiments 1 and 2 each consisted of 144 plants (4 species x 4 species-specific inocula sources, with 12 replicates for conspecific inoculum, 6 replicates for each of the three heterospecific inoculums, and 6 replicates for the control). Experiment 3 consisted of 120 plants (4 species x 4 species-specific inocula sources, with 12 replicates grown under conspecific adults in the common garden and 6 replicates grown under all three types of heterospecific adults). Plants in experiments 1 and 2 were divided among three experimental blocks in the greenhouse, while plants in experiment 3 were divided across the six plots of the common garden.

Seeds of each species were purchased from the same supplier as the common garden plants (Prairie Moon Nursery, Winona, MN) and were cold stratified in moist, sterilized sand for four weeks. Sand was sterilized by autoclaving for two hours. Seeds were germinated in commercial potting mix (Metro-Mix 360, Sun Gro Horticulture, Agawam, MA), sterilized by autoclaving for four hours, and grown under identical conditions in the greenhouse. The timeline for all three experiments is presented in SI Table S1.

Experiment 1 – Soil Inoculation: Seedlings were grown in 20.3cm square flats for 5 weeks after germination. Seedlings were then transplanted into 12.7cm round (1082mL) pots filled partially with sterilized background soil (50:50 mixture of Crider series silt-loam topsoil and coarse sand), which was sterilized by autoclaving twice for 4hrs, with a one-day rest period

in between. Soil inoculum was added at 10% v/v to the sterile background soil and the pots capped with another small layer of sterile background soil (Fig. 1A; *as in* Bauer *et al.* 2015). The live soil inoculum was obtained from second-year common garden plants using a 2.5 x 30 cm corer. Specifically, a total of 5-6 soil cores were collected per focal species from each common garden plot. Soil cores were pooled within plots from two replicate adult host plants, but not across plots or species. For the sterile control treatments, all remaining common garden soil was bulked and sterilized by autoclaving for four hours once, to keep the timing of the control treatments similar to the live soil treatments. Plant height and leaf number were measured one week after transplanting in the greenhouse as a metric of pre-treatment size. Height and leaf number were again measured mid-experiment and at harvest. Plants were harvested 16 weeks post-germination to obtain total biomass by rinsing soil from plant roots using a sieve, drying plant tissues for 72hrs, and weighing. Some plants experienced mild pest damage in the greenhouse, but inclusion of a damage covariate did not significantly alter our conclusions and so was not included in further analyses. One plant was removed from the final analyses due to death prior to harvest (leaving N=143).

Experiment 2 – Phyllosphere Inoculation: Phyllosphere inoculation included a series of inoculation treatments designed to mimic natural pathways for microbial colonization during plant growth (Christian et al. 2015). First, we exposed experimental plants to species-specific aboveground plant litter as an initial inoculation stage. Litter from the previous growing season, including leaf, stem and floral tissues, was collected directly from common garden donor plants in April 2015 (when plants are typically germinating or re-sprouting), pooled by host species (AN, CA, EP, or VM), and stored at 4°C until use in June 2015. Seeds from each species were germinated in commercial potting mix in individual 10cm square pots and seedlings grown for

four weeks before inoculation. We then placed four 10cm square pots (one individual pot for each study species) into four identical seedling flats, covered them with a clear plastic lid to maintain high humidity, and watered them from below. We inoculated seedlings by first distributing a thin layer of crumbled aboveground litter from either AN, CA, EP or VM across the surface of all plants growing within each flat, such that the seedlings of all four species were exposed to litter of only a single species. Litter was not applied to or intermixed with the soil. The treatment was maintained for one week to allow litter-associated microbiota to colonize the phyllosphere of experimental plants (Herre et al. 2005), but also to minimize any potential allelopathic or nutrient effects from litter addition. Litter was then removed and individual plants were transplanted into 12.7cm round (1082mL) pots filled with sterilized, background soil as in Experiment 1. After transplanting, plant height and leaf number were recorded as metrics of post-litter treatment size.

To prevent cross-contamination among treatments and to facilitate phyllosphere colonization, we created individual humidity chambers by inverting clear plastic cylinders (11.4cm diameter, 946 mL, Microwaveable Container, WebstaurantStore, Lancaster, PA) on top of the pots (Fig. 1B). In the second stage of phyllosphere inoculation, we collected fresh, mature leaves from the common garden donor plants and suspended them with a metal hook above the experimental plants inside the humidity cylinders (SI Fig. S2). Because AN, CA, EP, and VM have different leaf sizes and mass-per-unit-areas, we standardized leaf inoculum quantity across all four species by standardizing leaf area (e.g., smaller leaf sub-sections from large CA leaves, multiple leaves for small AN leaves, etc.) yielding leaf inoculum ‘sets’. Two leaf sets were used as inoculum sources for each experimental plant, one lower canopy leaf set and one mid-canopy leaf set, as microbial communities are known to undergo compositional succession as leaves age

(Hirose et al. 2013, Voříšková and Baldrian 2013). Leaves sampled from the common garden were chosen haphazardly and reflected the natural state of donor plants in the field (i.e., occasional presence of lesions, pustules, insect damage, etc.). To capture seasonal changes in phyllosphere communities and prevent leaf rot inside of the humidity chambers, leaf inoculum sets (both lower and mid-canopy leaves) were exchanged for fresh leaf material from the common garden every 2-3 weeks over the course of the experiment (i.e., four total sets). Control plants were exposed to neither litter nor mature leaf inocula sources. As in experiment 1, plant height and leaf number were measured mid-experiment and at harvest 16 weeks post-germination, when total dry-weight biomass was also determined. Thirteen plants were removed from the final analyses due to plant death prior to harvest (leaving N=131).

Experiment 3 – Field Inoculation: Seedlings of all four species were germinated in 20.3cm square flats and after three weeks they were transplanted into 2.3cm-square plug flats with sterilized Metro Mix. After four additional weeks of growth in the greenhouse, the root-bound plugs were transplanted in the common garden underneath individual adult plants of the same four species at a distance of 20-25cm from the crown and watered in (Fig. 1C). Experimental plants received no inoculation treatments prior to transplantation. All aboveground biomass was harvested 18-19 weeks post-germination. Belowground biomass was not harvested because roots were intermixed with those of neighboring plants. We measured soil moisture content (HH2 Moisture Meter, Theta Probe Soil Moisture Sensor ML2x, Delta-T Devices, Cambridge, England) and photosynthetically active radiation (PAR; AccuPAR LP-80 Ceptometer, Decagon Devices Inc., Pullman, WA, USA) for each transplant at harvest as potential covariates. While these one-time measures do not capture environmental variability over the growing season, they do reflect the relative effect of established adult plants on soil

moisture and light availability for experimental plants. Soil moisture was measured once at midday for each plant. PAR was measured using a 10cm probe held 13cm above ground level for each plant (as in Aspinwall *et al.* 2016), and averaged across three time points (mid-morning, mid-day, and mid-afternoon). Unexpectedly, experimental transplants in two of six common garden plots were killed by small mammal herbivory (leaving N=80). Additional plants experienced mortality under field conditions prior to plant harvest (leaving N=54), though analysis of survival probability revealed no significant differences in mortality among treatments.

Data Analysis: We used ANOVA to examine main effects of microbial ‘‘source’’ (donor species used to condition the soil or provide phyllosphere inocula), ‘‘species’’ (species being inoculated), and their interactions (‘source X species’) on dry-weight plant biomass, as a metric of host fitness, for all experiments. Within the interaction term, we also constructed *a priori* linear contrasts following Bever *et al.* (1997) and Mangan *et al.* (2010) to compare host growth in the presence of con- versus heterospecific microbiota and to test the potential for plant-microbiota feedbacks to stabilize or destabilize plant species coexistence. Therefore, we calculated two measures of plant-microbiota feedback:

1) “Net Overall Feedback” describes the net microbiota-induced feedback experienced by all species combinations and species in this study system (SI Data Files).

2) “Average Pairwise Feedback” takes the average of pairwise feedbacks experienced by each plant species for each species combination (SI Data Files). This feedback measurement describes the importance of microbiota-induced feedbacks as a trait for each of the four focal species used in this experiment (Mangan et al. 2010, Bauer et al. 2015).

To meet normality and homoscedasticity assumptions, square-root transformations were applied to total biomass and plant size in experiments 1 and 2, while a log-transformation was applied to shoot biomass in experiment 3. Additionally, to isolate initial effects of litter microbiota from subsequent mature leaf inoculations in experiment 2, we performed a separate feedback analysis on plant size after the 7-day litter inoculation, where plant size was computed as the product of height and leaf number. We also used repeated-measures ANOVA to evaluate the changes in plant size over time for experiments 1 and 2. Sphericity assumptions were not met and thus a multivariate approach to these data was performed. We used a backward model selection approach with AIC to test for the inclusion of soil moisture, PAR, and their interactions with 'source' and 'species' as potential covariates in the field experiment (significance level $\alpha < 0.10$). All data were analyzed in SAS 9.4. All figures were created using the 'ggplot2' package in R v.3.3.2.

RESULTS

Experiment 1 – PSFs: We did not find evidence for net overall feedback on host biomass in the plant-soil experiment ($p= 0.31$). The average pairwise PSF was negative for 3 of the 4 plant species, but positive for CA. However, average pairwise feedback was not significantly different from zero for any single species and was only marginally significant for AN ($p= 0.0626$; SI Table S2; Fig. 2A). Net overall PSF on plant size over time was not significant ($p= 0.29$), nor was average pairwise soil feedback on plant size over time significant for any single species (for all species: $p>0.10$; Fig. 3).

Experiment 2 – PPFs: By contrast, we found highly significant net overall feedback on host biomass in the plant-phyllosphere experiment ($F_{1,130}= 10.85, p= 0.0013$). While the strength

of average pairwise PPFs varied by species, the direction of feedback was negative and statistically significant for all four species (SI Table S2; Fig. 2B). Net overall PPF on plant size did not vary significantly over time ($p= 0.52$), nor did average pairwise feedback measures over time differ for any single species (for all species: $p>0.10$; Fig. 3). Intriguingly, plant size did show significant net overall PPF following the one-week litter inoculation period ($F_{1,130}= 14.04, p= 0.0003$). The average pairwise feedback experienced by experimental plants exposed to con- and heterospecific litter was also significantly negative for all four species (SI Table S2; Fig. 2C), though the magnitude of the feedback effects differed among species from estimates based on final biomass at harvest.

Experiment 3 – Field: We found significant net overall feedbacks on aboveground biomass in the field experiment ($F_{1,51}= 27.79, p< 0.0001$), where experimental transplants were exposed to both soil and phyllosphere inocula. The direction of average pairwise feedback was significantly negative for all four species (SI Table S2; Fig. 2D). Additionally, model selection analysis revealed that soil moisture at harvest was significantly negatively correlated with plant growth, but the effects varied among transplant species ($F_{1,51}= 12.15, p< 0.0001$; SI Fig. S3) and among adult donor species in the common garden ($F_{1,51}= 3.52, p= 0.029$; SI Fig. S3). Model terms including the ratio of ground-level PAR relative to canopy-level PAR did not significantly improve the model for aboveground biomass and thus were not included.

Live – Sterile inocula contrasts: The growth response to live versus sterile inocula differed in the two greenhouse inoculation experiments, thus we highlight those differences here. Live soil inocula increased plant biomass at harvest in experiment 1 relative to sterile controls, and response varied significantly by species ($F_{3,142}= 7.39, p= 0.0001$; Fig. 4). Specifically, VM exhibited the lowest net benefit to treatment with live soil relative to sterile soil (SI Fig. S4). We

also found that the difference in plant size between the live and sterile soil treatments varied over time and by species (*Wilk's Lambda= 0.797,* $F_{6,242}$*= 4.85, p< 0.0001*; Fig. 3). By contrast, in experiment 2, phyllosphere inocula reduced plant biomass at harvest relative to sterile controls, but this effect was only marginally significant ($F_{1,130}$*= 2.89, p= 0.093*; Fig. 4), and did not vary by species (*p= 0.38*; SI Fig. S4). Plant size did vary significantly over time in response to live versus sterile phyllosphere inocula (*Wilk's Lambda= 0.884,* $F_{2,107}$*= 7.05, p= 0.0013*; Fig. 3).

DISCUSSION

We found that phyllosphere microbiota induced negative average pairwise feedback for all four species tested (Fig. 2B), suggesting that negative feedbacks caused by host-specific phyllosphere microbiota can contribute to species coexistence by means of greater self-limitation. To our knowledge, this is the first experimental demonstration of PPFs and their potential community-level consequences. The negative feedback effect induced by phyllosphere microbiota, as measured by the feedback contrasts, was strong even though the direct fitness effect on plant hosts, as measured by the live-sterile contrast, was weakly negative and less significant (Fig. 4). Contrary to our original prediction, average pairwise soil feedbacks for all four species were consistently less negative and less significant than the average pairwise phyllosphere feedbacks under our experimental conditions, even though the direct fitness effect of live soil inocula on plant hosts was strongly positive (Fig. 4). The positive effect of soil inoculum may reflect in part the importance of mycorrhizae in these Asteraceae species (Smith and Read 2008). In the field experiment, where both PSF and PPF were occurring, average pairwise feedbacks were strongly negative and largely corroborated the results from the two greenhouse experiments despite a smaller sample size. Previous research has repeatedly

demonstrated that soil microbiota often have a negative effect on conspecific hosts and thereby a stabilizing effect on plant species coexistence (Kulmatiski et al. 2008, Mangan et al. 2010). Our results suggest that phyllosphere microbiota also contribute to plant species coexistence via negative feedbacks.

Our approach is unique compared to previous phyllosphere studies, given that we considered the horizontal spread of both visible and invisible, and pathogenic and mutualistic microbiota. In contrast to previous PSF experiments, which tested the importance of feedbacks from soil microbiota (Bever et al. 2012) or litter decomposition interactions (Meisner et al 2012), our study isolated the effects of host-specific phyllosphere microbiota on plant growth. Our results demonstrating strong negative effects also stand in contrast to the mutualistic role asserted for many phyllosphere microbes (e.g., fungal endophytes), most commonly inferred from inoculation of a limited number of microbial taxa onto a single host species (Arnold et al. 2003, Adame-Álvarez et al. 2014). The phyllosphere encompasses a wide range of organisms, including endo- and epiphytic bacteria and fungi, archaea, viruses, and other eukaryotes, as well as lesion-causing foliar pathogens and mutualists (Peñuelas and Terradas 2014). Therefore, while mutualists generally improve host fitness, the impacts of pathogenic phyllosphere microbiota may be greater under certain conditions, such as the warmer and more humid conditions found within our inoculation chambers. Alternatively, strong phyllosphere mutualists may be relatively rare among most plant groups. In addition, non-additive interactions between phyllosphere microbiota may determine the outcome of fitness effects on the host (May and Nelson 2014, Pattison et al. 2016). Future research should manipulate the make-up of phyllosphere communities to better elucidate microbial interactions and their combined impact on plant performance.

At the common garden site where all experimental inocula was collected, there are several naturally-occurring congeners and confamilials to the four study species, in addition to the other species of Asteraceae within the common garden itself (SI Methods). However, while all four experimental species are native to Indiana, there were no native conspecifics at the common garden site. It is therefore possible that the donor plants were colonized by generalist soil and phyllosphere microbiota not closely adapted to our particular host species (Parker et al. 2015), as well as by more Asteraceae-specific microbiota. Nevertheless, plant conditioning of the soil and phyllosphere had been occurring for more than one year prior to inocula collection and many plants were visually colonized by a variety of foliar pathogens and insect herbivores. Additionally, while the senesced litter inoculum had overwintered for five months, research shows that many phyllosphere colonizers of living tissues persist over this seasonal timeframe (Voříšková and Baldrian 2013).

Local adaptation between plants and their microbiota can influence PSF outcomes. A lack of co-adaptation between native plants and soil mutualists can result in reduced benefits (Rúa et al. 2016) and, accordingly, stronger negative feedbacks. Conversely, reduced host-specificity between plants and soil pathogens can lead to weaker pathogenic effects and weaker negative feedbacks (Cortois et al. 2016). However, the role that local adaptation plays in PPFs is less clear. Foliar pathogens can be locally adapted and exhibit stronger pathogenic effects (Laine et al. 2014), but how this influences plant-plant interactions, or differs for other phyllosphere functional groups, is uncertain (Greischar and Koskella 2007). Dispersal abilities of rhizo- and phyllosphere microbiota may also influence local adaptation and feedback outcomes. Phyllosphere communities are more strongly shaped by long-distance dispersal events via wind (David et al. 2015), whereas the soil matrix is more restrictive to long-distance propagule

movement. Thus, reduced dispersal in the soil may have lowered the probability for host-specific soil pathogens to accumulate, potentially leading to an underestimation of soil feedback strength.

Interestingly, we found a significant negative correlation between average pairwise PSF and PPF estimates among species, where there was a tradeoff in relative growth responses to con- versus heterospecific microbiota for soil versus phyllosphere inocula (Fig. 5). While this outcome is based on only four species, it represents a compelling pattern for further investigation. Mycorrhizal fungi play a key role as resource mutualists in the soil, though dependency varies among plant species (Smith and Read 2008). However, there is little evidence for an equivalent group of environmentally-acquired mutualists in the phyllosphere. Thus, plants that invest more in belowground mutualists (i.e., CA; *J. Bauer unpublished data*) may be more susceptible to aboveground pathogens. Conversely, plants that are less responsive to belowground microbiota (i.e., VM; SI Fig. S3) could associate with different suites of aboveground microbiota (Pattison et al. 2016) or be more resistant to aboveground pathogens. While researchers have advocated for the study of interactions between aboveground herbivores and pollinators with belowground functional groups (Schröter et al. 2004), research on interactions between above- and belowground microbiota is lacking (but see Rudgers & Orr 2009). This deficit should be addressed given the evidence for partial taxonomic and functional overlap of rhizo- and phyllosphere microbiota (Voříšková and Baldrian 2013, Bai et al. 2015). Manipulation of different microbial taxa could also generate insights into plant growth and defense strategies, and potential tradeoffs between them.

More generally, our experimental demonstration of both PSF and PPF raises a number of interesting questions in plant population dynamics and microbial ecology. For example, it is possible that previous studies on PSF in the greenhouse and field unintentionally included PPF

effects, especially if no physical barriers were placed between the soil and aboveground tissues, or between neighboring plant species. Previous results from field experiments evaluating plant community diversity-productivity relationships may reflect not only plant-plant and plant-rhizosphere interactions (Maron et al. 2011), but also plant-phyllosphere interactions. The effect of litter microbiota on phyllosphere community succession and plant-plant interactions has also not been previously considered. Similarly, it is possible that detached plant tissues (e.g., root fibers in soil inoculum, leaves in humidity chambers) could have emitted volatiles or other compounds that could have affected our results. We propose that future research should investigate the independent and combined impacts of phyllosphere and rhizosphere microbiota on plant-plant interactions across a range of species representing multiple functional groups and developmental ages. The fitness consequences of PSF and PPF could be distinguished by using physical barriers to alternately prevent, or allow, cross-colonization between the two microbial spheres. In parallel, the identities and overlap of microbiota associated with different plant tissues and species could be assessed using Next-Generation Sequencing, while quantifying the effect of inoculum density on the strength of PSF and PPF.

In conclusion, our research suggests that the functional interactions between soil and phyllosphere communities, their host plants, and their potential effects on plant species coexistence, are important avenues for future research. Both soil and phyllosphere microbiota should be considered together in a more general plant-microbiota feedback framework. This holistic approach promises to continue the theoretical and empirical advances achieved through use of the plant-soil feedback framework.

Acknowledgements

B.K.W. was supported by the National Institutes of Health (NIH) Genetics, Cellular & Molecular Sciences Training Grant and as a National Science Foundation (NSF) Graduate Research Fellow (GRF) during the course of the experiment and through writing of the manuscript. J.T.B was supported by the Agriculture and Food Research Initiative Competitive Grant No. 2016-67012-24680 from the USDA National Institute of Food and Agriculture. Funding support for establishment of the common garden at Bayles Rd. was provided by the Indiana University (IU) Research and Teaching Preserve. This work was supported in part by a grant to J.D.B by NSF DEB#1556664. We would like to thank K. Hoban, M. Zaret, and the IU Greenhouse Staff for assistance with the project, as well as members of the Clay and Bever labs for feedback on the manuscript, and the editors and anonymous reviewers at *Ecology Letters* whose comments helped to improve this paper.

LITERATURE CITED

Adame-Álvarez, R.-M., J. Mendiola-Soto, and M. Heil. 2014. Order of arrival shifts endophyte-pathogen interactions in bean from resistance induction to disease facilitation. FEMS Microbiology Letters 355:100–107.

Albornoz, F. E., T. I. Burgess, H. Lambers, H. Etchells, and E. Laliberté. 2016. Native soilborne pathogens equalize differences in competitive ability between plants of contrasting nutrient-acquisition strategies. Journal of Ecology:1–9.

Arnold, A. E., L. C. Mejía, D. Kyllo, E. I. Rojas, Z. Maynard, N. Robbins, and E. A. Herre. 2003. Fungal endophytes limit pathogen damage in a tropical tree. Proceedings of the National Academy of Sciences of the United States of America 100:15649–15654.

Aspinwall, M. J., P. A. Fay, C. V. Hawkes, D. B. Lowry, A. Khasanova, J. Bonnette, B. K. Whitaker, N. Johnson, and T. E. Juenger. 2016. Intraspecific variation in precipitation responses of a widespread C4 grass depends on site water limitation. Journal of Plant Ecology:rtw040.

Bagchi, R., R. E. Gallery, S. Gripenberg, S. J. Gurr, L. Narayan, C. E. Addis, R. P. Freckleton, and O. T. Lewis. 2014. Pathogens and insect herbivores drive rainforest plant diversity and composition. Nature 506:85–88.

Bai, Y., D. B. Müller, G. Srinivas, R. Garrido-Oter, E. Potthoff, M. Rott, N. Dombrowski, P. C. Münch, S. Spaepen, M. Remus-Emsermann, B. Hüttel, A. C. McHardy, J. A. Vorholt, and P. Schulze-Lefert. 2015. Functional overlap of the Arabidopsis leaf and root microbiota. Nature 528:364–369.

Bauer, J. T., K. M. L. Mack, and J. D. Bever. 2015. Plant-soil feedbacks as drivers of succession: evidence from remnant and restored tallgrass prairies. Ecosphere 6:1–12.

Bever, J. D., S. A. Mangan, and H. M. Alexander. 2015. Maintenance of plant species diversity by pathogens. Annual Review of Ecology, Evolution, and Systematics 46:305–325.

Bever, J. D., T. G. Platt, and E. R. Morton. 2012. Microbial population and community dynamics on plant roots and their feedbacks on plant communities. Annual Review of Microbiology 66:265–283.

Bever, J. D., K. M. Westover, and J. Antonovics. 1997. Incorporating the soil community into plant population dynamics: the utility of the feedback approach. Journal of Ecology 85:561–573.

Busby, P. E., K. G. Peay, and G. Newcombe. 2016. Common foliar fungi of Populus trichocarpa modify Melampsora rust disease severity. New Phytologist 209:1681–1692.

Callaway, R. M., G. C. Thelen, A. Rodriguez, and W. E. Holben. 2004. Soil biota and exotic plant invasion. Nature 427:731–733.

Casper, B. B., and J. P. Castelli. 2007. Evaluating plant-soil feedback together with competition in a serpentine grassland. Ecology Letters 10:394–400.

Christian, N., B. K. Whitaker, and K. Clay. 2015. Microbiomes: unifying animal and plant systems through the lens of community ecology theory. Frontiers in Microbiology 6:1–15.

Clay, K., J. Holah, and J. A. Rudgers. 2005. Herbivores cause a rapid increase in hereditary symbiosis and alter plant community composition. Proceedings of the National Academy of Sciences of the United States of America 102:12465–12470.

Cortois, R., T. Schröder-Georgi, A. Weigelt, W. H. van der Putten, and G. B. De Deyn. 2016. Plant-soil feedbacks: role of plant functional group and plant traits. Journal of Ecology 104:1608–1617.

David, A. S., E. W. Seabloom, and G. May. 2015. Plant host species and geographic distance

affect the structure of aboveground fungal symbiont communities, and environmental filtering affects belowground communities in a coastal dune ecosystem. Microbial Ecology 71:912–926.

Ehrenfeld, J. G., B. Ravit, and K. Elgersma. 2005. Feedback in the plant-soil system. Annual Review of Environment and Resources 30:75–115.

Greischar, M. A., and B. Koskella. 2007. A synthesis of experimental work on parasite local adaptation. Ecology Letters 10:418–434.

Herre, E. A., S. A. Van Bael, Z. Maynard, N. Robbins, J. Bischoff, A. E. Arnold, E. Rojas, L. C. Meija, R. A. Cordero, C. Woodward, and D. A. Kyllo. 2005. Tropical plants as chimera: some implications of foliar endophytic fungi for the study of host-plant defence, physiology and genetics. Pages 226–237 *in* D. F. R. P. Burslem, M. A. Pinard, and S. E. Hartley, editors. Biotic Interactions in the Tropics: Their Role in the Maintenence of Species Diversity. Cambridge University Press.

Herre, E. A., L. C. Mejía, D. A. Kyllo, E. Rojas, Z. Maynard, A. Butler, and S. A. Van Bael. 2007. Ecological implications of anti-pathogen effects of tropical fungal endophytes and mycorrhizae. Ecology 88:550–558.

Hirose, D., S. Matsuoka, and T. Osono. 2013. Assessment of the fungal diversity and succession of ligninolytic endophytes in Camellia japonica leaves using clone library analysis. Mycologia 105:837–843.

Kaneko, R., and S. Kaneko. 2004. The effect of bagging branches on levels of endophytic fungal infection in Japanese beech leaves. Forest Pathology 34:65–78.

Kardol, P., T. M. Bezemer, and W. H. van der Putten. 2006. Temporal variation in plant-soil feedback controls succession. Ecology Letters 9:1080–1088.

Kardol, P., G. F. (Ciska) Veen, F. Teste, and M. P. Perring. 2015. Peeking into the black box: a trait- based approach to predicting plant-soil feedback. New Phytologist 206:1–4.

Ke, P., T. Miki, and T. Ding. 2015. The soil microbial community predicts the importance of plant traits in plant-soil feedback. New Phytologist 206:329–341.

Klironomos, J. N. 2002. Feedback with soil biota contributes to plant rarity and invasiveness in communities. Nature 417:67–70.

Kulmatiski, A., K. H. Beard, J. R. Stevens, and S. M. Cobbold. 2008. Plant-soil feedbacks: a meta-analytical review. Ecology Letters 11:980–992.

Laine, A.-L., J. J. Burdon, A. Nemri, and P. H. Thrall. 2014. Host ecotype generates evolutionary and epidemiological divergence across a pathogen metapopulation. Proceedings of the Royal Society B: Biological Sciences 281:20140522.

Li, H.-Y., C.-A. Zhao, C.-J. Liu, and X.-F. Xu. 2010. Endophytic fungi diversity of aquatic/riparian plants and their antifungal activity in vitro. Journal of Microbiology 48:1–6.

Mangan, S. A., S. A. Schnitzer, E. A. Herre, K. M. L. Mack, M. C. Valencia, E. I. Sanchez, and J. D. Bever. 2010. Negative plant – soil feedback predicts tree-species relative abundance in a tropical forest. Nature 466:752–755.

Maron, J. L., M. Marler, J. N. Klironomos, and C. C. Cleveland. 2011. Soil fungal pathogens and the relationship between plant diversity and productivity. Ecology Letters 14:36–41.

May, G., and P. Nelson. 2014. Defensive mutualisms: do microbial interactions within hosts drive the evolution of defensive traits? Functional Ecology 28:356–363.

Meija, L. C., E. A. Herre, J. P. Sparks, K. Winter, M. N. Garcia, S. A. Van Bael, J. Stitt, Z. Shi, Y. Zhang, M. J. Guiltinan, and S. N. Maximova. 2014. Pervasive effects of a dominant foliar endophytic fungus on host genetic and phenotypic expression in a tropical tree.

Frontiers in Microbiology 5:1–16.

Meisner, A., W. de Boer, J. H. C. Cornelissen, and W. H. van der Putten. 2012. Reciprocal effects of litter from exotic and congeneric native plant species via soil nutrients. PLoS ONE 7:e31596.

Mejia, L. C., E. I. Rojas, Z. Maynard, S. Van Bael, A. E. Arnold, P. Hebbar, G. J. Samuels, N. Robbins, and E. A. Herre. 2008. Endophytic fungi as biocontrol agents of Theobroma cacao pathogens. Biological Control 46:4–14.

Mitchell, C. E., and A. G. Power. 2003. Release of invasive plants from fungal and viral pathogens. Nature 421:625–627.

Monteil, C. L., C. Guilbaud, C. Glaux, F. Lafolie, S. Soubeyrand, and C. E. Morris. 2012. Emigration of the plant pathogen Pseudomonas syringae from leaf litter contributes to its population dynamics in alpine snowpack. Environmental Microbiology 14:2099–2112.

Mordecai, E. A. 2011. Pathogen impacts on plant communities: Unifying theory, concepts, and empirical work. Ecological Monographs 81:429–441.

Packer, A., and K. Clay. 2000. Soil pathogens and spatial patterns of seedling mortality in a temperate tree. Nature 404:278–281.

Panaccione, D. G., W. T. Beaulieu, and D. Cook. 2014. Bioactive alkaloids in vertically transmitted fungal endophytes. Functional Ecology 28:299–314.

Parker, I. M., M. Saunders, M. Bontrager, A. P. Weitz, R. Hendricks, R. Magarey, K. Suiter, and G. S. Gilbert. 2015. Phylogenetic structure and host abundance drive disease pressure in communities. Nature 520:542–544.

Pattison, Z., H. Rumble, R. A. Tanner, L. Jin, and A. C. Gange. 2016. Positive plant-soil

feedbacks of the invasive Impatiens glandulifera and their effects on above-ground microbial communities. Weed Research.

Peñuelas, J., and J. Terradas. 2014. The foliar microbiome. Trends in Plant Science 19:278–280.

Petermann, J. S., A. J. F. Fergus, L. A. Turnbull, and B. Schmid. 2008. Janzen-Connell effects are widespread and strong enough to maintain diversity in grasslands. Ecology 89:2399–2406.

van der Putten, W. H., M. A. Bradford, E. P. Brinkman, T. F. J. van de Voorde, and G. F. Veen. 2016. Where, when and how plant-soil feedback matters in a changing world. Functional Ecology 30:1109–1121.

van der Putten, W. H., C. Van Dijk, and B. A. M. Peters. 1993. Plant-specific soil-borne diseases contribute to succession in foredune vegetation. Nature 362:53–56.

Revilla, T. A., G. F. (Ciska) Veen, M. B. Eppinga, and F. J. Weissing. 2013. Plant-soil feedbacks and the coexistence of competing plants. Theoretical Ecology 6:99–113.

Rodriguez, R. J., J. F. White Jr., A. E. Arnold, and R. S. Redman. 2009. Fungal endophytes: diversity and functional roles. The New Phytologist 182:314–330.

Rúa, M. A., A. Antoninka, P. M. Antunes, V. B. Chaudhary, C. Gehring, L. J. Lamit, B. J. Piculell, J. D. Bever, C. Zabinski, J. F. Meadow, M. J. Lajeunesse, B. G. Milligan, J. Karst, and J. D. Hoeksema. 2016. Home-field advantage? evidence of local adaptation among plants, soil, and arbuscular mycorrhizal fungi through meta-analysis. BMC Evolutionary Biology 16:1–15.

Rudgers, J. A., and S. Orr. 2009. Non-native grass alters growth of native tree species via leaf and soil microbes. Journal of Ecology 97:247–255.

Schnitzer, S., J. Klironomos, J. HilleRisLambers, L. L. Kinkel, P. B. Reich, K. Xiao, M. C.

Rillig, B. A. Sikes, R. M. Callaway, S. A. Mangan, E. H. van Nes, and M. Scheffer. 2011. Soil microbes drive the classic plant diversity-productivity pattern. Ecology 92:296–303.

Schröter, D., L. Brussaard, G. De Deyn, K. Poveda, V. K. Brown, M. P. Berg, D. A. Wardle, J. Moore, and D. H. Wall. 2004. Trophic interactions in a changing world : modelling aboveground – belowground interactions. Basic and Applied Ecology 5:515–528.

Smith, S. E., and D. J. Read. 2008. Mycorrhizal Symbiosis. 3rd edition. Academic Press, London.

Song, Z., P. G. Kennedy, F. J. Liew, and J. S. Schilling. 2016. Fungal endophytes as priority colonizers initiating wood decomposition. Functional Ecology:10.1111/1365-2435.12735.

Stergiopoulos, I., and T. R. Gordon. 2014. Cryptic fungal infections: the hidden agenda of plant pathogens. Frontiers in Plant Science 5:1–4.

Suryanarayanan, T. S. 2013. Endophyte research: going beyond isolation and metabolite documentation. Fungal Ecology 6:561–568.

U'Ren, J. M., and A. E. Arnold. 2016. Diversity, taxonomic composition, and functional aspects of fungal communities in living, senesced, and fallen leaves at five sites across North America. PeerJ:4:e2768.

van de Voorde, T. F. J., W. H. van der Putten, and T. M. Bezemer. 2011. Intra- and interspecific plant-soil interactions, soil legacies and priority effects during old-field succession. Journal of Ecology 99:945–953.

Voříšková, J., and P. Baldrian. 2013. Fungal community on decomposing leaf litter undergoes rapid successional changes. The ISME Journal 7:477–486.

Wilson, D. 1996. Manipulation of infection levels of horizontally transmitted fungal endophytes in the field. Mycological Research 100:827–830.

FIGURES AND TABLES

Fig. 1 Visual description of the three inoculation experiments performed. In experiment 1 (soil feedbacks), soil microbiota were "sourced" from adult donor plants in the common garden and inoculated into the pots of experimental plants (A). In experiment 2 (phyllosphere feedbacks), phyllosphere microbiota were sourced from aboveground tissues of adult donor plants and introduced into individual humidity chambers with experimental plants as the second part of the inoculation protocol (B). In experiment 3 (field), seedlings of all four species were transplanted at a distance of 20-25cm from the crown of an adult donor plant in the common garden, thus combining both soil and phyllosphere sources of microbiota inocula, as well as natural stressors (C). For ease of visualization, the adult donor plant depicted in panels A, B and C is *Vernonia missurica* with seedlings of all four species being inoculated (AN=*Aster novae-angliae*, CA=*Cacalia atriplicifolia*, EP=*Eupatorium perfoliatum*, VM=*Vernonia missurica*), but all other donor species were incorporated in the full, reciprocal design. A single gray arrow is shown in panels A and B illustrating inoculum transfer from adult donor plant to recipient plant.

Fig. 2 Average pairwise feedback strength on plant biomass and plant size differs by type of microbiota inoculum and species. Average pairwise feedback was estimated for each species, using square-root transformed total plant biomass in experiments 1 (A) and 2 (B). In experiment 2, average pairwise feedback experienced by each species as a result of litter inoculation alone (C) was estimated using a square-root transformation of plant size, computed as the product of height and leaf number. Average pairwise feedback was also estimated for each species using log-transformed shoot biomass at harvest in experiment 3 (D). In all cases, computed feedback estimates are based on transformed fitness metrics (e.g., plant size/biomass).

Error bars depict the standard error for the average pairwise feedback estimate, calculated for each species. Significant feedback estimates are marked as following (+ <0.10, * <0.05, ** <0.01, *** <0.001).

Fig. 3 Plant size over time varied by species and inoculum treatment. Relative fitness was estimated using a square-root transformation of plant size, computed as the product of height and leaf number. These raw data are shown in transformed units and have been jittered to aid in visualization. The top graph shows results for experiment 1, while the bottom graph shows results for experiment 2. Soil inoculation began after time point one in experiment 1, while in experiment 2 litter inoculation began prior time point one and mature leaf inoculations began after time point one and continued throughout until experiment end. Panels indicate which species was inoculated while line colors indicate which inoculum treatment was used.

Fig. 4 Growth response to live inoculum versus sterile inoculum differed by inoculum type. Live-Sterile contrast estimates were obtained using square-root transformed total plant biomass. Sterile inoculum treatments used included sterilized, bulk field soil in experiment 1 and the absence of tissue-based inoculum in experiment 2.

Fig. 5 Average pairwise soil-feedback estimates are negatively correlated with pairwise-phyllosphere feedback estimates across species *($p = 0.0196$)*. Computed average pairwise feedback estimates are based on square-root transformed total plant biomass measurements. The x-intercept for this regression, corresponding to a phyllosphere feedback estimate of zero, is -1.336. The y-intercept, corresponding to a soil feedback estimate of zero, is -0.904.

Figure 1

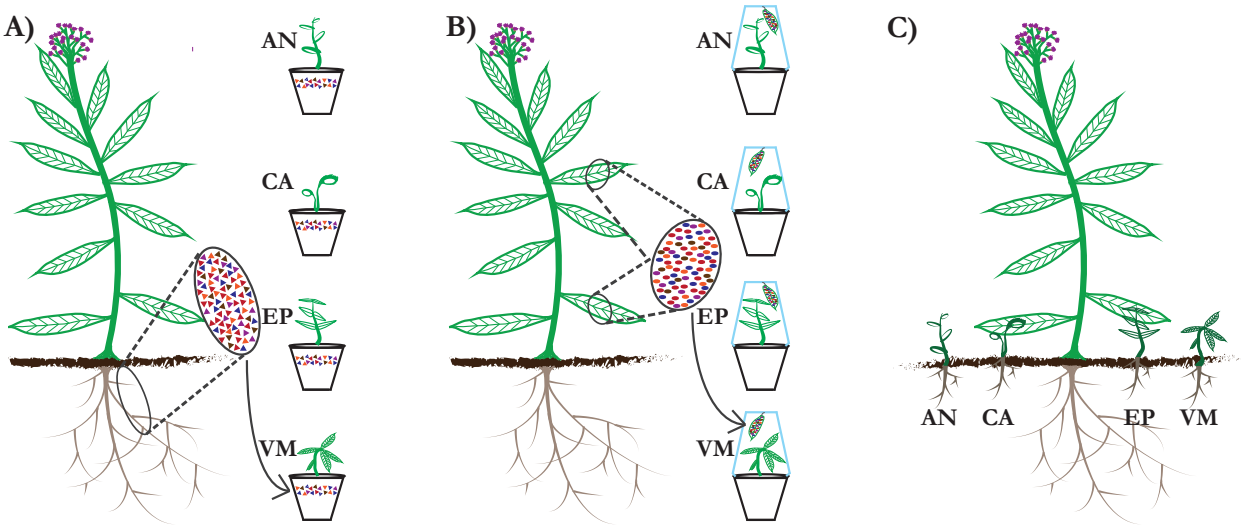

Figure 2

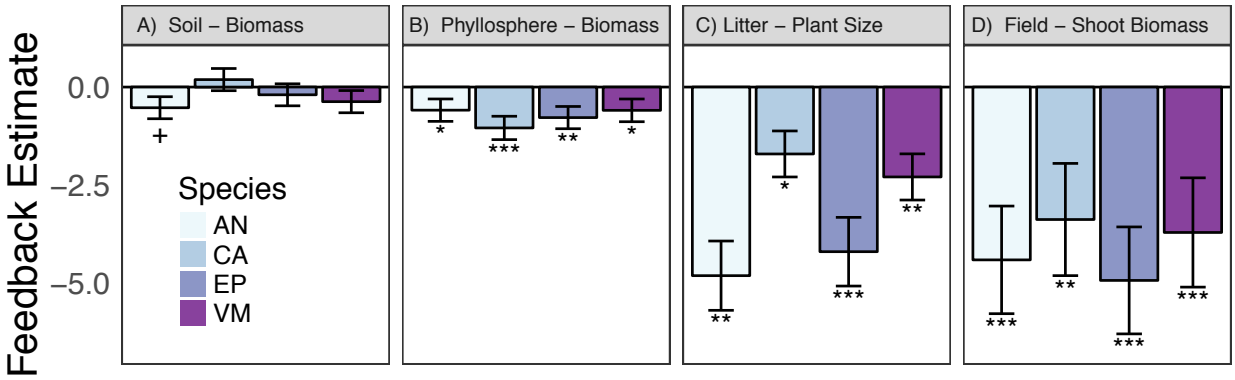
A) Soil – Biomass
B) Phyllosphere – Biomass
C) Litter – Plant Size
D) Field – Shoot Biomass
Feedback Estimate
0.0
−2.5
−5.0
Species
AN
CA
EP
VM
+
*
***
**
*
**
*
***
***
**
***
***

Figure 3

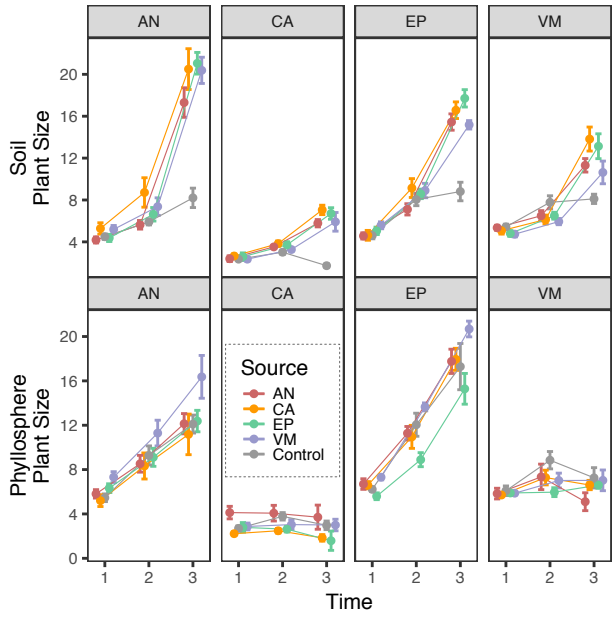
AN
CA
EP
VM
Soil
Plant Size
Phyllosphere
Plant Size
20
16
12
8
4
0
1
2
3
Time
Source
AN
CA
EP
VM
Control

Figure 4

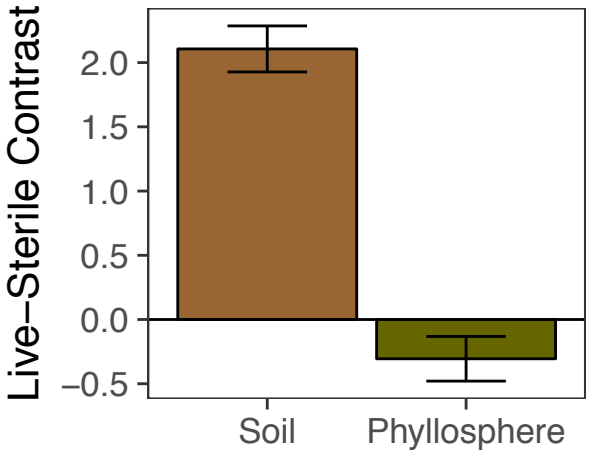

Figure 5

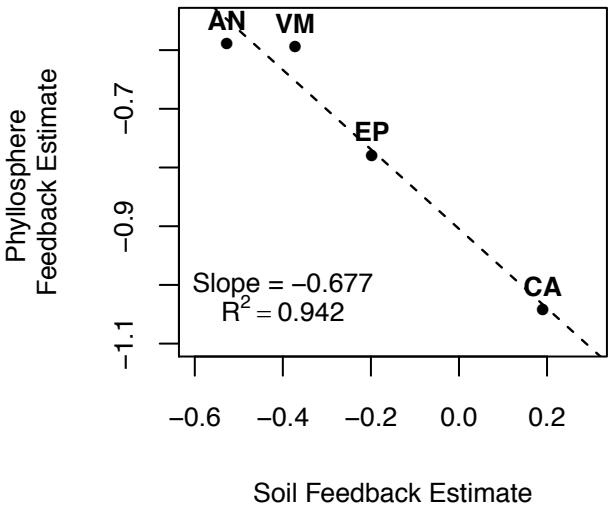
AN
VM
EP
CA
Slope = –0.677
R^2 = 0.942
Phyllosphere Feedback Estimate
–0.7
–0.9
–1.1
–0.6
–0.4
–0.2
0.0
0.2
Soil Feedback Estimate

Supporting Information

Fig. S1. – Topographic map showing the layout of the Asteraceae common garden plots at Bayles Rd., Bloomington, IN. Black squares show the location of the six replicated plots.

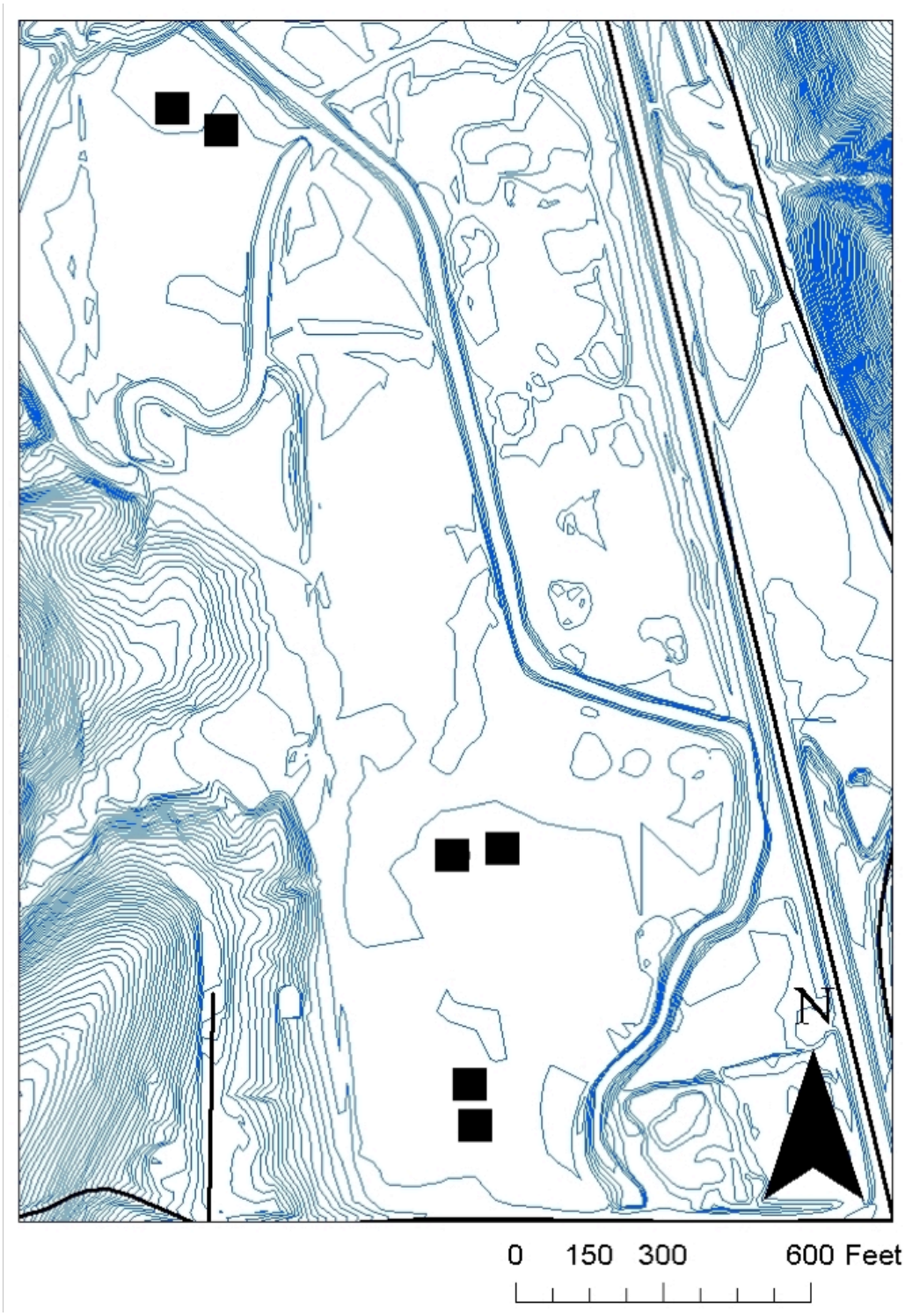

Methods – Description of the common garden.

Bayles Road is a former agricultural field that has been used for ecological research for the last 20 years. In each of the six plots, three individuals per species of 30 total species (28 species of Asteraceae and two species of Lobeliaceae) were planted. The common garden was established in the spring of 2014. Black landscaping cloth was used to limit plant invasions into the garden, but was supplemented by hand weeding when necessary. Individual plants were separated by 0.91m longitudinally and 0.76m laterally within each plot. The local plant community at Bayles Road includes grasses (e.g., *Andropogon virginicus, Lolium arundinaceum*, *Poa pratensis*, *Sorghum halapens, Tridens flavus*), forbs (e.g., *Asclepias syriaca, Erigeron annuus*, *Rubus spp.*, *Solidago spp., Toxicodendron radicans*, *Verbesina alternifolia, Vernonia spp.*), and several species of trees, which border the property (e.g., *Acer negundo, Acer saccharinum, Liriodendron tulipifera*, *Platanus occidentalis*).

The 30 common garden species included: *Actinomeris alternifolia, Antennaria plantaginifolia, Aster novae-angliae, Boltonia asteroides, Cacalia atriplicifolia, Cacalia plantaginea, Cirsium discolor, Coreopsis tripteris, Echinacea purpurea, Eupatorium coelestinum, Eupatorium perfoliatum, Eupatorium rugosum, Helenium autumnale, Helianthus grosseserratus, Heliopsis helianthoides, Hieracium canadense, Liatris spicata, Lobelia cardinalis, Lobelia spicata, Parthenium integrifolium, Prenanthes alba, Prenanthes racemosa, Ratibida pinnata, Rudbeckia hirta, Silphium perfoliatum, Solidago nemoralis, Verbesina helianthoides, Vernonia altissima, Vernonia fasciculata, Vernonia missurica*.

Table S1 – Experimental timeline (Year 2015).

April 13th	Purchased seeds and began cold stratification.
April 21st	Collected litter from common garden and stored until use.
May 11th	Germinated seeds.
June 1st	Transplanted Field plants into seed packs.
June 8th	Began litter inoculation treatment for plant-phyllosphere feedback plants.
June 15th	Ended leaf litter treatment. Transplanted plant-phyllosphere feedback plants into pots.
June 16th & 17th	Soil Cores collected.
June 16th & 17th	Transplanted plant-soil feedback plants into pots.
June 22nd & 23rd	First size measurements on plant-soil feedback and plant-phyllosphere feedback plants.
June 26th	Began live leaves inoculation treatment for plant-phyllosphere feedback plants.
July 1st	Transplanted Field plants under adult donor plants in the common garden.
July 1st	First size measurements on Field plants.
July 11th	Second live leaves inoculation treatment for plant-phyllosphere feedback plants.
July 15th	Second size measurements on plant-soil feedback plants.
July 22nd	Second size measurements on plant-phyllosphere feedback plants.
Aug 2nd	Third live leaves inoculation treatment for plant-phyllosphere feedback plants.
Aug 21st	Fourth live leaves inoculation treatment for plant-phyllosphere feedback plants.
Aug 31st & Sept 1st	Plant-soil feedback harvest. Third size measurements.
Sept 2nd - 4th	Plant-phyllosphere feedback harvest. Third size measurements.
Sept 17th	Soil moisture and light canopy measurements for Field plants under adult plants in common garden.
Sept 18th & 22nd	Field harvest. Second size measurements.

Table S2 – Model estimates gained from the *a priori* linear contrasts analysis.

	Soil – Biomass	Phyllosphere – Biomass	Phyllosphere – Post-Litter Plant Size	Field – Shoot Biomass
AN	-0.53±0.28 +	-0.59±0.29 *	-4.41±1.37 **	-4.81±0.88 ***
CA	0.19±0.28	-1.04±0.30 ***	-3.38±1.43 *	-1.71±0.59 **
EP	-0.20±0.28	-0.78±0.28 **	-4.93±1.36 ***	-4.20±0.88 ***
VM	-0.37±0.28	-0.59±0.29 *	-3.71±1.39 **	-2.29±0.59 ***
Live-Sterile	2.11±0.18 ***	-0.306±0.17 +	1.07±0.84	
Live-Sterile x Species	***	*NS*	*NS*	

Plant biomass data was used to compute average pairwise feedback estimates for each species (AN, CA, EP,VM), as well as for the live-sterile treatment comparison. In the soil- and phyllosphere-feedback experiments total seedling biomass was square-root transformed while in the field experiment shoot biomass was log-transformed. Additionally, in the phyllosphere-feedback experiment, average pairwise feedback estimates were obtained for square-root transformed plant size (height X leaf number) after litter inoculation. Significant feedback estimates are marked as following (+ <0.10, * <0.05, ** <0.01, *** <0.001). *NS* indicates a non-significant interaction in the Live-Sterile by Species contrast.

Fig. S2. – Example of a phyllosphere humidity chamber. Shown are the 12.7cm round pot, clear plastic cylinder humidity chamber, experimentally inoculated plant, and an example of the mature leaf inocula (in the back of the chamber), which was the second stage of inoculation in experiment 2.

Fig. S3. – Shoot biomass varies with soil moisture levels in the common garden and by identity of the transplant species (i.e., 'Species'; left panel) and among adult donor plant species in the common garden (i.e., 'Source'; right panel). Each point represents a single experimental plant. The biomass axis has been log transformed, but values shown are in untransformed units. Regression lines depict the relationship between aboveground plant biomass and soil moisture percent for each recipient species (left panel) or donor/source species (right panel). In the right side panel, it was not possible to get a regression estimate for the CA donor species.

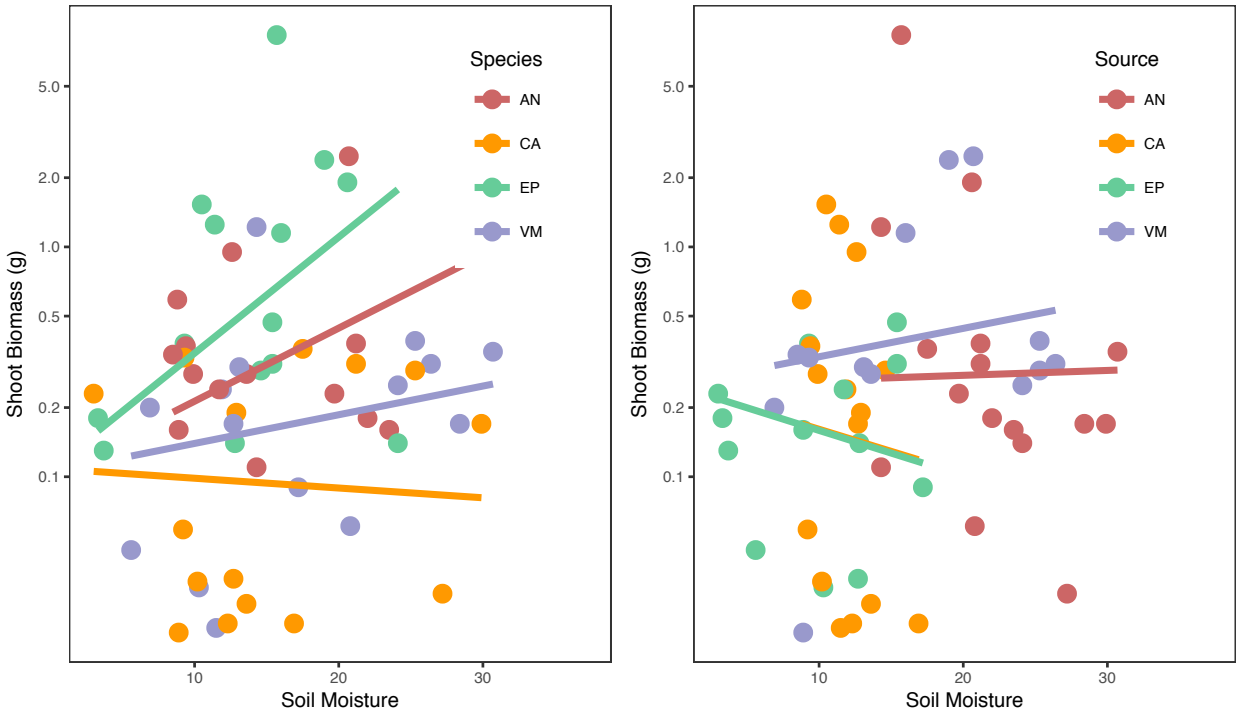

Fig. S4. – Growth response to live inoculum versus sterile inoculum differed by species in the soil experiment (Experiment 1; brown bars), but not in the phyllosphere experiment (Experiment 2; green bars). Shown are the log-response ratios (log-RR) for the average of the least-squares means of the live treatments, divided by the least-squares mean of the sterile control treatment. Panels depict response ratios for each experimental species. Positive values indicate increased growth with live inoculum relative to sterile control inoculum, while negative values indicate reduced growth with live inoculum. For simplification, the word phyllosphere in has been shortened to "Phyllo".

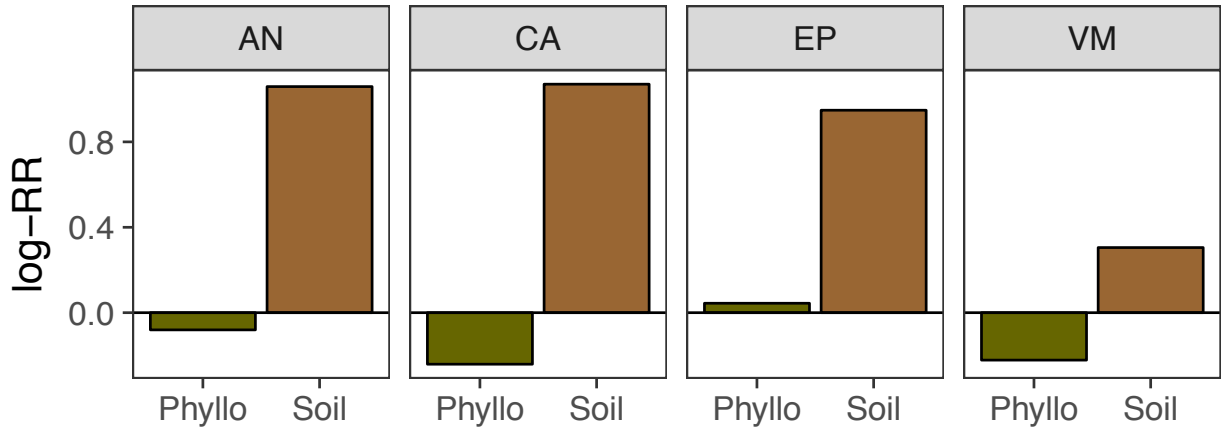

Title: Bacterial endophyte antagonism against a fungal pathogen *in vitro* does not predict efficacy *in planta*

Target Journal: Functional Ecology, New Phytologist, Microbial Ecology

Authors: Briana K. Whitaker[1*], Matthew G. Bakker[2]

[1] Department of Biology, Indiana University, Bloomington, IN

[2] Mycotoxin Prevention & Applied Microbiology research unit, USDA-ARS, Peoria, IL

Emails: brkawhit@indiana.edu; matt.bakker@usda.ars.gov

Author for correspondence: Briana K. Whitaker

Address: Department of Biology, Jordan Hall, 1001 E. 3rd St, Indiana University, Bloomington, IN, 47405-3700; Tel: (+1) 8128551674; Fax: (+1) 8128556705; Email: brkawhit@indiana.edu

Word Count: Abstract (293), Total (5857), Introduction (916), Materials and Methods (2706), Results (843), Discussion (1392); References (48), Figures (7), Color Figures (6), Tables (3)

Keywords: biocontrol, context-dependency, disease modification, Fusarium Head Blight, plant-growth promoting microbiota, wheat

ABSTRACT

All plants are colonized by a diverse array of microbiota, with impacts on host function that can span a continuum from beneficial to pathogenic. Endophytes, or microbiota that reside inside plant tissues, are increasingly seen as potentially useful symbionts for conferring disease suppression or abiotic stress tolerance. Common approaches to identify putatively beneficial symbionts rely on lab-based assays. However, few studies have directly contrasted functional roles inferred from *in vitro* tests with functional outcomes *in planta*. This can lead to a failure of candidate biocontrol agents when transferred to field conditions, where temperature and other environmental conditions are more variable. Our objective was to test whether bacterial-endophyte antagonism towards a plant pathogen *in vitro* would be predictive of disease outcomes *in planta*. Using two *in vitro* assays, we challenged bacterial endophytes isolated from wheat plants against *Fusarium graminearum*, a fungal pathogen of wheat that causes Fusarium head blight. A subset of isolates, ranging from weakly to strongly antagonistic in the *in vitro* assays, were selected for an *in planta* assay. All assays were performed under different temperature and carbon dioxide conditions to test the climatic dependency of the plant-fungal-bacterial interactions. We found that the degree of pathogen inhibition detected in the two *in vitro* assays was not predictive of the degree of pathogen load reduction *in planta*. This was true across temperature and carbon dioxide conditions chosen to reflect future climate change scenarios. Additionally, the outcome of the plant-fungal-bacterial interactions were environment-dependent and varied among bacterial isolates. Our results suggest that impacts of endophytes on plant performance cannot necessarily be inferred from simplified *in vitro* assays, and future research testing microbe-microbe interactions in the field, or *in planta*, should incorporate

environmental gradients to better understand context dependent outcomes in these tri-partite species interactions.

INTRODUCTION

Infectious diseases of wild and crop plants are important regulators of growth and yield in natural and agricultural systems (Savary et al. 2012, van der Putten et al. 2016). Non-pathogenic members within the plant microbiome are increasingly seen as important symbionts for disease alleviation in wild host systems (Arnold et al. 2003, Busby et al. 2016) and potentially as bio-control agents for disease suppression in agricultural systems (Mei and Flinn 2010, O'Callaghan 2016). However, it remains difficult to understand the ecology of these potentially beneficial microbiota given the innate complexity of host-pathogen-symbiont interactions that can occur simultaneously with variable abiotic conditions. Many research studies attempt to reduce the complexity of these species interactions by performing simplified laboratory experiments designed to compete microbial symbionts with plant pathogens of interest. However, there is uncertainty around the extent to which these tri-partite species interactions can be decomposed into pairwise interactions or extrapolated from the dramatically simplified environments of the laboratory. Thus, to understand the function of these putatively beneficial microbiota, a framework for lab-to-field based outcomes will be required.

For plant pathosystems where pathogen proliferation occurs within internal plant tissues, such as through vascular bundles, a fruitful starting criterion would be the identification of asymptomatic microbiota that also live internally within the host (i.e., endophytes). Fusarium head blight (FHB) is one such disease of wheat and barley, where the disease-causing agents (in North America, primarily members of the *Fusarium graminearum* species complex) can infect a

single floret on developing wheat inflorescences and then spread rapidly and internally via the vascular tissue and rachis (Bai and Shaner 2004). Endophytes have the potential to antagonize such pathogens directly via physical interaction within the host-tissue habitat (Porras-Alfaro and Bayman 2011). Wheat inflorescences also contain high levels of nutrients known to stimulate the growth of *Fusarium* species (Strange et al. 1974). FHB is a global and economically important disease, affecting crop yields directly via reduced grain-filling after infection and indirectly via the accumulation of a fungal-derived toxin (e.g., deoxynivalenol or nivalenol; McMullen et al. 2012). FHB also has similarities to many wild disease systems of grasses, where infection occurs via the inflorescence tissues and seed production is often aborted post-infection (Clay and Schardl 2002).

From a management perspective, endophytes are increasingly seen as important agents of disease control in agricultural and forestry systems, as well as more generally in microbial ecology (Busby et al. 2016). The mechanisms for disease reduction include direct competition for host habitat resources or habitat space, priming of the host immune system, or production of secondary metabolites that reduce the growth of microbial competitors (Porras-Alfaro and Bayman 2011). Endophytes have been identified as colonizers in all plant species studied to date (Peñuelas and Terradas 2014). Furthermore, endophytes have been isolated from many different host tissues ranging from roots to leaves and flowering organs, and can have impacts on their hosts spanning a continuum of mutualistic to pathogenic functional roles (Vacher et al. 2016). For these reasons, culturable endophytes, both bacterial and fungal, are increasingly being isolated for *in vitro* laboratory studies and to confirm the presence of metabolic traits inferred from metagenomic sequencing studies (Martiny et al. 2015). For agricultural scientists,

culturable endophytes have a potential use in preventative seed treatments, as an alternative to conventional biocide practices (Finkel et al. 2017).

Unfortunately, there has been little work exploring how environmental gradients drive phenotypic variability in microbial function and physiology *in vitro* or within internal host tissues, and how traits characterized in the lab may predict functional outcomes in nature (Hawkes and Connor 2017). For example, it is not clear how variability among endophytes in their resilience to climatic conditions affects their interactions with other microbial species (e.g., pathogens). Nor is it clear how environmental responsiveness among endophytes overlaps with host varieties that also vary in their response to environmental conditions, such as among plants with different heat and drought tolerances. One recent study demonstrated that the effects of foliar fungal endophyte inoculations on their grass hosts were dependent on soil moisture condition (Connor et al. 2017). On the other hand, another study of root endophyte interactions with non-gramineous, herbaceous hosts showed that while the environmental conditions tested affected plant growth directly, there was less effect on the endophyte-plant interactions (Kia et al. 2018). Thus, it may be necessary to consider a range of environmental conditions to better understand interactions between plants and endophytic symbionts.

Our objectives were to test whether measurements of bacterial endophyte interactions with *Fusarium graminearum in vitro* would be predictive of FHB disease outcomes *in planta* and to test whether host plant-pathogen-endophyte interactions vary over environmental gradients relevant to climate change. We predicted that 1) bacterial endophytes would vary in their antagonism towards the wheat fungal pathogen *in vitro* and 2) that bacterial endophyte antagonism of the pathogen *in vitro* would positively correlate with endophyte antagonism of the pathogen *in planta*, but that the correlation would be weak given the increased physical and

metabolic complexities of the plant habitat environment (Vacher et al. 2016). We also expected that 3) the environmental conditions across which pathogen antagonism was effective would vary among bacterial endophyte isolates. Lastly, we also predicted that 4) bacterial endophyte growth rate, as estimated using ribosomal RNA operon copy number, would influence *in vitro* interaction outcomes with the fungal pathogen. To test these questions, we performed a series of competition assays between bacterial endophytes and *Fusarium graminearum*, which increased in complexity from simplified environments *in vitro* to more realistic habitats *in planta*.

MATERIALS & METHODS

Overview of the Experimental Design

Endophytic bacteria were isolated from wheat (*Triticum aestivum*) plants grown in agricultural fields or research plots located across central Illinois, USA. A subset of this isolate collection was tested in two different *in vitro* assays, which were designed to represent common methods of identifying pathogen-suppressing microbial candidates under laboratory conditions. Based on the results of the *in vitro* assays, a subset of 12 isolates were then tested for their ability to reduce *F. graminearum* spread *in planta*. The 12 isolates spanned a range of *F. graminearum* inhibition outcomes *in vitro*, from weakly to strongly antagonistic. The assays were performed across various temperatures and atmospheric carbon dioxide (CO_2) concentrations in order to test the context-dependency of benefit from the plant-endophyte symbioses and to mimic current and projected summer climatic conditions in the central IL region over the next 50 years (IPCC 2014).

Wheat Tissue Sampling and Isolation of Bacterial Endophytes

Heads of winter wheat (variety unknown and variable across sites) were collected from four sites in central Illinois in May 2017 (Table 1). Wheat heads were clipped below the flag leaf and all tissues were processed within 24 hrs from collection. Heads were sorted on the basis of visual disease symptoms (i.e., any spots or lesions): none (0%), low (10-20% symptomatic spikelets), medium (>20-80%), or high (>80-100%). Wheat heads were dissected into flag leaf, stem (above the flag leaf but below the first spikelet), rachis, developing ovaries, the palea, glume and lemma tissues combined, and awns. Tissue processing and surface sterilization procedures varied by tissue type due to inherent structural differences among the more delicate to robust tissues (see Supporting Information [SI] Table S1 for details). Resulting dissected tissue fragments were plated on one of three types of agar media to increase the probability of isolating slow-growing bacteria (Bai et al 2015): Tryptone Glucose Yeast Extract (TGY), R2A (Oxoid, Basingstoke, UK), or minimal media (MM; recipes provided in SI Methods). All media types were amended with the antifungal nystatin (2.7μM).

An additional sampling effort was undertaken in July 2017, where entire heads of spring wheat plants (variety Glenn) were collected from a fifth site (Table 1). All wheat heads collected at this site had no detectable disease symptoms. Stems and rachii were dissected and sterilized as before. Ovaries were sterilized as before, but were additionally dissected longitudinally after sterilization and plated face-down to increase the surface area of internal tissues for culturing endophytes. No other spring wheat tissues were processed. Tissues were plated on TGY agar amended with nystatin (2.7μM) and additionally with vancomycin (17 μM) to diversify the recovery of gram-negative bacteria.

For both sampling efforts, tissue plates were incubated at 25°C for six to eight days. For all plates yielding bacterial growth, colonies were streaked onto TGY plates until pure cultures were produced. A summary of isolations is provided in Table 2. Pure stock cultures of all isolates were stored in 30% glycerol at -80°C. Bacterial isolates were provisionally identified using a Matrix Assisted Laser Desorption/Ionization (MALDI) Biotyper® (Bruker, Billerica, MA, USA), according to the recommended protocol. For those isolates that failed to yield a confident taxonomic identification to the genus level, and for all isolates used in experimental work, the 16S ribosomal RNA gene was amplified, purified, and sequenced (96 isolates; GenBank accessions MH178669-MH178739). From the 16S sequences, putative taxonomic assignments were made using the RDP naïve Bayesian classifier (Wang et al 2007). A visual taxonomic summary of the isolate collection was created using a hierarchical data visualization tool (i.e., Krona; SI Fig. S1; Ondov et al. 2011).

In Vitro *Dual Culture Assay*

Thirty-four isolates were selected for *in vitro* assays, with the aim of maximizing phylogenetic diversity and including isolates originating from a variety of plant tissues, media, and wheat types (Table 3). Antagonistic effects against *F. graminearum* were first assessed as dual cultures on TGY agar. Each isolate was grown in TGY broth overnight, spun down and washed with sterile water twice. Cell density was estimated using a Scepter™ handheld automated cell counter (Millipore Sigma, Burlington, MA, USA) and adjusted to 10^4 cells/mL. Each bacterial strain, or sterile water for the control, was drop-inoculated (10μL) at four equidistant points on a TGY plate (10cm diameter) and incubated in the dark for one day (21°C, 25°C, 29°C, or 33°C). Next, a 4mm diameter plug of *F. graminearum* strain GZ3639 (hereafter, *Fusarium*), obtained from the leading edge of a 3-day old culture grown on TGY agar at 25°C,

was placed at the center of each plate and incubated for an additional four days at the same experimental temperature as before (Shi et al. 2014).

The diameter of the fungal colony was measured in two perpendicular directions in alignment with the bacterial colonies, and averaged across two replicate plates (Herrera et al. 2016). An inhibition effect size for each isolate-temperature treatment (E_T) was calculated as follows:

$$E_T = (G_F - G_B)/G_F$$

Where G_F is the average growth of *Fusarium* in the non-inoculated control and G_B is the average growth of *Fusarium* in the presence of the bacterial endophyte (Comby et al. 2017). With this score, a value of 1 would indicate complete inhibition of the pathogen by the paired bacterial endophyte, while a value of 0 would indicate no effect of the bacterial endophyte on the pathogen. This experiment was performed in batches with control treatments in each batch. Measurements for each isolate-temperature treatment combination were compared only to their respective controls.

Preliminary results from a comparison of bacterial-fungal dual cultures incubated under ambient CO_2 (450ppm) and elevated CO_2 (1000ppm) at constant 25°C conditions showed no differences in fungal growth (r^2 = 94%) for this assay. Thus, these results are not presented.

In Vitro *Detached Spikelet Assay*

Bacterial interactions with *Fusarium* were further tested using an *in vitro* detached spikelet assay, following Comby et al. (2017). Cultures of each bacterial strain, which were the same 34 isolates as used for the dual culture assay, were grown in TGY broth overnight, spun down and washed with sterile water twice. Cell densities were adjusted to 10^5 cells/mL using

sterile Tween-20 solution (0.1%). For three bacterial isolates (C1, D6, N4), the concentration was adjusted to 10^4 cells/mL due to limited growth.

Spikelets from greenhouse-grown wheat plants (variety 'Glenn') at mid-anthesis were individually clipped and the awns removed. To increase the success of bacterial isolate establishment and to reduce surface contamination, detached spikelets were surface-sterilized by successive dipping for 3min in 70% ethanol, 2min in 0.5% NaOCl, 2min in 70% ethanol, and 2× 1min in sterile water. Spikelets were then vortexed for 30s with the bacterial solution, or with sterile 0.1% Tween-20 for the controls, blotted dry, placed in a single well of a 12-well culture plate filled with 0.3% (3g/L) water agar, and incubated in the dark (21°C, 25°C, 29°C, or 33°C). There were six replicates per isolate-temperature treatment combination.

After two days of incubation, five out of six spikelets were inoculated with *Fusarium* spores. The *Fusarium* spore suspension was created from a 7-day old culture grown in mung bean broth (SI Methods). The fungus was spun down, washed twice using sterile water, and adjusted to 10^5 conidia/mL using a sterile 0.1% Tween-20 solution. Spikelets to be inoculated were removed from the culture plate, sprayed with the fungal spore suspension using a spray atomizer, and then returned to the culture plate. To evaluate the effects of the bacteria alone on the spikelet, one spikelet was left pathogen-free (bacteria + / *Fusarium* –). Within each temperature treatment, one group of spikelets served as the negative control (bacteria – / *Fusarium* –) and another as the positive control (bacteria – / *Fusarium* +). All spikelets were incubated for an additional seven days.

Spikelets were rated from 0 to 4 on the basis of increasing necrosis of the plant tissue and presence of visible hyphae (see SI Fig. S2 for details). Negative controls and spikelets inoculated with bacteria alone did not manifest similar symptoms, but did produce visible bacterial growth.

A severity index was calculated as the average score across 5 replicates. An inhibition effect size for each temperature treatment (E_T) was calculated according to the same equation as for the dual culture assay, except that the severity index was used instead of *Fusarium* colony diameter.

Ribosomal RNA Operon Copy Number

For each of the 34 bacterial isolates tested in the two *in vitro* assays, the ribosomal RNA operon number within the bacterial genome (hereafter 'rrn') was estimated using the rrnDB database (Stoddard et al. 2015) as a metric of potential population growth rate and carbon-use efficiency (Roller et al. 2016). The rrn was determined at the genus-level as the average rrn among all curated genomes within the genus (as in Wu et al. 2017).

In Planta *Detached Head Assay*

To test *in planta* interactions between bacterial endophytes and *Fusarium*, a detached head assay was performed using a subset of 12 bacterial isolates. Heads were clipped above the flag leaf, but below the rachis (10 cm stem length), from greenhouse-grown wheat plants (variety 'Norm') at mid-anthesis. Detached heads were surface-disinfected: 20 min rinse under running tap water, 2 min in 0.1% NaOCl, and rinse with sterile water (Rossi et al. 2001). Wheat heads were then kept overnight in a bulk container filled with Murashige and Skoog (MS) media in a sterile flow hood. Simultaneously, overnight cultures of all 12 bacterial strains were grown as described above, washed, and adjusted to 10^5 cells/mL using sterile Tween-20 solution (0.1%). For the bacterial isolate C1, the concentration was adjusted to 10^4 cells/mL due to limited growth.

Replicate wheat heads were dipped for 30sec in the bacterial solution, individually placed in 50mL conical tubes filled with 25mL of MS media, and the opening of each conical tube sealed using parafilm to reduce evaporation and to hold the detached head upright. Each wheat

head was enclosed in a plastic bag to prevent overly-rapid drying and to reduce cross-contamination, and was spatially randomized in growth chambers. Growth chambers were set to either 25°C or 29°C, and either ambient (450 ppm) or elevated (1000 ppm) atmospheric CO_2 concentration, in a full factorial design. All growth chambers were set to 60% relative humidity and 12-hour days. Four replicate wheat heads were used per isolate-environment treatment. The assay was divided into three experimental sets due to the high number of isolate-environment treatment combinations, as well as to restrict usage of wheat heads to those grown only from the same group of plants in the greenhouse, which were all of the same age.

After two days, the plastic bags were removed and the wheat heads were inoculated with *Fusarium* as follows. Ten µL of a *Fusarium* spore suspension (prepared as described above, except using a 14 day-old liquid culture) was pipetted into an individual floret on the 7th spikelet from the top of the wheat head. Sterile 0.1% Tween-20 was used in lieu of the microbial treatments for the negative (bacteria - /*Fusarium* -) and positive controls (bacteria - / *Fusarium* +). After pathogen inoculation, wheat heads were enclosed in new plastic bags and incubated for an additional two days in the same conical tubes as before, after which the bags were removed and the wheat heads were scored for disease progression (% visually symptomatic spikelets). Four days after the fungal inoculation, wheat heads were clipped below the bottom spikelet and frozen at -80°C.

The density of *Fusarium* present in wheat head tissues (*Fusarium* load) was measured using quantitative polymerase chain reaction (qPCR). Wheat heads were lyophilized for 48hrs inside 2.5oz. aluminum screw top cans (Freund Container & Supply, Lisle, IL) and the tissue ground using four metallic ball bearings (9.525mm) on a Geno/Grinder 2010 (7min, 1600rpm; SPEX SamplePrep, Metuchen, NJ). DNA was extracted from 8 to 10mg of dried material using

the DNeasy PowerPlant Pro Kit (MO BIO Laboratories, Carlsbad, CA, USA). DNA concentration was quantified using the Quant-iT™ dsDNA assay kit (high sensitivity; Life Technologies, Carlsbad, CA) on a CFX96 instrument (Bio-Rad, Hercules, CA).

qPCR was also run on the CFX96 instrument. The reaction mixture consisted of 10µL SsoFast EvaGreen master mix (Bio-Rad Laboratories Inc., Hercules, CA), 1µL each of the upstream and downstream primers (final [0.5µM]), 7µL water, and 1µL DNA template (20ng/µL). The primers used to quantify *Fusarium* load targeted the TRI5 gene, which encodes the trichodiene synthase enzyme responsible for the first dedicated step in the biosynthesis of trichothecene mycotoxins (forward = TCTATGGCCCAAGGACCTGT, reverse = ACGCTCATCGTCGAATTCCT). The thermocycling program consisted of 2min at 98°C, followed by 40 cycles of denaturing for 10s at 95°C, annealing and extension for 30s at 58°C, and plate read. To minimize error associated with variation in DNA extraction efficiency, pathogen DNA abundance was expressed relative to host plant DNA abundance (i.e., *Fusarium* load) using a paired qPCR reaction, with identical PCR conditions, for the wheat translation elongation factor 1-α gene (Nicolaisen 2009; forward = TCTCTGGGTTTGAGGGTGAC, reverse = GGCCCTTGTACCAGTCAAGGT). Three technical replicates were run for all samples.

To better account for variation between samples in the concentration of PCR inhibitors, as well as run-to-run variation between plates, the LinRegPCR program was used to estimate PCR amplification efficiencies for each technical replicate (Ruijter et al. 2009). Starting quantities were calculated with correction for variable amplification efficiencies (Ruijter et al. 2009), as:

$$N_o = N_t / E^{C_q}$$

Where N_o is the starting concentration (in arbitrary fluorescence units), N_t is the fluorescence intensity threshold, C_q is the cycle number at which the fluorescent signal crosses the fluorescence intensity threshold, and E is the amplification factor averaged across technical replicates. An amplification factor of E=2 indicates perfect doubling with each PCR cycle (i.e., 100% efficiency). All samples had an average amplification factor above 1.70 and low variability between technical replicates (i.e., a coefficient of variation < 0.50 for the amplification efficiencies). Samples that failed to meet these criteria were either re-run after dilution of the DNA template (10ng/μL) or, where one technical replicate was obviously divergent in quality, the remaining two replicates were used to compute sample averages.

Statistical Analyses

In vitro assays – We used linear models to test the effect of temperature and bacterial isolate on inhibition effect sizes in the *in vitro* assays. Tukey's post-hoc test was used to determine the significance of differences between temperature groups in inhibition effect size ($\alpha < 0.05$). Principal components analysis (PCA; function 'prcomp') was performed for each *in vitro* assay, where the input data consisted of centered and standardized inhibition effect size values across the four temperatures. For the detached spikelet assay, two variables were transformed to meet assumptions of normality, specifically E_{21} was log-transformed and E_{33} was squared. A procrustes analysis was used to test the similarity between the dual culture and detached spikelet PCA configurations (function *protest*, package 'vegan '; Oksanen et al. 2017). Additionally, linear models were used to test the correlation between bacterial isolates' inhibition effect sizes across temperature levels. The results of each PCA were compared to the rrn using linear models to test the hypothesis that bacterial growth rate influences *in vitro* interaction outcomes with *Fusarium*.

In planta assays – Linear models were used to test for differences in *Fusarium* load based on bacterial isolate, temperature, and CO_2 treatments. Experimental set was also included as a fixed effect. A generalized linear model, with a binomial distribution, was used to test the effect of the same predictors on the percentage of visually symptomatic spikelets, where the response variable tested was a ratio of the visibly infected to total number of spikelets per wheat head. The percentage of visually symptomatic spikelets and *Fusarium* load were also compared using a generalized linear model.

Marginal means estimates were used to compute an *in planta*, inhibition effect size (E_T) for each bacterial treatment relative to the bacteria - / *Fusarium* + control treatment. The function 'emmeans' was used to estimate the marginal mean for each bacterial or control treatment, averaged across all environmental treatments, based on the results of the *Fusarium* load models (package 'emmeans'; Lenth et al. 2018). Lastly, to test whether *in vitro* antagonism against the fungus was predictive of *in planta* disease outcomes, linear models were used to compare the PCA results for each *in vitro* assay to the inhibition effect sizes calculated for the *in planta* assay.

All statistical analyses were conducted in R (v.3.4.3).

RESULTS

In Vitro Assays

On average across all temperatures, every bacterial isolate reduced the growth of *Fusarium* in the dual culture assay (range 3-52% reduction; Fig.1A), and reduced severity scores in the detached spikelet assays (range 21-89% reduction; Fig.1B). There was a clear inhibition zone present for 5 out of 34 of the bacterial isolates in the dual culture assay (2 *Bacillus*, 2 *Serratia*, 1 *Paenibacillus*). Interestingly, the top six performing isolates in the dual culture assay

were all *Bacillus* spp., while in contrast the top six performing isolates in the detached spikelet assay were either *Pseudomonas* spp. or *Paenibacillus* spp. Raw measurements of *Fusarium* growth in both *in vitro* assays was greatest at 25°C and most restricted at the highest temperature (33°C). However, the average inhibition effect size increased steadily with increasing temperatures (for both assays, $p < 0.0001$; SI Fig. S3 A,B).

For both the dual culture and detached spikelet assays, a principal components ordination captured effectiveness of reducing *Fusarium* growth along the first component axis (Fig. 2A,B). This outcome was persistent across temperatures, as indicated by the strong loading of inhibition effect size variables for all four temperature treatments onto the PC-1 axis. For the dual culture assay, the inhibition effect size variable loadings were: 21°C = 0.472, 25°C = 0.550, 29°C = 0.524, 33°C = 0.447 (Fig. 2A). The patterns were similar for the detached spikelet assay, though the inhibition effect size variables for the warmer temperatures loaded more strongly than did the coolest temperature: 21°C = 0.409, 25°C = 0.557, 29°C = 0.542, 33°C = 0.479 (Fig. 2B). Overall, the PC-1 axis for the dual culture assay explained 77.5% of the variability in the ability of the isolates to reduce fungal growth across temperatures, while the PC-1 axis for the detached spikelet assay explained 69.2%. Thus, for both *in vitro* assays, the PC-1 axis divided the isolates along a spectrum from weak to strong antagonists of fungal growth and/or spikelet disease severity. Based on the sequential loading of each temperature effect size variable onto the PC-2 axis in both assays (Fig. 2A,B), the PC-2 axis divided the isolates into those that were more effective antagonists at cooler temperatures versus at warmer temperatures.

A comparison of the PCA ordinations revealed little congruence in bacterial isolate position between the two *in vitro* assays (correlation = 0.279, $p = 0.19$). Similarly, inhibition effect sizes in the dual culture assay were not predictive of effect sizes in the detached spikelet

assay (for all temperatures, $p > 0.10$). The rrn, as a metric of population growth rate, was a marginally significant predictor of the PC-1 axis for the dual culture assay ($F_{1,32} = 3.98$, $p = 0.0546$, Adj. $R^2 = 0.083$; Fig. 3), where bacterial isolates from genera with higher average rrn tended to be stronger antagonists than bacterial isolates from genera with lower average rrn. The rrn was not predictive of the PC-1 axis in the detached spikelet assay ($p = 0.305$; data not shown).

In Planta Assay

Fusarium load, assessed via qPCR, within the detached wheat heads was significantly affected by a three-way interaction between temperature, atmospheric CO_2 concentration, and the identity of the inoculated bacterial isolate ($F_{13,162} = 1.89$, $p = 0.0345$; whole model Adj. $R^2 = 0.26$). These results were such that, for any given combination of temperature and CO_2 treatments, *Fusarium* load varied by the identity of the co-inoculated bacterial isolate (Fig. 4). Across the main effect of bacterial treatment, *Fusarium* load spanned a range from low (i.e., near the negative control) to high (i.e., near the positive control; $F_{13,162} = 3.42$, $p = 0.0001$; Fig. 4).

Temperature alone also significantly affected *Fusarium* load, with reduced fungal growth at the higher temperature (i.e., 29°C; $F_{1,162} = 14.84$, $p = 0.0002$; Fig. 5A). There was a trend for reduced *Fusarium* load under elevated CO_2 conditions, but this was not significant as a standalone main effect ($p = 0.107$; Fig. 5B). There was no detectable effect of experimental set on *Fusarium* load ($p = 0.969$).

Visual assessment of disease progression was a poor match for assessment of pathogen load by qPCR. The percentage of visually symptomatic spikelets was significantly greater at 29°C relative to the 25°C ($\chi^2_{1,162} = 9.05$, $p = 0.0026$; SI Fig. S4A), but did not vary by CO_2 treatment ($p = 0.508$; SI Fig. S4B) or by the identity of the inoculated bacterial isolate ($p =$

0.913). The percentage of visually symptomatic spikelets did vary by experimental set ($\chi^2_{2,162}$ = *7.36, p = 0.0253*; SI Fig. S4C). Additionally, *Fusarium* load was significantly negatively correlated with the percentage of visually symptomatic spikelets ($\chi^2_{1,218}$ = *5.45, p = 0.0195*; Fig. 6).

In Vitro to In Planta Comparison

In vitro results failed to predict disease reduction outcomes *in planta*. Linear models indicated that the PC-1 axis in the dual culture assay did not significantly predict the inhibition effect sizes in the detached head assay (*p= 0.291*; Fig. 7A). Similarly, the PC-1 axis from the detached spikelet also did not significantly predict the detached head assay effect sizes (*p= 0.932*; Fig. 7B).

DISCUSSION

Overall, we found that our *in vitro* assays were poor predictors of *Fusarium* growth *in planta*, contrary to our original prediction. However, in both the dual culture and detached spikelet assays all 34 bacterial isolates tested effectively reduced the growth of *Fusarium*, indicating that all isolates had at least partial efficacy against the plant pathogen under laboratory conditions. The two *in vitro* assays each divided the bacterial isolates along a spectrum from weak to strong antagonists of the wheat fungal pathogen, though the two assays were not concordant with one another. In the dual culture assay, but not the detached spikelet assay, bacterial isolates with greater rrn tended to be more effective against *Fusarium*, potentially supporting the hypothesis that the dual culture assay measured bacterial population growth rate, in part, as a metric of competitive ability. Lastly, across all assays, the outcome of the bacterial-fungal interaction varied as a function of the environmental condition, with increasing

effectiveness of the bacteria at higher temperatures in the *in vitro* assays and greater performance of the fungus at cooler temperatures in the *in planta* assay, indicating environmental dependency to the microbial interactions.

Across all bacterial treatments in the *in planta* assay, *Fusarium* load was significantly greater at the lower temperature condition (i.e., 25°C), which could be partially indicative of increased fungal performance under more moderate temperature conditions (Pietikäinen et al. 2005). Interestingly, bacterial effectiveness against the fungal pathogen *in vitro* was also reduced at the lower temperatures, again indicating greater fitness of the fungus at cooler temperatures. We found no detectable differences in the bacterial-*Fusarium* interactions across atmospheric CO_2 conditions *in vitro* (data not presented), however *Fusarium* load was marginally reduced under elevated CO_2 *in planta*, possibly as a result of increased carbon access and defense allocation for the plant host (Ainsworth et al. 2002).

Additionally, our results showed a negative correlation between *Fusarium* load and the percentage of visually symptomatic spikelets. Overall, this could indicate that external symptoms of disease progression surpassed the internal proliferation of *Fusarium* growth. For instance, it is known that visual assessment of disease symptoms can be difficult and prone to human error (Siou et al. 2014). Thus, it is possible that our visual assessments instead captured higher rates of plant senescence (i.e., premature bleaching of plant tissue) that were in fact caused by faster metabolic rates and increased ethylene signaling under the elevated CO_2 treatments (Seneweera et al. 2003). Alternatively, death of the rachis tissue may have cut off resource supply to higher portions of the head, leading to bleaching symptoms even in the absence of the pathogen in those tissues (Bai and Shaner 2004). These results highlight the utility of assays involving

physiologically active plant substrates as an important contextual habitat for plant-pathogen-endophyte interactions.

Despite the now well-recognized idea that microbiota can mediate plant host function (Friesen et al. 2011), there has been surprisingly little work exploring the context-dependency of endophyte-mediated disease outcomes across realistic environmental gradients (Busby et al. 2016). In our study, temperature and CO_2 conditions interacted to alter the effect of endophytic bacteria on *Fusarium* load in planta. For example, some bacterial isolates performed better under ambient CO_2 conditions (e.g., G12 – *Terribacillus sp.*), while other bacterial isolates performed better under elevated CO_2 (e.g., Q16 – *Paenibacillus sp.*). Recent work has also shown context-dependent benefits to plant hosts from fungal endophytes under differential soil moisture (Giauque and Hawkes 2013) and nutrient (Nelson et al. 2018) conditions. However, few studies have performed multi-factorial, climate experiments and measured disease outcomes in the presence of a beneficial symbiont (but see Rúa et al. 2014).

It is perhaps surprising that we did not find a greater concordance between our two *in vitro* assays in the effectiveness of different bacterial isolates against *Fusarium* (Fig. 2). Previous research by Comby et al. (2017) also found that many *Bacillus* isolates did well against the selected pathogen in dual culture plate competition assays, but that the *Bacillus* isolates were not as effective in a detached spikelet assay. We suggest that this outcome may be due to the inherent differences among bacterial lineages in the average number of ribosomal RNA genomic copies (Kembel et al. 2012), which is a correlate of maximum population growth rate (Roller et al. 2016) and potentially indicative of a competitive life history strategy (Stevenson and Schmidt 2004). Differences among bacterial isolates in competitive life history strategies may have allowed more competitive bacterial isolates to reduce *Fusarium* growth when contested in initial,

spatially-segregated colonies on media, but would not have been beneficial in the detached spikelet assay, where the bacterial and fungal populations were intermixed on the plant substrate. While our analysis of rrn in the *in vitro* assays was exploratory, and cannot be fully separated from bacterial genus identity, we suggest that future research should experimentally test this bacterial trait in the context of plant symbioses. For example, different bacterial lineages may perform better in different plant habitats as a function of their innate population growth rates (Roller et al. 2016), such as on plant debris at the end of the growing season, or internally inside living plant tissue.

Our sampling efforts identified a wide array of bacterial endophytes, representing many different bacterial genera (SI Fig. S1). Several of the genera we identified have previously been reported as plant-growth promoting in the wheat-*Fusarium* system. For example, two of the top four best-performing bacterial isolates from our *in planta* assay were *Paenibacillus sp.* (i.e., Q16 & Q22; Fig. 4), which have been isolated from wheat seeds and demonstrated to be effective against *F. graminearum in vitro* and in greenhouse trials in wheat (He et al. 2009, Herrera et al. 2016). Several previous studies have also identified *Bacillus spp.* as inhibitors of *F. graminearum* growth and production of the mycotoxin deoxynivalenol (Shi et al. 2014, Zhao et al. 2014, Palazzini et al. 2016). *Bacillus spp.* are particularly attractive from a commercialization standpoint, due to their ability to form heat-resistant spores and survive seed-treatment processes (Yánez-Mendizabal et al. 2012). However, in our own study the *Bacillus spp.* did not perform well in either the detached spikelet or detached head assay. In general, there are few *Fusarium*-active biocontrol products for wheat that have reached commercialization (O'Callaghan 2016), Cerall® being an exception, which is comprised of a seed treatment of the bacterial species *Pseudomonas chloroaphis* ("BioAgri AB" 2018).

Our results demonstrate the importance of considering a spectrum of effectiveness from *in vitro* assays when designing *in planta* or field experiments. However, across all of the assays tested here, the bacterial isolate was always inoculated prior to inoculation of the fungal pathogen. Recent work has shown that order of arrival (i.e., priority effects) can affect microbial interactions in plant hosts and determine effectiveness of biocontrol agents (Adame-Álvarez et al. 2014, Schoneberg et al. 2015). We also did not assess the extent of endophytic bacterial establishment in the *in planta* assay, which will be necessary for future studies to identify the mode of action for pathogen antagonism inside plant tissues. Future research should also seek to test the effectiveness of employing a consortia of bacterial isolates against plant pathogens versus single endophytic isolates (O'Callaghan 2016), and then compare these microbial treatments to conventional agricultural practices, such as fungicide application.

In conclusion, our results demonstrate the utility of using a more holistic approach to screen microbial antagonists of disease-causing agents. The two *in vitro* assays tested here were designed to mimic simple lab protocols used to rank microbial endophytes by their effectiveness against an undesired outcome (e.g., pathogen proliferation). However, neither assay was able to successfully predict disease reduction outcomes *in planta*. Microbial endophytes, like macroorganisms, experience trade-offs in growth (Litchman et al. 2015) that can affect their ability to thrive in environments of differing nutritional quality (e.g., lab media vs. plant tissues), physical complexity, or climatic conditions. To better understand these trade-offs in growth, particularly for microbial symbionts of hosts, will require tests across multiple environmental conditions (Hawkes and Connor 2017) and a greater consideration for the underlying traits that drive microbial species interactions *in vitro*. The ability to culture microbiota represents a great opportunity to study microbial species outside of the host environment, under controlled

experimental conditions. However, it is also imperative that future studies are designed to better consider the complexity of microbial species growth and trade-offs under both *in vitro* and *in vivo* conditions.

Acknowledgements

The authors would like to thank Mr. Jake Brown and Mr. Jeff Bender, as well as Drs. Martha Vaughan, Chris Dunlap, and Mark Busman, for their assistance with the project and identification of sampling sites, as well as Dr. Keith Clay for editorial comments on earlier versions of the manuscript. B.K.W. was supported by an NSF Graduate Research Fellow and by the NSF Graduate Research Internship Program, hosted through a research agreement with the U.S. Department of Agriculture (USDA). Partial funding for this work was provided by the USDA ARS National Program for Food Safety. Mention of trade names or commercial products is solely for the purpose of providing specific information and does not imply recommendation or endorsement by USDA. USDA is an equal opportunity provider and employer.

LITERATURE CITED

Adame-Álvarez, R.-M., J. Mendiola-Soto, and M. Heil. 2014. Order of arrival shifts endophyte-pathogen interactions in bean from resistance induction to disease facilitation. FEMS Microbiology Letters 355:100–107.

Ainsworth, E. A., P. A. Davey, C. J. Bernacchi, O. C. Dermody, E. A. Heaton, D. J. Moore, P. B. Morgan, S. L. Naidu, H. S. Y. Ra, X. G. Zhu, P. S. Curtis, and S. P. Long. 2002. A meta-analysis of elevated [CO_2] effects on soybean (*Glycine max*) physiology, growth and yield. Global Change Biology 8:695–709.

Arnold, A. E., L. C. Mejía, D. Kyllo, E. I. Rojas, Z. Maynard, N. Robbins, and E. A. Herre. 2003. Fungal endophytes limit pathogen damage in a tropical tree. Proceedings of the National Academy of Sciences of the United States of America 100:15649–15654.

Bai, G., and G. Shaner. 2004. Management and resistance in wheat and barley to Fusarium head blight. Annual Review of Phytopathology 42:135–161.

BioAgri AB. 2018. . https://www.bioagri.se/produkter/produktbibliotek/cerall/.

Busby, P. E., M. Ridout, and G. Newcombe. 2016. Fungal endophytes: modifiers of plant disease. Plant Molecular Biology 90:645–655.

Clay, K., and C. Schardl. 2002. Evolutionary origins and ecological consequences of endophyte symbiosis with grasses. The American Naturalist 160:S99–S127.

Comby, M., M. Gacoin, M. Robineau, F. Rabenoelina, S. Ptas, J. Dupont, C. Profizi, and F. Baillieul. 2017. Screening of wheat endophytes as biological control agents against Fusarium head blight using two different *in vitro* tests. Microbiological Research 202:11–20.

Connor, E. W., M. Sandy, and C. V. Hawkes. 2017. Microbial tools in agriculture require an ecological context: Stress-dependent non-additive symbiont interactions. Agronomy Journal 109:917–926.

Finkel, O. M., G. Castrillo, S. H. Paredes, I. S. González, and J. L. Dangl. 2017. Understanding and exploiting plant beneficial microbes. Current Opinion in Plant Biology 38:155–163.

Friesen, M. L., S. S. Porter, S. C. Stark, E. J. von Wettberg, J. L. Sachs, and E. Martinez-Romero. 2011. Microbially mediated plant functional traits. Annual Review of Ecology, Evolution, and Systematics 42:23–46.

Giauque, H., and C. V Hawkes. 2013. Climate affects symbiotic fungal endophyte diversity and performance. American Journal of Botany 100:1435–1444.

Hawkes, C. V, and E. W. Connor. 2017. Translating phytobiomes from theory to practice: ecological and evolutionary considerations. Phytobiomes 1:57–69.

He, J., G. J. Boland, and T. Zhou. 2009. Concurrent selection for microbial suppression of *Fusarium graminearum*, Fusarium head blight and deoxynivalenol in wheat. Journal of Applied Microbiology 106:1805–1817.

Herrera, S. D., C. Grossi, M. Zawoznik, and M. D. Groppa. 2016. Wheat seeds harbour bacterial endophytes with potential as plant growth promoters and biocontrol agents of *Fusarium graminearum*. Microbiological Research 186–187:37–43.

IPCC. 2014. Climate change 2014: Synthesis Report. Contribution of Working Groups I, II, II to the Fifth Assessment Report of the Intergovernmental Panel on Climate Change [Core Writing Team R.K. Pachauri and L.A. Meyer (eds.)]. IPCC, Geneva, Switzerland.

Kembel, S. W., M. Wu, J. A. Eisen, and J. L. Green. 2012. Incorporating 16S gene copy number information improves estimates of microbial diversity and abundance. PLoS Computational

Biology 10:1–11.

Kia, S. H., M. Jurkechova, K. Glynou, M. Piepenbring, and J. G. Maciá-Vicente. 2018. The effects of fungal root endophytes on plant growth are stable along gradients of abiotic habitat conditions. FEMS Microbiology Ecology 94:1–10.

Lenth, R., H. Singmann, J. Love, P. Buerkner, and M. Herve. 2018. "emmeans" Estimated Marginal Means Package.

Litchman, E., K. F. Edwards, and C. A. Klausmeier. 2015. Microbial resource utilization traits and trade-offs: Implications for community structure, functioning, and biogeochemical impacts at present and in the future. Frontiers in Microbiology 6:1–10.

Martiny, J. B. H., S. E. Jones, J. T. Lennon, and A. C. Martiny. 2015. Microbiomes in light of traits: A phylogenetic perspective. Science 350:aac9323-1.

McMullen, M., G. Bergstrom, E. De Wolf, R. Dill-Macky, D. Hershman, G. Shaner, and D. Van Sanford. 2012. A unified effort to fight an enemy of wheat and barley: Fusarium head blight. Plant Disease 96:1712–1728.

Mei, C., and B. Flinn. 2010. The use of beneficial microbial endophytes for plant biomass and stress tolerance improvement. Recent Patents on Biotechnology 4:81–95.

Nelson, J. M., D. A. Hauser, R. Hinson, and A. J. Shaw. 2018. A novel experimental system using the liverwort *Marchantia polymorpha* and its fungal endophytes reveals diverse and context-dependent effects. New Phytologist 218:1217–1232.

O'Callaghan, M. 2016. Microbial inoculation of seed for improved crop performance: issues and opportunities. Applied Microbiology and Biotechnology 100:5729–5746.

Oksanen, J., F. G. Blanchet, M. Friendly, R. Kindt, P. Legendre, D. McGlinn, P. R. Minchin, R. B. O'Hara, G. L. Simpson, P. Solymos, M. H. H. Stevens, E. Szoecs, and H. Wagner. 2017.

"vegan" Community Ecology Package.

Ondov, B. D., N. H. Bergman, and A. M. Phillippy. 2011. Interactive metagenomic visualization in a Web browser. BMC Bioinformatics 12.

Palazzini, J. M., E. Alberione, A. Torres, C. Donat, J. Köhl, and S. Chulze. 2016. Biological control of *Fusarium graminearum sensu stricto*, causal agent of Fusarium head blight of wheat, using formulated antagonists under field conditions in Argentina. Biological Control 94:56–61.

Peñuelas, J., and J. Terradas. 2014. The foliar microbiome. Trends in Plant Science 19:278–280.

Pietikäinen, J., M. Pettersson, and E. Bååth. 2005. Comparison of temperature effects on soil respiration and bacterial and fungal growth rates. FEMS Microbiology Ecology 52:49–58.

Porras-Alfaro, A., and P. Bayman. 2011. Hidden fungi, emergent properties: endophytes and microbiomes. Annual Review of Phytopathology 49:291–315.

van der Putten, W. H., M. A. Bradford, E. P. Brinkman, T. F. J. van de Voorde, and G. F. Veen. 2016. Where, when and how plant-soil feedback matters in a changing world. Functional Ecology 30:1109–1121.

Roller, B. R. K., S. F. Stoddard, and T. M. Schmidt. 2016. Exploiting rRNA operon copy number to investigate bacterial reproductive strategies. Nature Microbiology 1:1–7.

Rossi, V., A. Ravanetti, E. Pattori, and S. Giosuè. 2001. Influence of temperature and humidity on the infection of wheat spikes by some fungi causing Fusarium head blight. Journal of Plant Pathology 83:189–198.

Rúa, M. A., R. L. McCulley, and C. E. Mitchell. 2014. Climate drivers, host identity and fungal endophyte infection determine virus prevalence in a grassland ecosystem. Journal of Ecology 102:690–699.

Ruijter, J. M., C. Ramakers, W. M. H. Hoogaars, Y. Karlen, O. Bakker, M. J. B. van den hoff, and A. F. M. Moorman. 2009. Amplification efficiency: Linking baseline and bias in the analysis of quantitative PCR data. Nucleic Acids Research 37.

Savary, S., A. Ficke, J. N. Aubertot, and C. Hollier. 2012. Crop losses due to diseases and their implications for global food production losses and food security. Food Security 4:519–537.

Schoneberg, A., T. Musa, R. T. Voegele, and S. Vogelgsang. 2015. The potential of antagonistic fungi for control of *Fusarium graminearum* and *Fusarium crookwellense* varies depending on the experimental approach. Journal of Applied Microbiology 118:1165–1179.

Seneweera, S., S. K. Aben, A. S. Basra, B. Jones, and J. P. Conroy. 2003. Involvement of ethylene in the morphological and developmental response of rice to elevated atmospheric CO_2 concentrations. Plant Growth Regulation 39:143–153.

Shi, C., P. Yan, J. Li, H. Wu, Q. Li, and S. Guan. 2014. Biocontrol of *Fusarium graminearum* growth and deoxynivalenol production in wheat kernels with bacterial antagonists. International Journal of Environmental Research and Public Health 11:1094–1105.

Siou, D., S. Gélisse, V. Laval, C. Repinçay, R. Canalès, F. Suffert, and C. Lannou. 2014. Effect of wheat spike infection timing on Fusarium head blight development and mycotoxin accumulation. Plant Pathology 63:390–399.

Stevenson, B. S., and T. M. Schmidt. 2004. Life history implications of rRNA gene copy number in *Escherichia coli*. Society 70:6670–6677.

Stoddard, S. F., B. J. Smith, R. Hein, B. R. K. Roller, and T. M. Schmidt. 2015. rrnDB: Improved tools for interpreting rRNA gene abundance in bacteria and archaea and a new foundation for future development. Nucleic Acids Research 43:D593–D598.

Strange, R. N., J. R. Majer, and H. Smith. 1974. The isolation and identification of choline and

betaine as the two major components in anthers and wheat germ that stimulate *Fusarium graminearum in vitro*. Physiological Plant Pathology 4:277–290.

Vacher, C., A. Hampe, A. Porté, U. Sauer, S. Compant, and C. E. Morris. 2016. The phyllosphere: microbial jungle at the plant-climate interface. Annu. Rev. Ecol. Evol. Syst.:in press.

Wu, L., Y. Yang, S. Chen, Z. Jason Shi, M. Zhao, Z. Zhu, S. Yang, Y. Qu, Q. Ma, Z. He, J. Zhou, and Q. He. 2017. Microbial functional trait of rRNA operon copy numbers increases with organic levels in anaerobic digesters. ISME Journal 11:2874–2878.

Yánez-Mendizabal, V., I. Viñas, J. Usall, T. Cañamás, and N. Teixidó. 2012. Endospore production allows using spray-drying as a possible formulation system of the biocontrol agent *Bacillus subtilis* CPA-8. Biotechnology Letters 34:729–735.

Zhao, Y., J. N. Selvaraj, F. Xing, L. Zhou, Y. Wang, H. Song, X. Tan, L. Sun, L. Sangare, Y. M. E. Folly, and Y. Liu. 2014. Antagonistic action of *Bacillus subtilis* strain SG6 on *Fusarium graminearum*. PLoS ONE 9:1–11.

FIGURES AND TABLES

Table 1 – Description of sites used in bacterial endophyte sampling effort.

Site	Latitude	Longitude	Disease Incidence	Wheat Type	Tissues Processed
1	40°40’06”N	88°46’56”W	None	Winter	F,S,R,V,PGL,A
2	40°28’47”N	89°40’49”W	20-100%	Winter	F,S,R,V,PGL
3	40°29’25”N	89°41’32”W	30-100%	Winter	F,S,R,V,PGL
4	40°29’39”N	89°41’6”W	0-30%	Winter	F,S,R,V,PGL
5	40°42’30”N	89°36’56”W	None	Spring	S,R,V

Disease Incidence indicates variability among sites in the percentage of spikelets per wheat head that had any visual disease symptoms. For the tissues processed: F=flag leaf, S=stem, R=rachis, V=ovaries, PGL=palea & glume & lemma, and A=awns.

Table 2 – Summary of bacterial endophyte isolations.

	Type	F	S	R	V	PGL	A
Tissue	Winter	28	5	4	5	80	29
	Spring		19	32	108		
		TGY	**R2A**	**MM**	**TGY+Vancomycin**		
Media	Winter	72	57	22			
	Spring				159		
		None	**Low**	**Med**	**Hi**		
Disease	Winter	81	25	18	27		
	Spring	159					
		S1	**S2**	**S3**	**S4**	**S5**	
Site	Winter	66	21	32	32		
	Spring					159	

Bacterial endophytes were sampled from across two wheat types (winter, spring); six tissue types (F=flag leaf, S=stem, R=rachis, V=ovaries, PGL=palea & glume & lemma, and A=awns); three types of agar media (TGY=Tryptone-Glucose-Yeast, R2A=Reasoner's 2A agar, and MM=Minimal Media); four levels of disease, where disease describes the percentage of symptomatic spikelets for specific wheat heads from which bacteria were isolated; and five field sites. Counts represent the number of isolations made within each category – the same 310 isolates are divided in different ways in each section.

Table 3 – List of bacterial isolates used in the *in vitro* experiments.

Bacterial Class	ID	Bacterial Genus	Site	Disease Status	Media	Tissue Type
Bacilli	A6	*Bacillus*	S1	None	M	A
	A10	*Paenibacillus* *	S1	None	T	A
	A22	*Bacillus*	S1	None	T	A
	A28	*Paenibacillus*	S1	None	R	A
	A30	*Bacillus* *	S1	None	R	A
	B12	*Bacillus*	S1	None	R	PGL
	B15	*Bacillus*	S1	None	R	PGL
	G3	*Bacillus*	S2	Low	T	PGL
	G9	*Bacillus*	S2	Med	T	PGL
	G11	*Paenibacillus*	S2	Med	T	PGL
	G12	*Terribacillus* *	S2	Med	T	PGL
	G14	*Bacillus*	S2	Med	R	PGL
	O1	*Bacillus*	S3	Hi	R	R
	Q10	*Lysinibacillus* *	S4	Low	T	PGL
	Q16	*Paenibacillus* *	S4	Low	R	PGL
	Q22	*Paenibacillus* *	S4	Low	R	PGL
	T1	*Bacillus*	S4	None	T	R
	U2	*Bacillus*	S4	Low	R	S
Gammaproteobacteria	A17	*Pseudomonas*	S1	None	R	A
	C1	*Xanthomonas* *	S1	None	T	V
	D2	*Pseudomonas*	S1	None	M	F
	D6	*Pseudomonas*	S1	None	T	F
	F2	*Pseudomonas*	S1	None	T	S
	N4	*Pseduomonas* *	S3	Hi	T	F
	U1	*Pantoea*	S4	None	M	S
	W14	*Acinetobacter* *	S5	None	T+VAN	S
	X1	*Enterobacteriaceae (Kosakonia –low conf.)*	S5	None	T+VAN	R
	X15	*Stenotrophomonas*	S5	None	T+VAN	R
	Y1	*Pantoea*	S5	None	T+VAN	V
	Y2	*Serratia* *	S5	None	T+VAN	V
	Y8	*Pantoea*	S5	None	T+VAN	V
	Y11	*Pseudomonas* *	S5	None	T+VAN	V
	Y43	*Enterobacteriaceae (Kosakonia –low conf.)*	S5	None	T+VAN	V
	Y108	*Serratia* *	S5	None	T+VAN	V

Taxonomic assignment is presented at the genus level. Isolates are sorted by bacterial class. The site and disease status of the wheat heads sampled are shown, as well as the type of agar medium

and the plant tissue on which they were isolated. Bacterial ID is given as a letter-number code used for simplicity and presentation in figures. An asterisk indicates the bacterial isolate was also used in the *in planta* assay.

Figure 1 – All bacterial isolates reduce the growth of *Fusarium in vitro*. Barplots are shown for the A) Dual Culture Assay and B) Detached Spikelet Assay. Bacterial isolates are ordered from lowest (i.e., no impact) to greatest (i.e., high inhibition) average effect size for each assay. The y-axis has been inverted to aid in interpretation of the effect size metric. The 12 isolates selected for the *in planta* assay are also indicated.

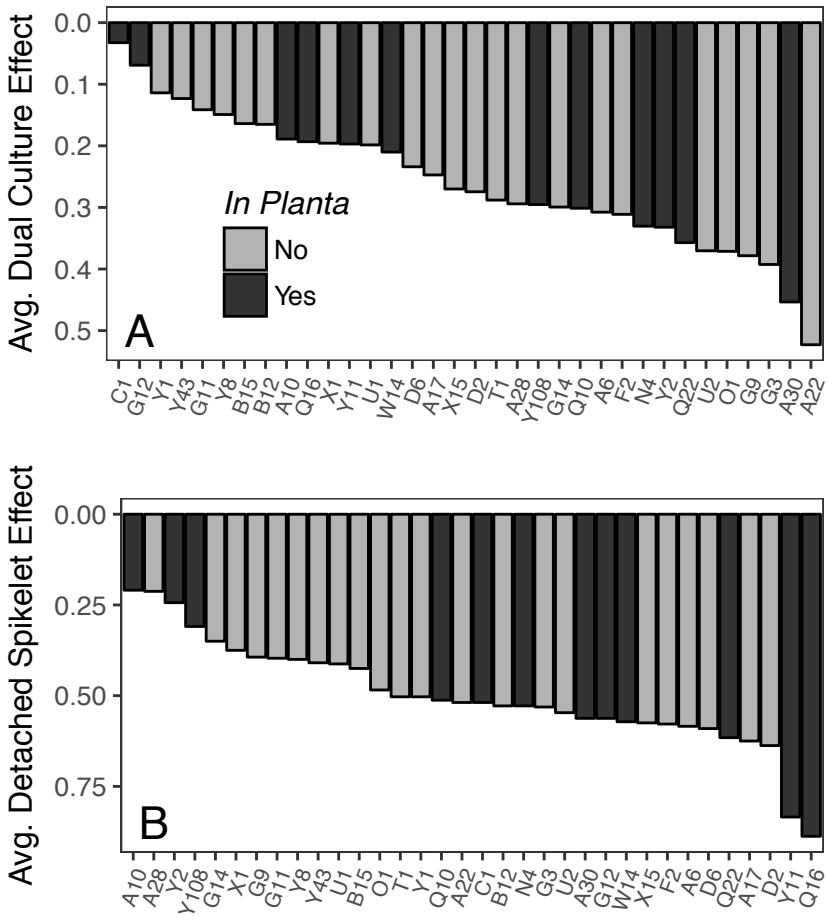

Figure 2 – Principal components analysis divided bacterial isolates along a continuum of weak to strong antagonists for both the A) Dual Culture Assay and B) Detached Spikelet assays. Vectors indicate the inhibition effect sizes (E_T) for each of four temperatures. Ellipses represent a confidence interval (one standard deviation, 0.68) for the two represented bacterial classes. Letter-number codes describe the Bacterial ID (*see Table 3 for reference*). Percentage of variance explained is provided for each axis.

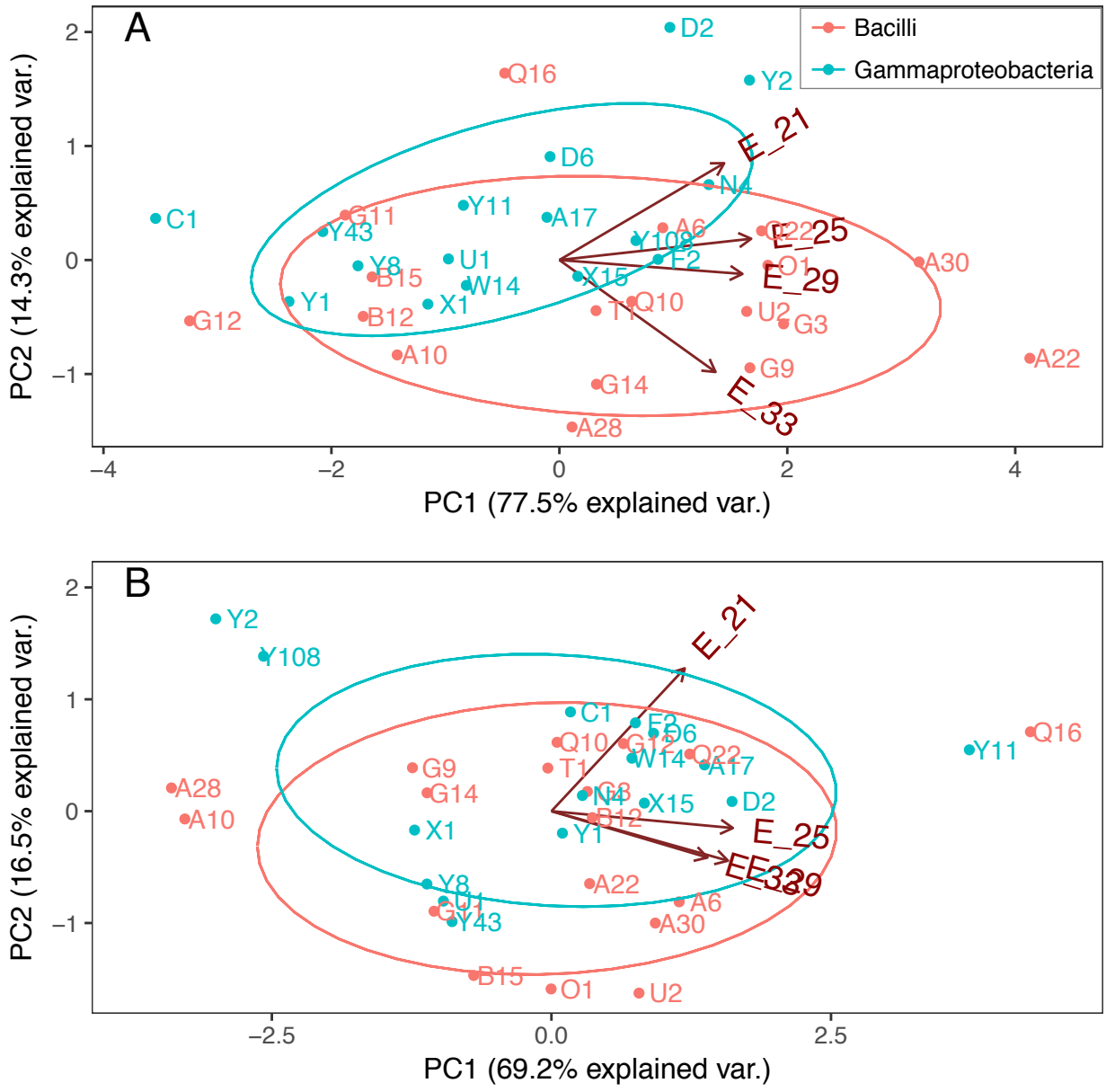

Figure 3 – Bacterial antagonism against *Fusarium* in the dual culture assay increased marginally with increasing ribosomal RNA operon number (rrn). A regression of the average genus-level rrn is plotted against the dual culture assay PC-1 axis score, which divided the bacterial isolates along a continuum from weak to strong antagonists (blue-dashed line). Each point represents a single bacterial isolate.

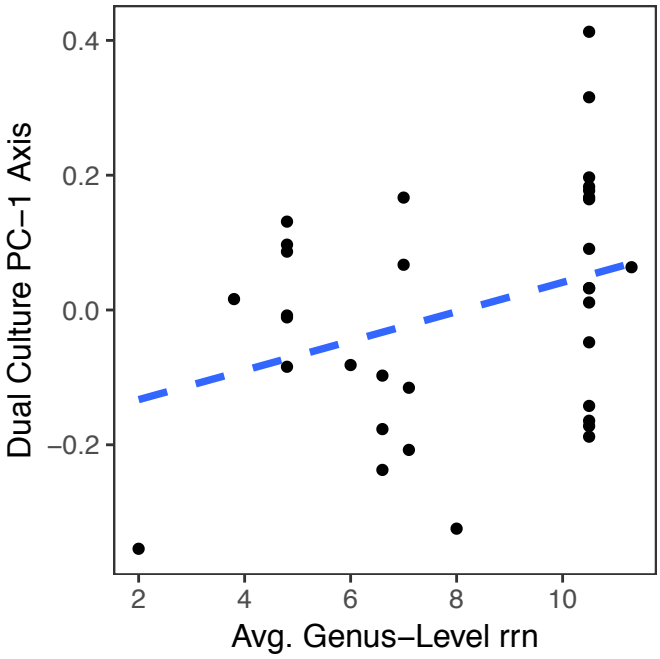

Figure 4 – The ability of bacterial isolates to reduce *Fusarium* load *in planta* varied by temperature and CO_2 condition. Boxplots indicate variation in *Fusarium* load (*F. graminearum* to *T. aestivum* gene copy ratio) and are displayed for each bacterial treatment and the controls. The x-axis is shown on a log scale. Letter-number codes describe the Bacterial ID (*see Table 3 for reference*), where 'B-/F+' denotes the positive control (bacteria - / *Fusarium* +) and 'B-/F-' denotes the negative control (bacteria - /*Fusarium* -). For the ambient and elevated atmospheric CO_2 treatments, the abbreviations 'Amb.' and 'Elev.' are used, respectively

(*see next page*)

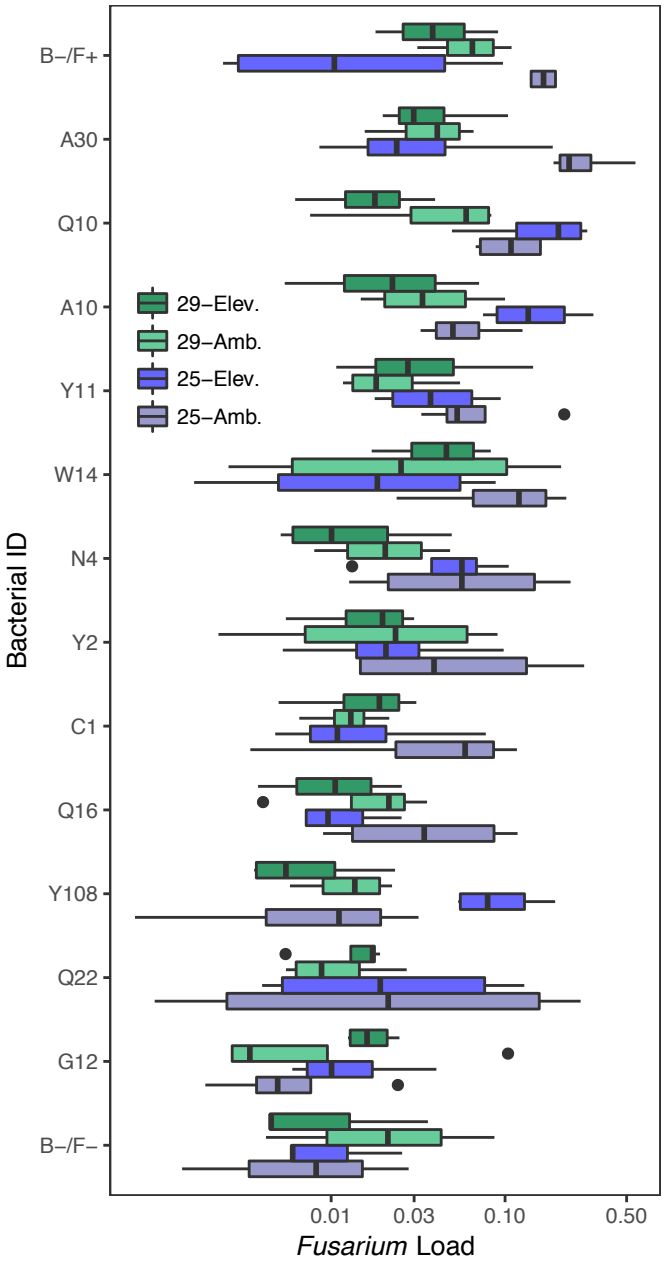
B−/F+
A30
Q10
A10
Y11
W14
N4
Y2
C1
Q16
Y108
Q22
G12
B−/F−
Bacterial ID
29−Elev.
29−Amb.
25−Elev.
25−Amb.
0.01
0.03
0.10
0.50
Fusarium Load

Figure 5 – *Fusarium* load *in planta* was A) significantly reduced under the higher temperature and B) marginally reduced under the elevated CO_2 treatments. Boxplots indicate variation in *Fusarium* load (*F. graminearum* to *T. aestivum* gene copy ratio). The y-axes are shown on a log scale. Each point represents a measurement for a single experimental wheat head.

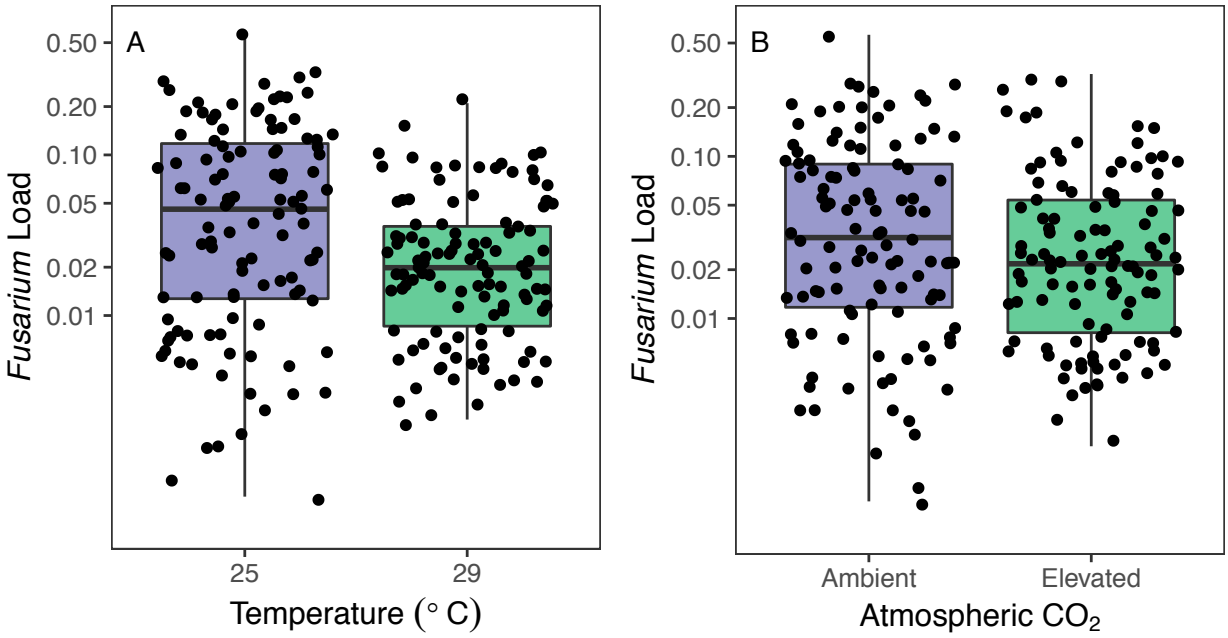

Figure 6 – *Fusarium* load significantly negatively correlated with the percentage of symptomatic spikelets *in planta*. A regression of *Fusarium* load plotted against the percentage of infected spikelets (blue-dashed line). The x-axis is shown on a log scale. Each point represents a measurement for a single experimental wheat head.

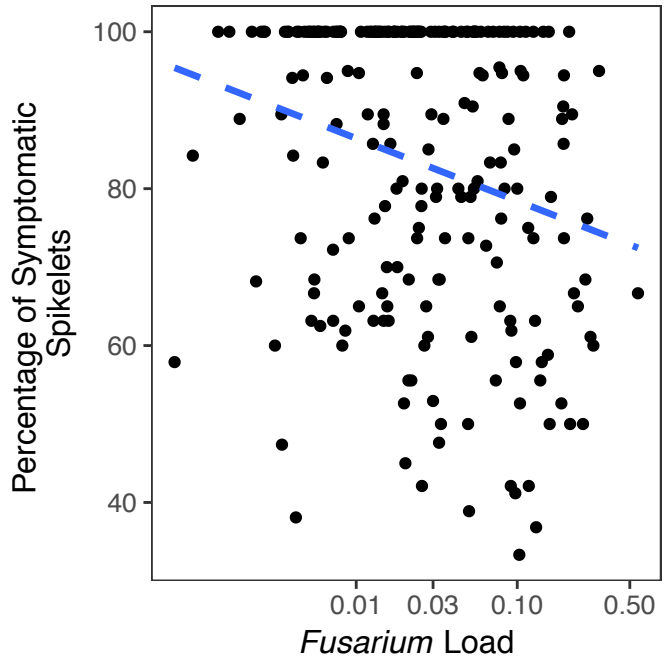

Figure 7 – *In vitro* measurements of bacterial antagonism against the *Fusarium* pathogen do not significantly predict disease outcomes *in planta*. A regression of the PC-1 axis from A) the dual culture assay and B) the detached spikelet assay plotted against the effect size on *Fusarium* load in the detached head assay (blue-dashed lines). Each point and letter-number code is used for a single Bacterial ID (*see Table 3 for reference*).

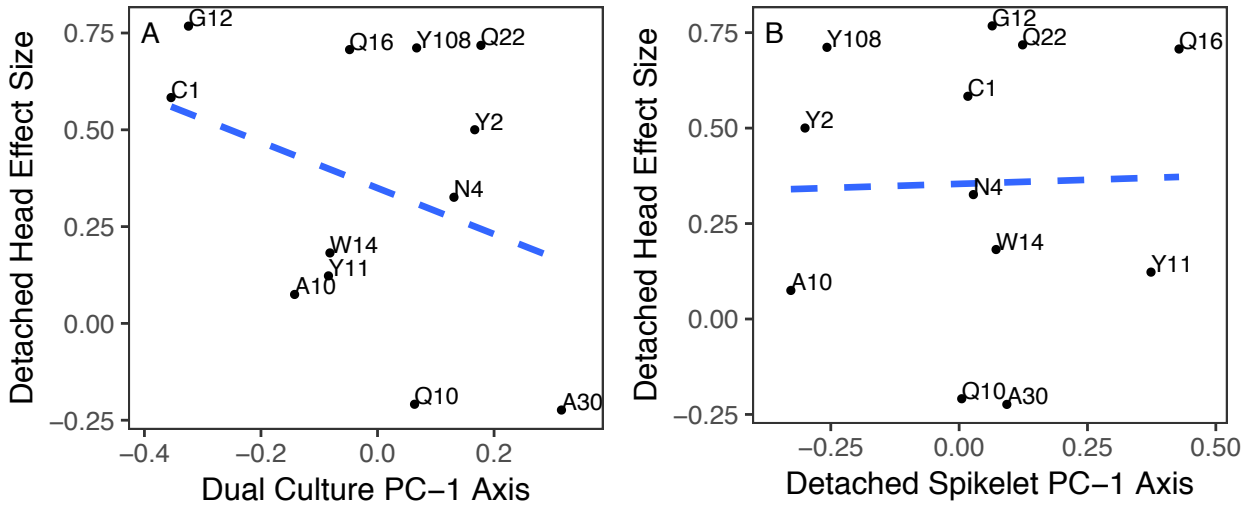

SUPPORTING INFORMATION

Table S1 – Description of Tissue Processing and Surface Sterilization

Tissue	Pre-Sterilization Processing	Sterilization Procedure	Post-Sterilization Processing
S &R	Cut into 3cm sections	30s in 70% ethanol, 3min in 0.5% NaOCl, 30s in 70% ethanol, three sterile H_2O rinses, dried on a sterile tissue	Cut into 1cm sections, dissected longitudinally, both halves plated facing down
F	Cut into ¼ cm^2 square fragments	30s in 70% ethanol, 2min in 0.5% NaOCl, 30s in 70% ethanol, three sterile H_2O rinses, dried on a sterile wipe	4 fragments haphazardly selected and plated 4 per plate
V	(none)		
PGL	(none)	30s in 70% ethanol, three sterile H_2O rinses, dried on a sterile wipe	4 per plate
A	Haphazardly cut to random lengths		3-4 per plate

SI METHODS

Media Recipes

Minimal Medium (MM) – 1 Liter – 1.6g Na_2HPO_4 + 1.0g KH_2PO_4 + 0.5g $MgSO_4 \cdot 7H_2O$ + 0.5g $NaNO_3$ + 0.5g $(NH_4)_2SO_4$ + 25mg $CaCl_2 \cdot 2H_2O$ + 1mL trace metals solution (TekNova, Sterile 1000x Trace Metals Mixture, Cat.No. T1001). After autoclaving and cooling, add: 1 mL Vitamin Supplement (ATCC®, MD-VS™).

Tryptone/Glucose/Yeast (TGY) – 1 Liter – 5g tryptone + 1g glucose/dextrose + 5g yeast extract + 1g K_2HPO_4 + 20g agar. For broth, simply omit the agar.

Mung Bean Broth – 1 Liter – 40g Mung Beans. Bring water to a boil first, then add mung beans and boil for 10min. Allow broth to cool, then strain using a colander and autoclave.

Figure S1 – Graphical summary for the taxonomic breadth of recovered bacterial endophytes of wheat inflorescence, stem, and flag leaf tissues. Shown is the proportion of isolates belonging to each taxon, from the rank of phylum (inner ring) to genus (outer ring).

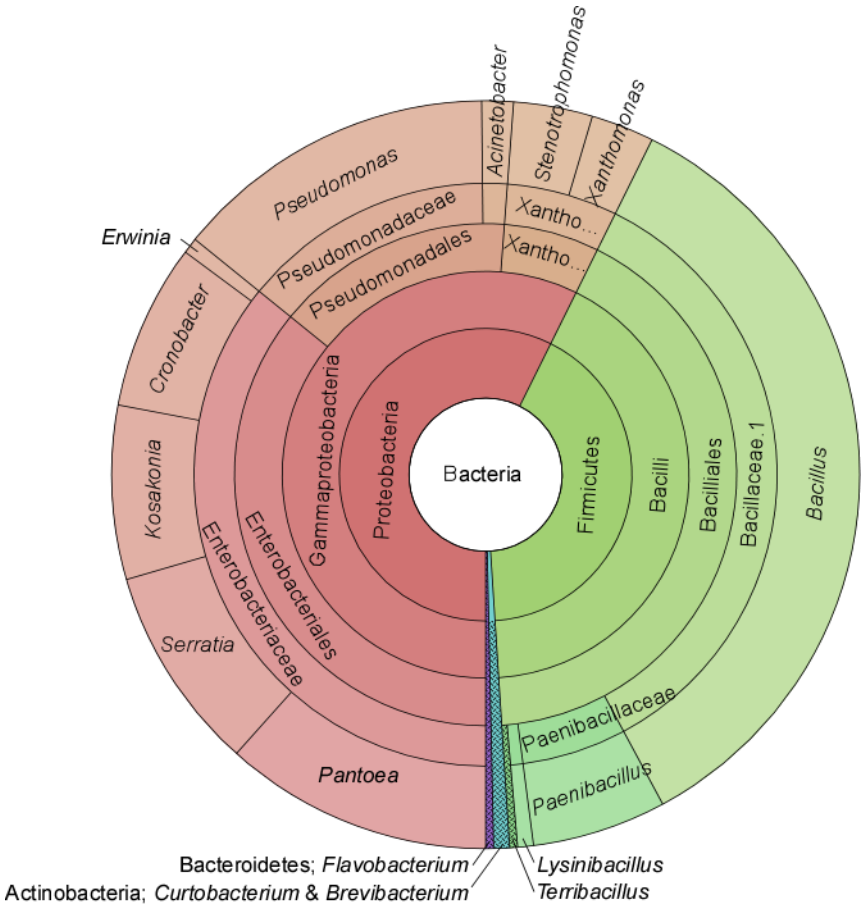

Figure S2 – Detached spikelet assay rating system. Photographs depict representative spikelets in each category, from 0-4, with increasing levels of necrosis or visible hyphae.

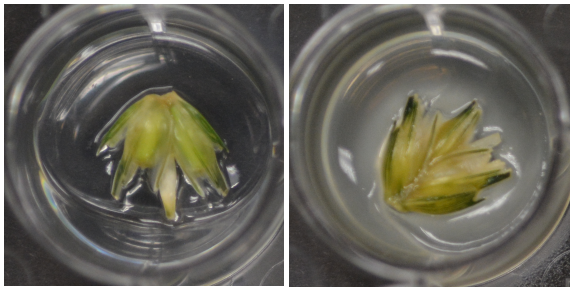

Level 0 – no damage or hyphal growth

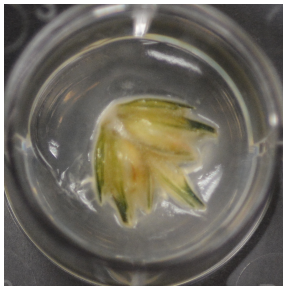

Level 1 – visible symptoms of necrosis (red coloration)

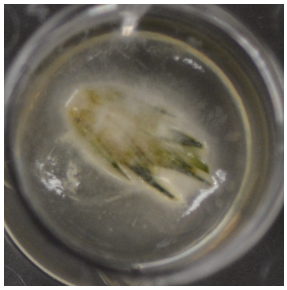

Level 2 – visible hyphae

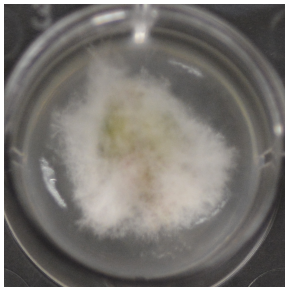

Level 3 – increasing production of hyphae

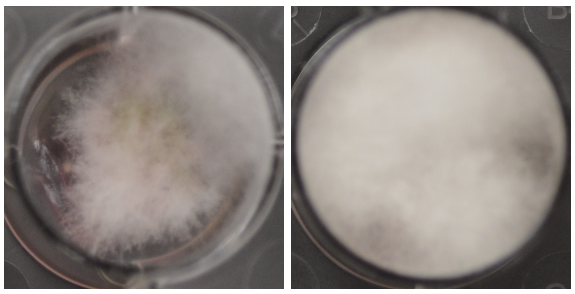

Level 4 – red coloration to media, hyphal growth has reached walls of culture-plate well

Figure S3 – Effect size varies by temperature treatment in both A) Dual Culture and B) Detached Spikelet Assays. Each point represents a measurement for a single bacteria-temperature treatment combination. Letters denote the significant differences between groups. Boxplots indicate variation in effect sizes across temperatures (E_T).

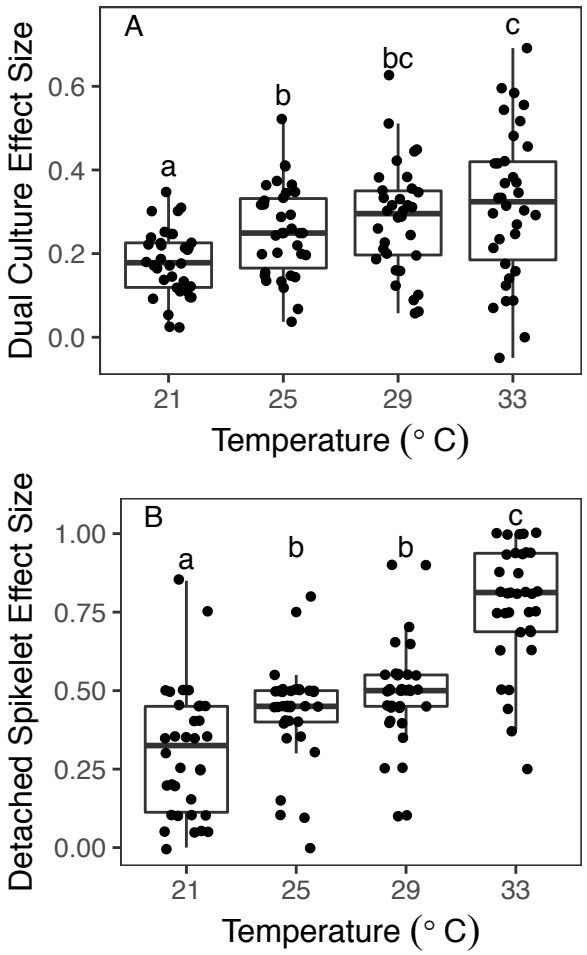

Figure S4 – Percentage of symptomatic spikelets varied by experimental factors. Density curves indicate variation in the percentage of visibly infected spikelets among A) temperature and B) atmospheric CO_2 treatments. Kernel density functions represent a smooth version of histograms. For C) experimental sets, the boxplots indicate variation in the percentage of visibly infected spikelets and each point represents a measurement for a single experimental wheat head. Percentage has been abbreviated as 'Perc.".

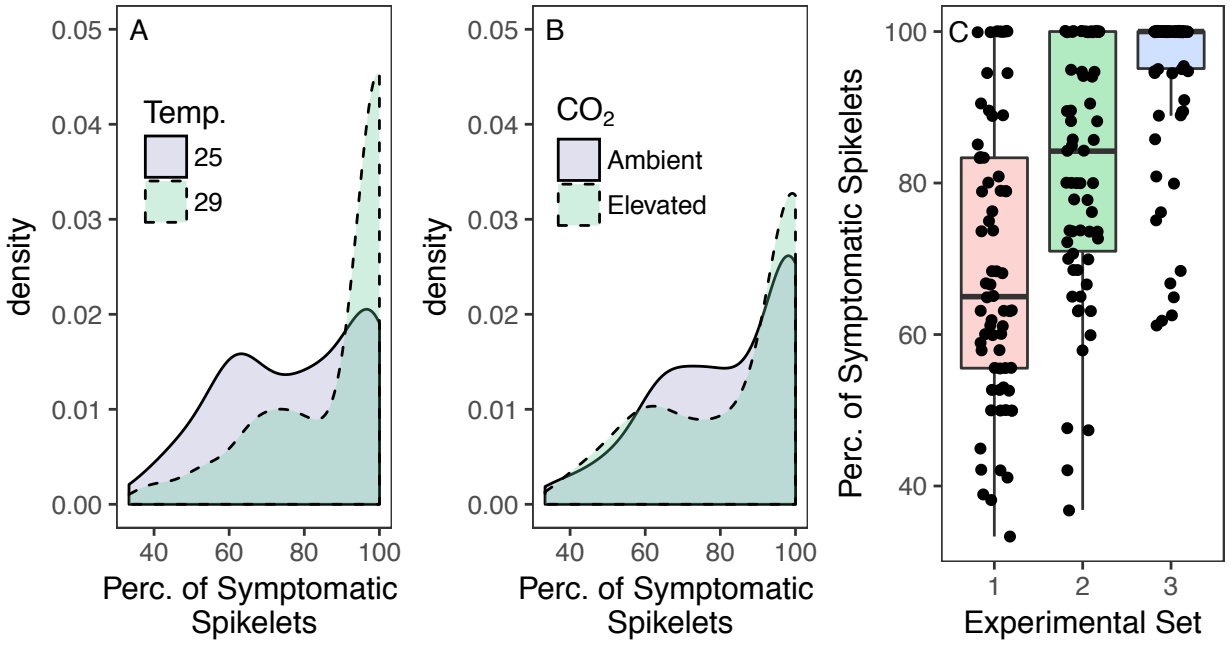

Conclusion

The task of a community ecologist can be a difficult one. One major goal being to understand the inherent complexity of the biotic and abiotic world, a task made challenging given that these dynamics can vary across multiple spatial and temporal scales. My research has attempted to employ manipulatory experimental designs, in order to test questions about the structure and function of microbial communities in the plant phyllosphere. This has included using a reciprocal transplant study, where replicate individuals of three host varieties were planted into field sites representing the historic home for each host variety. The contrast of host genetics with local environment allowed me to test a twist on the classic nature versus nurture question, within the context of microbial ecology. Similarly, using a common garden experiment, where the goal was to minimize variation in environmental conditions and microbial exposure, I instead manipulated host species identity using an explicit phylogenetic framework, to study the role of evolutionary history in structuring plant microbial communities. I expanded on this concept of host specificity in the phyllosphere to test a novel extension and adaptation of the plant soil feedback framework, dubbed plant-phyllosphere feedbacks. In this work, I demonstrated that, at least under some experimental conditions, phyllosphere microbial communities can have greater impacts on plant-plant interactions than rhizosphere communities, via the differential fitness consequences of exposure to con- versus heterospecific microbial inoculum. Lastly, through the simultaneous manipulation of environmental conditions and identity of bacterial endophytes, I tested how plant-bacteria interactions with a fungal pathogen can be mediated by the abiotic environment.

The impact of my dissertation work demonstrates the complexity, and potentially previously underestimated importance, of aboveground microbial communities (i.e., the

phyllosphere) in plant hosts. My work has combined multiple spatial scales of study, with manipulatory experimentation, and hypothesis-driven research to better uncover the hidden and cryptic nature of our world's tiniest creatures.

Dr. Briana K. Whitaker
Department of Biology, Indiana University
1001 E. 3rd Street, Bloomington, IN 47405
brkawhit@indiana.edu, (812) 855-1674
http://brianakwhitaker.wixsite.com/ecology

EDUCATION

2018 (July) **Doctor of Philosophy**
Indiana University at Bloomington (IUB)
Department of Biology; Evolution, Ecology, and Behavior (EEB) Program
Committee: Keith Clay (Advisor), Heather Reynolds, Jay Lennon, Curt Lively
GPA: 3.95

2012 **Bachelor of Science in Biology**, *Geography & Chemistry Minors*
University of North Carolina at Chapel Hill (UNC-CH)
Awarded: Honors in Biology --- *for defense of original research*
Degree Honors: Highest Distinction
Dean's List: Fall 2008 - Spring 2012
GPA: 3.869

2008 **N.C. School of Science and Mathematics (NCSSM)**, Durham, NC
Specialized Secondary School for Science, Math, and Technology
GPA: 3.96

RESEARCH EXPERIENCE

2013 – 2018 **Graduate Student Researcher**, IUB
- Plant-Microbial Ecology, Dr. Keith Clay
- Conducting studies on the relative importance of host genetic background and environmental conditions in driving endophyte community assembly.
- Manipulating con- and hetero-specific microbial inocula to study the consequences for host fitness and population dynamics.

2012 – 2013 **Research Technician**, U. of Texas at Austin & USDA-ARS, Temple, TX
- Plant Physiology, Drs. Tom Juenger, Phillip Fay, & Michael J. Aspinwall
- Executed experiments and measured diverse morphological and physiological traits on the grass species *Panicum virgatum* (Switchgrass) and *Panicum hallii* in the field and lab.

2011 – 2012 **Honors Thesis Student**, UNC-CH
- Plant Virus Ecology, Drs. Charles E. Mitchell & Megan A. Rúa
- Project Title – "Host Nutrient Status Stimulates Viral Pathogen Production, *Bromus hordeaceus* and Barley Yellow Dwarf Virus (BYDV)"

2010 **NSF REU**, UNC-CH

- Plant Virus Ecology, Drs. Charles E. Mitchell & Megan A. Rúa
- Project Title – "Analysis of individual and interactive effects of Barley Yellow Dwarf Virus (BYDV) and clipping on the grass species *Bromus carinatus* and *Bromus hordeaceus*."

2009 – 2010 **Undergraduate Research Assistant**, UNC-CH
- Biophysics, Drs. Richard Superfine & Briana Carstens Fiser
- Developed a fabrication and micro-contact printing method for elastomeric micro-posts. Expanded the experiment from low to high throughput.

GRANTS, FELLOWSHIPS & AWARDS

2017 **Outstanding Student Award**, **for best paper**, ESA Student Section ($100)
2017 **H. Kolodziejski Award**, **for mentorship**, Center for the Integrative Study of Animal Behavior ($750)
2017 **NSF Doctoral Dissertation Improvement Grant** (DDIG) – ($20,143)
2017 **NSF Graduate Research Internship Program** (GRIP), internship at USDA-ARS in Peoria, IL with Dr. Matthew Bakker ($5,000)
2017 **NIMBioS Workshop** (invited). Microbial traits. University of Tennessee, Knoxville
2015 **Daffodil Society Scholarship**, IUB Department of Biology ($1,000)
2015 **Fred Seward Award**, IUB Department of Biology ($2,500)
2015 **McCormick Science Grant**, IUB ($2,500)
2015 **Prairie Biotic Research Grant**, Prairie Biotic Research Inc. ($999.10)
2015 **Brackenridge Scholarship**, IUB Department of Biology ($2,000)
2015 **NIMBioS Graduate Attendee –** Workshop on Current Issues in Statistical Ecology,
University of Tennessee, Knoxville
2014 **Provost's Travel Award for Women in Science**, IUB ($209)
2014 **NSF Graduate Research Fellowship** (GRF) for 3yrs – ($100,000 + *tuition support*)
2014 **IUB Floyd Plant and Fungal Biology Summer Fellowship** ($617)
2014 **IAS Senior Grants**, Indiana Academy of Sciences ($2,993)
2014 **IURTP Field Research Award**, IU Research & Teaching Preserve ($495)
2013 **NIH Genetics, Cellular & Molecular Sciences Training Grant** (1yr) – ($25,000)
2013 **NSF Graduate Research Fellowship** (GRF) **–** **Honorable Mention**
2012 **John A. Couch Award**, UNC-CH – **Research Excellence in Plant Biology**
2012 **Francis J. LeClair Award**, UNC-CH – **Academic Excellence in Plant Sciences**
2011 **UNC-CH Summer Undergraduate Research Fellowship (SURF)** – Mitchell Lab ($3,000)
2010 **Leonard and Rose Herring Study Abroad Scholarship**, UNC-CH
2010 **Ginsburg Study Abroad Scholarship**, Ben-Gurion University
2010 **NSF Research Experience for Undergraduates (REU)** – Mitchell Lab ($5,850)
2010 **NSF and *Science* Magazine 2009 Visualization Challenge –**
- **Honorable Mention in Photography** – Taylor, R., ***Whitaker, B.K.***, & Carstens, B.L. "Flower Power". *Science*. 2010. Vol. 327. p. 954 – 955.

2009 **UNC-CH Science & Math Achievement & Resourcefulness Track (SMART) Scholar** – Research Placement and Grant – Dr. Richard Superfine Lab, Biophysics

2008 – 2012 **Fred Morrison Scholarship**, UNC-CH

PUBLICATIONS

Refereed Journal Articles:

Whitaker, B.K., Bauer, J., Bever, J.D., & Clay, K. (2017) Negative plant-phyllosphere feedbacks in native Asteraceae hosts – a novel extension of the plant-soil feedback framework. *Ecology Letters.* doi: 10.1111/ele.12805. -- *Awarded Best Student Paper at 2017 ESA Annual Meeting, by ESA Student Section.*

Aspinwall, M.S. et al. (including **Whitaker, B.K.**). (2016) Intraspecific variation in precipitation responses of a widespread C_4 grass depends on site water limitation. *Journal of Plant Ecology*. doi:10.1093/jpe/rtw040.

Christian, N.*, **Whitaker, B.K.***, & Clay, K. (***Equal contribution*) (2015) Microbiomes: unifying animal and plant systems through the lens of community ecology theory. *Frontiers in Microbiology*. **6**(869). doi:10.3389/fmicb.2015.00869. -- *Featured in "Frontiers Spotlight 2015" - Top 20 most viewed and downloaded articles across all Frontiers journals in 2015.*

Whitaker, B.K., Rúa, M.A., & Mitchell, C.E. (2015) Viral pathogen production in a wild grass host driven by host growth and soil nitrogen. *New Phytologist.* **207**(3). doi: 10.1111/nph.13369.

Book Chapters:

Christian, N., **Whitaker, B.K.**, & Clay, K. (2017) A novel framework for decoding fungal endophyte diversity. Published in The Fungal Community: Its Organization and Role in the Ecosystem.

Manuscripts in Review or Preparation:

Whitaker, B.K., Christian, N., Chai, Q., & Clay, K. (2018) Phylogenetic relatedness of Asteraceae hosts determines foliar microbiome community assembly in a common garden environment. *In Review at Molecular Ecology.*

Whitaker, B.K., Reynolds, H., & Clay, K. (2018) Local Environment, and not Ecotype, is the primary driver of microbiome community assembly in *Panicum virgatum* (Switchgrass). *In Review at Ecology.*

Whitaker, B.K., & Bakker, M.G. (2018) Bacterial endophyte antagonism *in vitro* does not predict protection from a fungal pathogen *in planta*. *In Preparation.*

PRESENTATIONS (*invited*)

2018 **USDA-ARS, Mycotoxin Prevention & Applied Microbiology Meeting** – Isolation and identification of seed endophytic bacteria in wheat *(Triticum*

aestivum) and their role in inhibition of the pathogen *Fusarium graminearum* across variable environmental conditions. Peoria, IL

2017 **Bradley University, Department of Biology** The Nature vs. Nurture Debate: Does who you are, or where you are, matter most? Peoria, IL

PRESENTATIONS (*other*)

2017 **Ecological Society for America (ESA)** –Foliar microbiome community assembly driven by phylogenetic relatedness of Asteraceae hosts in a common garden. COS 31-2. Portland, OR

2017 **Midwestern Ecology & Evolution Conference (MEEC)** – Foliar microbiome community assembly driven by phylogenetic relatedness of Asteraceae hosts in a common garden. Urbana-Champaign, IL

2016 **ESA** – A novel extension and investigation of the plant-soil feedback framework for phyllosphere microbial communities. COS 73-6. Ft. Lauderdale, FL

2015 **MEEC** – Ecotype by environment interactions drive microbiome community assembly in *Panicum virgatum* (switchgrass). Bloomington, IN

2013 **ESA** – Genotypic variation in traits controlling carbon uptake responses to precipitation in Switchgrass. Authors: Fay, P.A. et al. (including **Whitaker, B.K.**). COS 75-2. Minneapolis, MN.

2013 **ESA** – Growth and physiological plasticity among differentially adapted genotypes of a widespread C_4 grass under altered precipitation. Authors: Aspinwall, M.S. et al. (including **Whitaker, B.K.**). COS 6-1. Minneapolis, MN.

2012 **John K. Koeppe Undergraduate Research Symposium** –Host nutrient status stimulates viral pathogen production. Chapel Hill, NC.

POSTERS

2017 **MEEC** –*presented by a mentored student* Con- and heterospecific leaf litter induces negative feedback in Asteraceae species. Urbana-Champaign, IL

2015 **ESA** – Environment, and not ecotype, is the primary driver of microbiome community assembly in *Panicum virgatum* (Switchgrass). PS 24-31. Baltimore, MD

2013 **ESA** –Viral pathogen production and virus-plant interactions are controlled by nitrogen and phosphorus supply. PS 88-135. Minneapolis, MN.

2012 **Thirteenth Annual Celebration of Undergraduate Research** – Nutrient application to external host environment stimulates internal viral-pathogen titer. Chapel Hill, NC

2009 **Biophysics Symposium** –Elastomeric microposts: Force sensing at the cellular level. Chapel Hill, NC

TEACHING & MENTORING

2013 – 2016 **Assistant Science Instructor,** IU Biology Outreach
Clear Creek & Fairview Elementary Schools, Kindergarten & 3rd Grade

2016 **Course Instructor**, IU Foundations in Science and Mathematics Program
Introduction to Biology, Accelerated High School Summer Program

2013 **Associate Course Instructor,** IUB
Dept. of Biology, Course (L-111) Evolution, Ecology, & Diversity

2014 – Present	**Research Mentor** of Undergraduate Student(s) M. Zaret – (Aug 2015 – May 2018) – Presented Posters at Regional & National Meetings KC Cifizzari – (Jan 2017 – July 2018) M. Iang – (May 2017 – May 2018) I. Carrico – (May 2017 – May 2018) K. Hoban – Graduated with B.S. Biology – (Aug 2015 – May 2016) C. Ciresi – STARS Program – (Mar 2014 – May 2015)

SERVICE

2016 – 2018	**Editor-At-Large, ScIU Blog**, IUB
2014 – 2015	**Committee Leader, Ecology Lunch Bunch,** IUB
2014	**Midwestern Ecology & Evolution Conference Planning Committee**

SCIENTIFIC OUTREACH

2016 – 2018	**ScIU Blog**, IUB – Editor, Writer, & Peer Reviewer for campus science blog
2014 – 2015	**Girls Incorporated Summer Science Camp**, IUB – Program Leader/Organizer
2015	**Women in STIM Mentoring Circles**, IUB – Female Graduate Student Mentor
2014	**Jim Holland Summer Enrichment Program**, IUB – Program Leader
2009 – 2012	**Eno River Association,** Durham, NC – Invasive Plant Removal & Conservation

BIBLIOGRAPHY

Google Scholar: https://scholar.google.com/citations?user=epm3p_sAAAAJ&hl=en
ORCID: http://orcid.org/0000-0003-2522-9672
ResearchGate: https://www.researchgate.net/profile/Briana_Whitaker